Novel Manufacturing Processes for Polymer Bead Foams

by

Eung Kee (Richard) Lee

A thesis submitted in conformity with the requirements for the Degree of Doctor of Philosophy

Department of Materials Science and Engineering
University of Toronto

Novel Manufacturing Processes for Polymer Bead Foams

Richard E. K. Lee
Degree of Doctor of Philosophy, 2010
Department of Materials Science and Engineering
University of Toronto

ABSTRACT

Polymer bead foams are manufactured through a sintering process using foamed polymer beads. It is worth emphasis that the bead foam technology is the only process that can produce 3-dimensionally shaped foam products with ultra-low densities. This unique feature of bead foam process has been attracting enormous attentions from various foam industries. However the conventional bead foam processes still have some limitations associated with manufacturing productivity and safety during the treatment. This thesis deals with novel approaches to innovative and cost-effective manufacturing processes for polystyrene (PS) and polypropylene (PP) bead foam materials, based on thorough understanding of the scientific issues in bead foam technologies. This study also demonstrates the feasibility of new processes by conducting a series of foaming experiments such as batch foaming and continuous extrusion foaming as well as steam chest molding which is a critical common process for all bead foam products. In addition, this study aimed at developing new bead foam processes based on the relationship between the cellular structure and processing/material parameters. When it comes to expandable PS (EPS) bead process, research efforts have been made to eliminate n-pentane which has some disadvantages related to its flammability and low boiling temperature. In addition, the bi-celullar PS foams that feature the superior thermal-insulation property was

manufactured through continuous extrusion foaming process. With regard to expanded PP (EPP) bead process, research efforts were focused on the development of cost-effective continuous foaming process in order to resolve the high cost issue of conventional EPP beads. These research strategies were designed on the basis of the comprehension of thermoplastic foaming, steam chest molding process and gas dissolution/diffusion phenomena. The results in the thesis provided considerable introductory and advanced knowledge about the bead foam technologies so that further promising researches can be performed to invent entirely new bead foam materials such as ultrahigh–temperature-durable bead foam products, biodegradable bead foams, other highly functional bead foam products aside from EPS and EPP bead foams.

Acknowledgements

First of all, I would like to give all the glory to my God Jesus Christ, as I admit that he is my father and a savor of my life. He faithfully led my way during my study at the University of Toronto, and also thankfully supplied physical power and wisdom to me.

I feel so grateful and indebted to my supervisors, Prof. Chul B. Park and Prof. Hani E. Naguib, for having helped me not just with research work but with financial support for me and my family in Canada. Besides, I would also like to thank my Ph.D. committee professors, Prof. Zhirui Wang, Prof. Zheng Hong. Lu, Prof. Glenn Hibbard and Prof. Vipin Kumar, for the willingness to serve on my dissertation committee and for their valuable comments and impressive suggestions as well.

Personally it was unthinkable for me to finish my Ph.D. study safe and sound without many colleagues in the Microcellular Plastics Manufacturing Laboratory. I deeply thank Dr. Jin Wang, Dr. Edward Zhang, Dr. Wenge Zheng, Gangjian Guo, Qingping Guo, Guangming Li, Chunmin Wang, Taher Azdast, Wanrudee Kaewmesri, Florien Gunkel, Ivan Gutierrez, Dr. Zhenjin Zhu, Dr. Wenli Zhu, Gary Li, Jing Wang, Mohamed Serry, Dr. Kuboki, Dr. Kumar, Dr. Maridass, Dr. Kamal, Dr. Wenli Zhu, Dr. Wentao Zhai, Mohamed Hassan, Hongtao Zhang, Jeff Wu, Kelly Zhang, Mingyi Wang, Nan Chen, Prof. Behravesh, Raymond Chu, Mr. Koyama, Reza Nofar, Kamlesh, Changwei Zhu, Dr. Saleh, and April Binnie. I will never forget their help and friendship.

On top of it, I can’t help but thank my Korean colleagues; Big brother Kevin Y.H. Lee, Dr. Young-Seok Kim, Dr. Chi-sung Song, Alex Lee, Ryan S.G. Kim, Myung-Jae Lee, Patrick Lee, Taekyun Yoo, John Lee, Dr. Kyung-Min Lee, Jong-chan Park, Dr.

Yong-Rak Moon, Dr. Sung-Min Kim, Dr. Jae-Kyoung Kim, Heesup Nam, Sue Chang, Peter U. Jung (and his family as well), Esther Lee, Eunji In and Dr. Choonghee Jo. The time and the tremendous fun that we shared in Toronto will be unforgettable even in the future. My gratitude is extended to Prof. Young-wook Kim, Prof. Bosung Shin, and Prof. Dong-won Jung for their good advices and sincere comments in various aspects. I also wish to acknowledge Prof. Dong-woo Cho at POSTEC in Korea not only for lots of treats to Soju but also for showing an ideal role-model for me. Subsequently I also want to say thank you to Yoon-Hyun Choi about tremendous help with my successful adjustment in Canadian life.

I truly feel obligated to acknowledge LG Hausys Corp. and LG Chemical Corp. since I could not get through with my study without their financial support. I wish I will be able to be conducive to the prosperity of the companies.

Last but not least, I would like to thank my parents, parents-in-law, two brothers, a brother-in-law for their constant love and prayer for my PhD study. Finally it is time to thank my lovely wife, Kyoungsun, my daughter, Hyunmin and son, Daniel. Frankly, I don’t even know how much I owed my family during my study, because they did their best to support me by sacrificing themselves. Now all I can do is to pledge that I will give it my best shot to love them and to make them happy in the rest of my life.

TABLE OF CONTENTS

CHAPTER 5. BI-CELLULAR POLYSTYRENE FOAM

CHAPTER 6. ANALYSIS OF EPP IN AN AUTOCLAVE PROCESS

CHAPTER 7. EXTRUSION FOAMING OF PROPYLENE-ETHYLENE COPOLYMERS FOR EPP APPLICATION

CHAPTER 8. STUDY ON STEAM CHEST MOLDING PROCESS FOR EPP BEAD FOAMS

CHAPTER 9. SUMMARY OF CONTRIBUTION AND RECOMMENDATIONS

LIST OF TABLES

LIST OF FIGURES

NOMENCLATURE

CBA	=	Chemical blowing agents
PBA	=	Physical blowing agents
EPS	=	Expandable polystyrene
EPP	=	Expanded polypropylene
HFCs	=	Hydrofluorocarbons
PS	=	Polystyrene
PP	=	Polypropylene
SDS	=	Sodium Dodecyl Sulfate
c_s	=	Solubility of gas in the polymer (cm^3/g or $g_{gas}/g_{polymer}$)
H	=	Henry's law constant (cm^3 [STP]/g-Pa)
p_s	=	Saturation pressure
R	=	Gas constant (J/K)
H_o	=	Solubility coefficient constant (cm^3 [STP]/g-Pa)
ΔH_s	=	Molar heat of sorption (J)
D	=	Diffusivity
D_o	=	Diffusivity coefficient constant (cm^2/s)
E_d	=	Activation energy (J)
W	=	Required work to generate a bubble
γ_{pb}	=	Surface tension
A_b	=	Surface area,
V_b	=	Bubble of volume
ΔG^*_{homo}	=	Gibbs free energy in homogeneous nucleation

$\dot{N}$	=	Homogeneous nucleation rate
C_o	=	Concentration of gas molecules in solution
f_o	=	Frequency factor of gas molecules joining the nucleus
k	=	Boltzman constant
r	=	Critical radius
σ	=	Surface tension
Δp	=	Pressure difference between the bubble and the melt.
N_1	=	Heterogeneous nucleation rate
ΔG^*_{het}	=	Gibbs free energy in heterogeneous nucleation
γ^3_{bp}	=	Surface energy of the polymer-bubble interface
ΔP	=	Gas pressure used to diffuse the gas into the polymer
θ	=	Wetting angle of the polymer-additive gas interface.
dP/dt	=	Pressure drop rate
P_{sat}	=	Saturation pressure
ρ_f	=	Foam density , g/cm^3
ρ	=	Density of unfoamed sample, g/cm^3
M	=	Mass of foam sample, g
V	=	Volume of foam sample, cm^3
Φ	=	Volume expansion ratio,
V_f	=	Void fraction
N_0	=	Cell density
N	=	Number of bubbles in the micrograph
a	=	Area of the micrograph

M	=	Magnification factor of the micrograph
MFI	=	Melt flow index
DSC	=	Differential Scanning Calorimeter
T_m	=	Melting temperature
T_c	=	Crystallization temperature
ΔH_{exp}	=	Experimental heat of fusion heat of fusion
χ_c	=	Degree of crystallinity
ΔH^*	=	Heat of fusion of the fully crystalline polymer

Chapter 1

Introduction

1.1. Bead Foam Technology

Polymer bead foams with various 3-dimensional shapes can be manufactured using a sintering process of foamed beads. One of most frequently used bead foams is polystyrene (PS) bead foams. They are widely used in disposable coffee cups, coolers or cushioning material in packaging. Expandable PS (EPS) beads are polymerized in the form of fine polystyrene beads that contain 4 to 7 wt% of n-pentane, which means that the EPS beads are in an unfoamed state when they are sold and transported to a variety of molding manufacturers. Thus, the bulk density of the EPS beads is about 0.64 g/cm^3 and the transportation cost is reasonable. Molding manufacturers can perform pre-expansion with the expandable PS (EPS) beads using a pre-expander system. The pre-expanded beads have to be stabilized in a silo. This period is for the pressure equilibrium between internal cells and atmosphere. Following the stabilization period, the beads are ready to go through steam chest molding. It is the general procedure to fabricate EPS bead foams in industry.

The second most popular bead foams are expanded polypropylene (EPP) bead foams that are generally used as automotive parts and high-end packaging materials that require high dimensional stability and superior elasticity. Figure 1.1 shows how EPP bead foams are being used in the automotive industry [1]. Particularly most of bumper-cores in cars are made of EPP bead foams with 15 times of volume expansion ratio. Other advantages of EPP are superior recyclability and environmental friendliness.

Aside from EPS and EPP, expanded polyethylene (EPE) and expanded poly lactic acid (EPLA) bead foams are recently drawing much of attentions due to their biodegradability and large application potentials. It is known that the bead foam process is the only technology to achieve 3-dimensional structure foams with very low density down to about 20 kg/m^3. Generally extrusion foaming can continuously produce just 2-dimensional foam profiles with various densities. In the case of injection foam molding, it is possible to produce 3-dimensional shaped foams. However, the maximum volume expansion ratio is limited to just 2 to 3 times. In this aspect, bead foam technology is considered highly promising and worthy of extensive study.

1.2. Thermoplastic Foams

Thermoplastic foams consist of at least two phases: solid polymer matrix and a gaseous phase that contributes to the formation of cells [2]. In general foamed polymer products possess various unique characteristics compared to their solid counterparts, such as higher specific tensile strength, higher toughness, and superior thermal and sound insulation properties [3-7]. In addition, polymer foams are much lighter than their solid counterparts. This unique feature of thermoplastic foams keeps stimulating customers and manufacturers to find new lucrative application areas. It is estimated that the global production of thermoplastic foam in 2001 is more

than five million tons [8]. The market volume gradually continues to grow every year.

The major processing methods used to produce thermoplastic foams are batch foaming [9-11], extrusion foaming [12–18], injection foam molding [19-22], rotational molding [23-25], and compression foam molding [26, 27]. Often times, extrusion foaming and injection foam molding are preferred to other processes due to higher productivity.

1.3. Classification of Thermoplastic Foams

Generally thermoplastic foams can be categorized according to cell size, foam density, and cell structure. Firstly, depending on cell size and cell population density, thermoplastic foams can be classified to conventional foams, fine-celled foams, and microcellular foams (Table 1.1) [28]. Foam density can also be a criterion for classification of thermoplastic foams; high-density foams (i.e., less than 4 times expansion), medium density foams (i.e., between 4 and 10 times expansion), and low-density foams (i.e., more than 10 times expansion). High-density foams are usually used for construction materials, furniture, and transportation products, whereas low-density foams are mainly used for impact absorption, sound insulation, and packaging materials [29]. To classify thermoplastic foams based on cell structure, they can be divided into the open-cell foams and the closed-cell foams. The open-cell foams feature inter-connected cells. On the other hand, the closed-cell foams have no openings in cell walls. Many researchers have been paying attentions to the open-cell foams because of their excellent sound-insulating effect. However closed-cell foams are highly preferred for bead foam process in order to achieve further expansion of each cell in foamed beads.

1.4. Research Motivation

In spite of the fact that thermoplastic foaming technology has evolved quite a lot over the last decades, bead foam processes are still holding some drawbacks and significant challenges. As to the conventional EPS bead foam process, the blowing agent, n-pentane, is a volatile organic compound (VOC), which leads to the risk of explosion and fire during the transportation and the storage of large amount of EPS beads. Another issue is a limited shelf life of EPS beads. Since the low boiling point of n-pentane is as low as 36.1 ^{o}C, the pentane dissolved in the beads can gradually diffuse out and accordingly the bead quality deteriorates over time. On this account, many researchers have been trying to develop the VOC-free EPS bead foam technology for a long time. In addition to that, industrial needs toward EPS foams with superior thermal-insulation effect have skyrocketed due to the fast growth of construction material market.

When it comes to EPP bead foams, the high price of EPP bead foams is restricting the expansion of the market volume even if they have excellent mechanical properties that are suitable for numerous engineering purposes. It is not only because the current processs is a batch foaming that is less productive than extrusion foaming, but also because the transportation cost of EPP beads with extremely low bulk densities. Moreover, it is known that enormous investment is required to build the autoclave batch foaming system for traditional EPP beads.

1.5. Objectives of Thesis

The main purpose of this research is to develop and demonstrate the feasibility of novel manufacturing processes of EPS and EPP bead foams, based on the scientific understanding of the conventional bead foam processes.

The first objective is to quantify the solubility and the diffusivity of n-pentane in PS and PP at room temperature and atmospheric pressure. The results of this study will account for why EPS bead foam process can not be applied to EPP beads and for why expandable PP beads are not commercially available.

The second objective in this thesis is to develop a novel EPS bead foam process where the final EPS beads contain no VOC at all. As mentioned earlier, the current EPS bead foam technology has disadvantages concerning VOC issues.

Thirdly, this thesis study also aims at developing extrusion foaming process that can produce PS foam with superior thermal-insulation characteristics by controlling cellular structure. It is desirable to attain bi-cellular cell structure in the PS foam to minimize the thermal conductivity. It is expected that the expanded PS beads with bi-cellular structure will form PS bead foams having the improved thermal insulation property.

The fourth objective is to thoroughly comprehend the conventional manufacturing process of EPP beads, including the generation of a beta-crystal structure while going through the autoclave foaming process.

The fifth objective is to demonstrate the viability of continuous extrusion foaming for producing affordable EPP beads compared to conventional ones. For this research, two kinds of ethylene-propylene copolymers will be investigated regarding extrusion foaming behaviors.

The final objective is to understand and optimize the steam chest molding process which plays a critical role in shaping the final 3-dimensional foam products.

1.6. Organization of Thesis

Comprehensive introduction about the dissertation is given in the Chapter 1 along with its motivation and objectives. This is followed by a series of literature reviews on principles of thermoplastic foaming and bead foam processes in Chapter 2. Subsequently Chapter 3 explores the gas transport phenomena through the quantitative measurement of solubility and diffusivity of n-pentane in PS and PP at ambient conditions. Chapter 4 will discuss the strategy and experimental results about the development of a novel EPS bead foam process without VOC. In Chapter 5, extrusion foaming study will be deployed in an attempt to achieve bi-cellular PS foams. In Chapter 6, the detailed information on both the existing EPP manufacturing process and the formation of beta-crystals in PP beads is disclosed. Chapter 7 deals with continuous extrusion foaming of ethylene-propylene copolymers for a cost-effective way of manufacturing EPP beads. In Chapter 8, actual execution of steam chest molding with conventional EPP beads as well as the experimental results will be discussed in order to fundamentally understand the detailed mechanism of bead expansion and sintering. Finally Chapter 9 covers major contributions of the thesis and recommendations for future research. Table 1.3 shows the overall outline of the thesis study.

1.7. References

[1] BASF Website, http://www.basf.com/group/products-and-industries/index

[2] D. Klempner, and V. Sendijarevic, *Handbook of Polymeric Foams and Foam Technology, 2nd Edition*, Hanser Publsihers, 6 (2004)

[3] D. F.Baldwin, and N. P. Suh, *SPE ANTEC Tech. Papers*, 38, 1503 (1992)

[4] D. I. Collias, D. G. Baird, and R. J. M. Borggreve, *Polymer*, 35, 3978 (1994)

[5] D. I. Collias, and D. G. Baird, *Polym. Eng. Sci.*, 35, 1167 (1995)

[6] K. A. Seeler, and V. Kumar, *Journal of Reinforced Plastics and Composites*, 12, 359 (1993)

[7] L. M. Matuana, C. B. Park, and J. J. Balantinecz, *Cellular Polymers*, 17, 1 (1998)

[8] J. L. Throne, *Thermoplastic Foam Extrusion*, Hanser Publishers, New York, 112 (2004)

[9] Y. Ema, M. Ikeya, and M. Okamoto, *Polymer*, 47, 5350 (2006)

[10] J. Reignier, J. Tatiboue¨t, and R. Gendron, *Polymer*, 47, 5012 (2006)

[11] M. Shimbo, D. F. Baldwin, and N. P. Suh, *Polym. Eng. Sci.*, 35, 1387 (1995).

[12] P. C. Lee, G. Li, J. W. S. Lee and C. B. Park, *J. Celullar Plastics*, 43, 431 (2007)

[13] D. I. Collias, and D. G. Baird, R. J. M. Borggreve, *Polymer*, 25, 3978 (1994)

[14] D. I. Collias, and D. G. Baird, *Polym. Eng. Sci.*, 35, 1167 (1995)

[15] E. P. Giannelis, *Adv. Mater.*, 8, 29 (1996)

[16] M. Okamoto, P. H. Nam, P. Maiti, T. Kotaka, N. Hasegawa, and A. Usuki, *Nanoletters*, 1, 295 (2001)

[17] X. Han, C. Zeng, L. J. Lee, K. W. Kurt, D. L. Tomasko, *SPE ANTEC Tech. Papers*, 48, Paper #354 (2002)

[18] M. Kwak, M. Lee, and B. K. Lee, *SPE ANTEC Tech. Papers*, 48, Paper #381 (2002)

[19] C.A. Villamizar, and C. D. Han, *Polym. Eng. Sci.*,18, 699 (1978)

[20] D. Maldas, B. V. Kokta, and C. Daneault, *J. Vinyl. Technol.*, 11, 2 (1989)

[21] N. E. Zafeiropoluos, C. A. Baillie, and F. L. Matthews, *Adv. Compos. Lett.*, 9, 291 (2000)

[22] G. Cantero, A. Arbelaiz, R. Llano-Ponte, and I. Mondragon, *Comp. Sci. Techno*. 63 1247 (2003)

[23] A. Arbelaiz, B. Fernandez, G. Cantero, R. Llano-Ponte, A. Valea, and I. Mondragon, *Compos. Part A*, 36, 1637 (2005)

[24] P. Balasuriya, L. Ye, Y. Mai, and J. Wu, *J. Appl. Polym. Sci.*, 83, 2505 (2002)

[25] B. V. Kokta, D. Maldas, C. Daneault, and P. Beland, *Poly. Plast. Technol. Eng.*, 29, 87 (1990)

[26] B. N. Kokta, D. Maldas, C. Daneault, and P. Beland, *J. Vinyl. Technol.*, 12, 146 (1990)

[27] K. L. Pickering, A. Abdalla, C. Ji, A. G. McDonald, and R.A. Franich, *Composites: Part A*, 34, 915 (2003)

[28] K. C. Frisch, J. H. Saunders, *Plastics Foams*, Marcel Dekker Inc., New York, 24 (1972)

[29] J. L. Throne, *Thermoplastic Foams*, Sherwood Publishers, Ohio, 39 (1996)

Table 1.1 Foam classification by cell size and cell population density.

Foam type	**Cell size**	**Cell population density**
Conventional	> 300 μm	< 10^6 cell/cm^3
Fine-celled	10 - 300 μm	10^6 - 10^9 cell/cm^3
Microcellular	< 10 μm	> 10^9 cell/cm^3

Table 1.2. Outline of thesis work

	EPS Bead Foam	EPP Bead Foam	Remark
Conventional Process	**Suspension polymerization** - Risk of fire - Global warming potential	**Batch foaming in autoclave (Ch.6)** - Low productivity - High bead price	To comprehend existing technologies and their limitations
	Gas transport phenomena of n-pentane in PS and PP **(Ch.3)**		To explain why EPS technology can not be applied to EPP
Novel Manufacturing Process	VOC-free EPS bead foam process **(Ch.4)** PS Foam with high thermal insulation **(Ch.5)**	Continuous extrusion foaming process **(Ch.7)**	To develop renovative new processes
Common Issues	Optimum condition for steam chest molding process **(Ch.8)**		To understand the basic principles of steam chest molding process

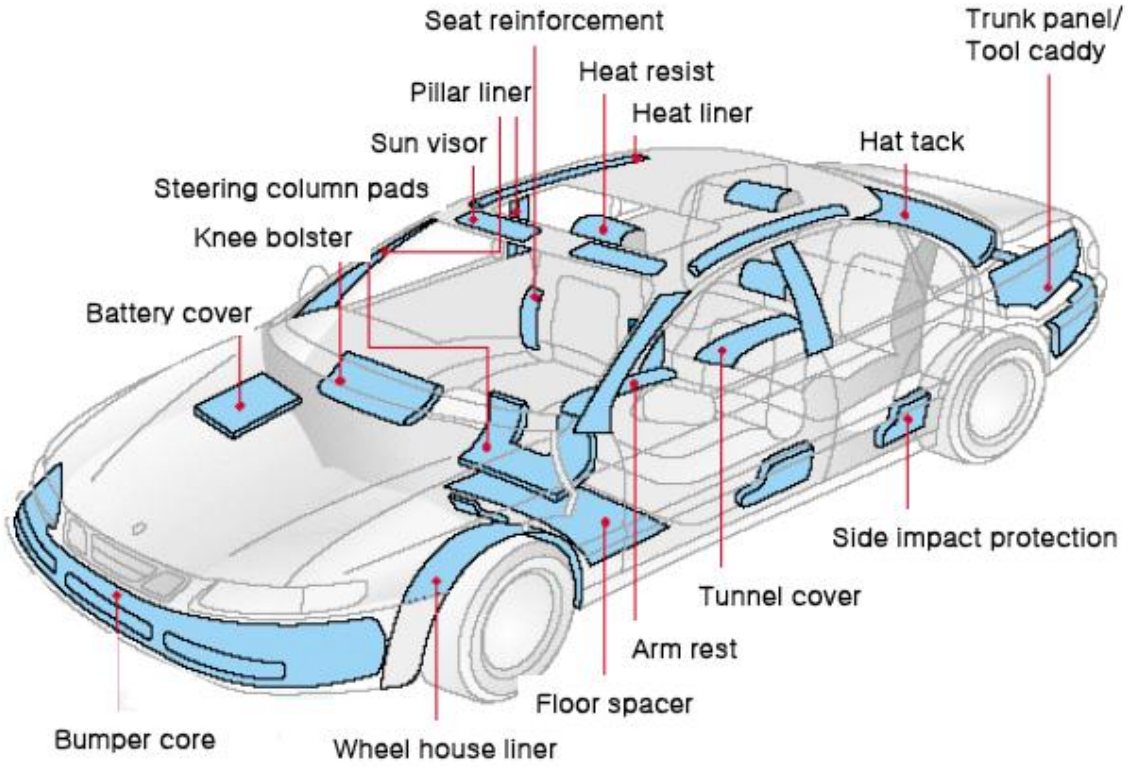

Figure 1.1. EPP bead foams used as automotive parts [1].

Chapter 2

Theoretical Background and Literature Review

This chapter is designed to deal with both the previous researches and the basic information on the fundamental principles of thermoplastic microcellular foaming, methods to characterize foam structures, and the conventional processes of manufacturing EPS/EPP bead foams.

2.1. Thermoplastic Microcellular Foams

Now that the bead foam process can be conducted with foamed polymer beads, the quality of expanded beads is crucial for determining the final physical properties of the polymer bead foams. Accordingly, it is essential to understand the mechanism and the procedure of thermoplastic microcellular foam process in order to take control of the cell morphology of foamed polymer beads.

2.1.1. Blowing Agents for Foaming

In general, thermoplastic foams can be blown with either a chemical blowing agent (CBA) or a physical blowing agent (PBA). CBAs are substances that can decompose at a certain processing temperature, thus evolve gases like CO_2 and/or N_2. Commonly solid organic and inorganic substances (such as azodicarbonamide and sodium bicarbonate) are used as CBAs. Specifically CBAs are divided by their enthalpy of reaction into two groups including exothermic and endothermic foaming agents. The chemical reaction that generates the gas can either absorb energy (endothermic) or release energy (exothermic). PBAs are materials that are injected into the polymer system in either a liquid or gas phase. Some PBAs such as pentane or isopropyl alcohol have a low boiling point and remain in a liquid state in the polymer melt under pressure [1]. When the pressure is released, the phase change of the foaming agent from liquid to vapor happens immediately and the vapor comes out of the solution with the polymer, thereby expanding the polymer melt. As the boiling point of a gas decreases, the volatility of the gas increases. Higher volatility or vapor pressure requires more pressure to keep the gas in its liquid phase in the polymer melt. Another type of PBA is inert gases, such as N_2 or CO_2. Inertness represents the reactivity and corrosiveness of a gas to the polymer, any additive, the machinery, or the surrounding environment. As a blowing agent becomes more inert, it is less reactive (or corrosive) to its surroundings. These inert gases dissolve as vapors in the polymer melt and diffuse out of the solution as vapors to expand the polymer melt. The solubility of the gases affects the final density. Both CO_2 and N_2 have relatively low solubility in polyolefin matrices, compared to hydrocarbon blowing agents such as butane or pentane.

In the traditional foam processing, the most frequently incorporated blowing agents are FCs, CFCs, n-pentane, and n-butane [2]. These blowing agents have high solubilities, and can

thus be dissolved in large quantities into the polymer matrices. For example, the solubility of FC-114 in polystyrene is above 20 wt% at a pressure of 6.9 MPa and at a temperature of 200°C [3]. These blowing agents allow for a foam structure that has high void fraction at low processing pressure and large volume expansion due to the smaller amount of gas loss. Since these blowing agents have low diffusivities due to their larger molecular size, the gas loss out of the foamed extrudate is substantially reduced [2]. Therefore, the final foam product can have a low foam density. Despite all the advantages of the conventional foaming blowing agents, some serious environmental and safety issues still exist. The use of CFCs was prohibited according to the Montreal Protocol [4], signed by 24 countries in 1987. Other blowing agents such as n-pentane and n-butane are hazardous because of their high flammability.

2.1.2. Microcellular Foam Processing

Extremely high cell population density for polymeric foams can be achieved by inducing an abrupt thermodynamic instability in a homogeneous polymer/gas solution. After the formation of polymer/gas solution, the cells should be nucleated and preserved by controlling their growth until the gas bubbles are stabilized [5]. The microcellular foaming system should have the following essential processing mechanisms to successfully achieve these conditions: a mechanism for completely dissolving a large and soluble amount of a blowing agent into polymer melt under high processing pressure; a mechanism for inducing a thermodynamic instability in the homogeneous polymer/gas solution formed earlier; and a mechanism for controlling the bubble growth while preventing them from coalescing and collapsing.

2.1.3. Principles of Microcellular Foam Processing

In general, microcellular foam processing consists of three major steps; 1) formation of polymer/gas solution, 2) cell nucleation, and 3) cell growth. These basic processing steps are applied to batch foam as well as extrusion foaming.

2.1.3.1. Formation of Polymer/Gas Solution

The first step of microcellular foaming is to achieve homogeneous polymer/blowing agent solution. The uniformity of the polymer/gas solution significantly affects the final cell morphology as well as the mechanical properties. In particular, the amount of blowing agent injected should be below the solubility limit of the processing pressure and temperature in order to ensure complete mixing and dissolving of gas into the polymer. This must be carefully controlled because large voids will form if an excess amount of blowing agent exists and cannot be dissolved into the polymer. For this reason, it is crucial to determine the solubility (or the amount) of blowing agent that can be absorbed and dissolved into the polymer at different processing temperatures and pressures. This information is necessary for the production of microcellular foam in order to avoid the presence of large voids.

The maximum solubility of gas into polymers can vary, depending on the system pressure and temperature and can be estimated by Henry's law [4]:

$$c_s = H p_s \tag{2.1}$$

where c_s is the solubility of gas in the polymer in cm^3/g or $g_{gas}/g_{polymer}$, H is Henry's law constant (cm^3 [STP]/g-Pa), and p_s is the saturation pressure in Pa. The constant H is a function of temperature described by:

$$H = H_o \exp(-\frac{\Delta H_s}{RT}) \tag{2.2}$$

where R is a gas constant in J/K, T is the temperature in K, H_o is a solubility coefficient constant (cm^3 [STP]/g-Pa), ΔH_s is the molar heat of sorption in J. The molar heat of sorption, ΔH_s, can be either a negative or positive value, depending on the polymer-gas system. Equations (2.1) and (2.2) can be used to estimate the solubility of a blowing agent in the polymer at a certain processing pressure and temperature. The estimation of the solubility of CO_2 in some polymers can be found in some research papers [6,7]. Based on the polymer flow rate in extrusion, the gas flow rate can be controlled so that the gas-to-polymer weight ratio may be maintained below the solubility limit.

When it comes to gas diffusivity in polymer, the diffusivity (*D)* is mainly a function of temperature, and this can be represented as the following equation [8,9]:

$$D = D_o \exp(-\frac{E_d}{RT}) \tag{2.3}$$

where D_o is the diffusivity coefficient constant in cm^2/s, and E_d is the activation energy for diffusion in J. Thus, the diffusion rate can be increased by processing the plastic/gas mixture at a higher temperature. In a continuous process, retaining undissolved gas pockets in the polymer matrix is possible when an excess amount of gas is injected. Therefore, it is critical to ensure that the amount of gas injected is below the solubility limit in the processing conditions. However, one advantage of using the extrusion foaming process is the reduction in dissolution time

because of higher gas diffusivity at the high processing temperature. This makes the extrusion process a more cost-effective method. In addition to the proper amount of gas injection, a sufficient amount of dissolution time is required to generate a uniform solution. Although the appropriate amount of gas can be injected, it does not necessarily guarantee the formation of a uniform solution. If the required time of gas diffusion in the polymer matrix is longer than the melt residential time inside the system between gas injection and nucleation, it is obvious that a uniform solution would not be achieved. Park *et al.* [10] investigated the diffusion behavior in an extrusion process containing a mixing screw. It was observed that shear mixing caused by the screw rotation promotes convective diffusion. In convective diffusion, the screw motion creates the contact between a high gas concentration region (gas bubble) and a low gas concentration region (polymer melt). Furthermore, by stretching gas bubbles in the shear field generated by the motion of the screw which enhances the diffusion process, the interfacial area will be increased, thereby improving the diffusion mechanism. In addition, a dissolution enhancing device containing static mixers in the extrusion system will enhance the dissolution process by generating shear fields as the mixing elements are reorienting the melt along the flow direction, thus promoting solution formation.

2.1.3.2. Cell Nucleation

Cell nucleation is an important step in fine-celled or microcellular foaming processes. Cell nucleation can be defined as a transformation of small clusters of gas molecules into energetically stable groups or pockets. In order to create bubbles in liquids or polymer melts, a minimum amount of energy must be given to the system so that it can break the free energy barrier. This energy can be provided by heating or through a pressure drop. Two types of

nucleation mechanisms can be observed: homogeneous and heterogeneous nucleation. Homogeneous nucleation is a type of nucleation where cells are nucleated randomly throughout the liquid or polymer melt matrix. It requires higher nucleation energy than heterogeneous nucleation. Heterogeneous nucleation is defined as nucleation at certain preferred sites, such as on the phase boundary, or sites provided by the additive particles.

In the case of homogeneous nucleation, the classical nucleation theory has been used to describe the nucleation behavior in microcellular foaming by Colton and Suh [11]. In this theory, the required work to generate a bubble of radius r in a liquid is given by

$$W = \gamma_{pb} A_b - \Delta P V_b \tag{2.4}$$

where the first term, $\gamma_{pb} A_b$, is the work required to create a bubble with surface tension, γ_{pb}, and surface area, A_b, and the second term, $\Delta P V_b$, is the work done by the expansion of gas inside a bubble of volume V_b. The difference between the two terms is the actual work required to generate a cell. After the substitution of geometric equations of a sphere for A_b and V_b, the equation becomes as follows:

$$W = 4\pi r^2 \gamma_{pb} - \frac{4}{3}\pi r^3 \Delta P \tag{2.5}$$

In order for the bubble to grow spontaneously, the maximum energy barrier must be overcome. If the induced energy in the system is lower than the maximum energy, the bubble, which is smaller than the critical bubble size, collapses. The amount of free energy can be calculated by differentiating W with respect to r from the previous equation.

$$\Delta G^*_{\text{hom}} = \frac{16\pi\gamma_{pb}^3}{3\Delta P^2} \tag{2.6}$$

The cell nucleation rate, $\dot{N}$ (bubbles/m$^3 \cdot$ sec), can be defined as follows [12]:

$$\dot{N} = C_o f_o \exp(-\frac{\Delta G^*}{kT}) \tag{2.7}$$

where C_o is the concentration of gas molecules in the solution, f_o is the frequency factor of gas molecules joining the nucleus, and k is the Boltzman constant.

According to the classical nucleation theory, a greater number of cells can be nucleated as the saturation pressure, ΔP, increases. The saturation pressure can be estimated as the gas concentration in the polymer according to Henry's law (Equation 2.1). When the amount of gas in the polymer increases, the chance to nucleate more cells also increases. Even though the classical nucleation theory yields very valuable information about the pressure drop and cell nucleation relationship, it does not predict the effect of the pressure drop rate on cell nucleation. The effect of the pressure drop rate on nucleation is another important parameter and should be carefully examined. In the classical nucleation theory, an instantaneous pressure drop and instantaneous nucleation are assumed and thus, the nucleation rate, $\dot{N}$ of Equation (2.7) corresponds to the number of nucleated cells. However, in reality, the pressure drop is not instantaneous and happens over a finite time period. The nucleation rate will be affected based on how fast the pressure drops, or based on the pressure drop rate. The effect of the pressure drop rate on cell nucleation is as follows: the faster the pressure drop, the more that cells are nucleated [13]. Since the higher pressure drop rate requires a shorter time period, the already nucleated cells do not have a chance to grow a great deal. Therefore, more gas is utilized for cell nucleation and less is used for cell growth. As a result, high cell density foams or microcellular foams can be produced with high pressure drop rate dies.

The other type of cell nucleation is heterogeneous cell nucleation that is promoted at some preferred sites. Although the mechanism of heterogeneous cell nucleation in the polymer

foaming process has not been thoroughly elucidated due to its complexity, it is well known that cell population density in the foam structure can be significantly enhanced by blending some fillers [14]. In many cases, foams with some additives or fillers have higher cell density compared to those without additives [15]. However, the fundamental studies on the nucleation enhancement behavior with these additives have not been investigated in depth. Chen *et al.* [16] from Trexel Inc., investigated the mechanism of heterogeneous nucleation with filled polymers. The hypothesis of this process is that the undissolved gas between the polymer and the additives creates cells when the system pressure drops during the foaming process. Within the heterogeneous nucleation theory, certain sites or spots in the polymer matrix which contain undissolved gas may become cells, provided that the size of the spots is larger than the following critical value [16]:

$$r = \frac{2\sigma}{\Delta p} \tag{2.8}$$

where r is critical radius, σ is the surface tension and Δp is the pressure difference between the bubble and the melt. Micro-pores on the polymer-additive interface can act as cracks or defects. During the mixing process, the polymer melt may not be able to fill these micro-pores and gaps between two phases completely due to the surface tension. From the above equation, it is evident that the surface tension force increases as the radius, r, becomes smaller. Therefore, the pores cannot be filled, although the pressure difference between the polymer melt and micro-pores is larger. This creates some space for the gas to accumulate, thereby yielding cell nucleation. It was experimentally verified that a certain amount of gas accumulates at the polymer-additive interface and that the spots where gas accumulates generate cells if the size of the spots is larger than the critical value. This explains why heterogeneous nucleation generally requires much less

gas to produce fine-celled structures compared to homogeneous nucleation. The rate at which the bubbles nucleate heterogeneously is given by the following equation [16]:

$$N_1 = C_1 f_1 \exp(\frac{-\Delta G^*_{het}}{kT}) \tag{2.9}$$

where C_1 is the concentration of gas molecules, f_1 is the frequency factor of gas molecules joining the nucleus, k is the Boltzman's constant, and T is the temperature in K. ΔG^*_{het} is Gibbs free energy and can be expressed for heterogeneous nucleation, which occurs at smooth planar surfaces as follows (see Figure 2.1 (a)):

$$\Delta G^*_{het} = \frac{16\pi\gamma^3_{bp}}{3\Delta P^2} F(\theta_c) \tag{2.10}$$

where γ^3_{bp} is the surface energy of the polymer-bubble interface, ΔP is the gas pressure used to diffuse the gas into the polymer. $F(\theta_c)$, which is the reduction of energy due to the inclusion of additives (nucleants), can be expressed as follows:

$$F(\theta_c) = (\frac{1}{4})(2 + \cos\theta)(1 - \cos\theta)^2 \tag{2.11}$$

where θ_c is the contact angle of the polymer-additive gas interface.

As for the polymeric foaming processes, the surface geometry of the nucleating sites, which depends on the nucleating agents themselves, the presence of unknown additives or impurities and the nature of the internal walls of equipment, varies from one site to another. Therefore, instead of assuming that all nucleating sites are either smooth planar surfaces, observable cell nucleation can take place in conical cavities that exhibit geometries consistent with the image presented in Figure 2.1 (b) where the semiconical angles, β are randomly

distributed between 0 and 90° at different nucleating sites. In this case, $F(\theta_c,\beta)$ is the reduction of energy, which can be expressed as follows [17]

$$F(\theta_c,\beta)=\frac{1}{4}[2-2\sin(\theta_c-\beta)+\frac{\cos\theta_c\cos^2(\theta_c-\beta)}{\sin\beta}] \tag{2.12}$$

As the phase boundaries between the additive and the polymer matrix have a lower free energy barrier for nucleation than homogeneous nucleation, nucleation is more likely to occur at these sites. The number of cells nucleated can be controlled by the amount of additives [18,19]. Also, if the additive particle size is fine graded (less than a micron) and well dispersed in the polymer matrix, a uniformly distributed microcell structure can be produced [18]. Lee *et al.* [20] examined the gas absorption behavior of polymer systems to explain heterogeneous nucleation in mineral filled polymers: HDPE with/without talc, and PVC with/without $CaCO_3$. It was suggested that the accumulated gas in the filler-polymer interface helps to create cells in the foaming process. Ramesh *et al.* [21] developed a model for heterogeneous nucleation in the blend of PS and high impact polystyrene (HIPS) based on the presence of microvoids.

2.1.3.3. Cell Growth

Once the numerous fine cells are nucleated, most of them can continue to grow because of gas diffusion from the polymer matrix. Since the pressure inside the cells is greater than the surrounding pressure, cells tend to grow so as to decrease the pressure difference between the inside and the outside [22]. The cell growth mechanism is affected by the viscosity, diffusion coefficient, gas concentration, and the number of nucleated cells. The temperature can control the amount of cell growth, which then affects two important parameters: diffusivity and melt viscosity. For instance, if the temperature decreases, the diffusivity of gas decreases and the melt

viscosity of the matrix increases, thus, decreasing the cell growth rate. In the foaming process, maintaining the gas in the polymer matrix by close temperature control is essential for achieving good cell growth and thus, high volume expansion. In microcellular foams, because the cell size is very small and the cell density is very high, the cell wall thickness separating the two cells is smaller and the rate of growth is faster than in conventional foams.

Nevertheless, this may also cause cell coalescence, which is not desirable [23]. If the cells coalesce during cell growth, the initial cell density will be deteriorated. As nucleated cells grow, adjacent cells will begin to touch each other. These contiguous cells tend to coalesce because the total free energy is lowered by reducing the surface area of cells via cell coalescence [24]. It may be noted that the shear field generated during the shaping process tends to stretch nucleated bubbles, which further accelerates cell coalescence [25]. When the cell density is deteriorated, the mechanical and thermal properties are deteriorated as well. Although Baldwin *et al.* [26] attempted to prevent cell coalescence in the die by pressurizing the nucleated polymer solution during shaping, the extruded foam structure showed that many adjacent cells were coalesced and that the cell density was deteriorated. Considering the difficulty of maintaining high backpressure in the shaping die in case of a large cross section of extruded foam, it may not be realistic to prevent cell coalescence by controlling the pressure alone in the shaping die. Park *et al.* [25] proposed a method of suppressing cell coalescence by increasing the melt strength of polymer via temperature control in microcellular extrusion processing. The melt strength, by definition, may be treated as a degree of resistance to the extensional flow of the cell wall during the drainage of polymer in the cell wall when volume expansion takes place. Therefore, the cell wall stability can improve when the melt strength increases [27].

2.2. Batch Processing

As for the batch process, a polymer sample is first loaded in a high-pressure chamber where the sample can be saturated with an inert gas (such as CO_2 or N_2) under high pressure at ambient temperatures. A thermodynamic instability is then induced by rapidly lowering the solubility of the gas in the polymer. This is accomplished by releasing the pressure and heating the sample. This expansion drives the nucleation of a large number of microcells and the nucleated cells grow to produce the foam expansion. Because of the low rate of gas diffusion into the polymer at room temperature, an exceptionally long time is required for the saturation of the polymer with gas, which is the major disadvantage of the batch process.

The batch foaming process used to generate cellular foamed structures in the composites is not likely to be implemented in the industrial production of foams because it is not cost effective. The microcellular batch foaming process is time-consuming because of the multiple steps in the production of foamed samples [28]. In order to overcome the shortcomings of the batch process, a cost-effective, continuous microcellular was developed based on the same concept of thermodynamic instability that is found in the batch process.

2.3. Extrusion Foaming

One of the most important features of extrusion foaming is that polymer foams can be manufactured in a continuous process unlike batch foaming. It is well known that extrusion foaming have relatively higher productivity than batch foaming. As a blowing agent for extrusion foaming, CBA or PBA can be used depending on target foam properties as well as material characteristics. Compared to CBA, the PBA-based processing (such as environmentally friendly CO_2 and N_2) does not have decomposition temperature limitations and as such, can be

processed below the critical temperatures. Furthermore, it involves lower cost, and in general, can produce better cell morphology.

As shown in Figure 2, there are several basic steps for continuous extrusion foaming with a PBA: (a) uniform formation of a polymer/gas solution, (b) cell nucleation, (c) cell growth, and (d) timely solidification of the polymer melt. Cell nucleation occurs in a rapid-pressure-drop nucleation die [29]. The generation of a large number of bubble nuclei inside the polymer melt can be achieved by subjecting the polymer/gas solution to a thermodynamic instability. The thermodynamic instability can be induced by lowering the solubility of gas in the solution and by introducing a rapid pressure drop, which results in the nucleation of a large quantity of micro-cells. Cell nucleation is a very critical step, as it directly influences the number of cells created in the polymer matrix. The nucleated cells continue to grow upon exiting the die and cell growth stops either when all the gas dissolved in the plastic matrix is depleted or when the matrix becomes too stiff due to cooling, to allow further growth. There are two critical issues involved in cell growth: cell coalescence and cell collapse. Park and Behravesh [30] developed effective strategies that can prevent cell coalescence and gas escape in the cell growth stage. Cell coalescence can be suppressed by cooling the polymer/gas solution homogeneously, which increases the melt strength. Whereas, gas escape can be controlled by cooling the surface of the extrudate to form a solid skin layer, thereby, blocking the gas from escaping from the polymer. When the polymer melt is extruded out of the die and its temperature decreases, it will solidify through glassification or crystallization. Timely solidification is important, for a delayed solidification may result in gas loss, whereas solidification that is too fast will not produce a desired volume expansion ratio (or density reduction) [31].

- Theory of Filamentary Die Design in Foam Extrusion

The geometries of the filamentary dies, i.e. the die diameter and the die length induce different die pressures and different pressure drop rates, and consequently, different final foam structures. Xu et al. [32] designed three interchangeable groups of 9 dies with the same pressure or the same pressure drop rate. They assumed that the polymer melt was described by a "power law model" and that the theoretical die pressure and pressure drop rate are calculated using Equations 2.13~2.15 [33].

$$P_{die} = -2m\frac{L}{R^{3n+1}}\left[\left(3+\frac{1}{n}\right)\frac{Q}{\pi}\right]^{n} \tag{2.13}$$

$$t_{residence} \approx \frac{L}{v_{avg}} = \frac{L}{Q/\pi R^2} = \frac{\pi R^2 L}{Q} \tag{2.14}$$

$$\frac{dp}{dt} \approx \frac{P_{die}}{t_{residence}} = -2m\left(3+\frac{1}{n}\right)^{n}\left(\frac{Q}{\pi R^2}\right)^{n+1} \tag{2.15}$$

Equation 2.13 calculates the pressure drop along the capillary die land with a constant cross section; Equation 2.14 calculates the average residence time inside the capillary and Equation 2.15, obtained by dividing Equation 2.13 over Equation 2.14, calculates the pressure drop rate.

- Governing Mechanism of Volume Expansion

Naguib et al. carefully analyzed experimental results of extrusion foaming at various processing conditions. They concluded that the final volume expansion ratio of extruded PP foams blown with n-butane was governed either by the loss of the blowing agent through the foam skin or the crystallization of polymer matrix [34].

The diffusivity of blowing agents at elevated temperatures is very high. Therefore, gas can easily escape from the extruded foam because of its higher diffusivity at elevated temperatures. In addition, as the cell expansion increases, the thickness of the cell wall decreases and the resulting rate of gas diffusion between cells increases. Consequently, the rate of gas escape from the foam to the environment increases. Gas escape through the thin cell walls decreases the amount of gas that is available for the growth of cells, resulting in lowered expansion. Moreover, if the cells do not solidify quickly enough, they tend to shrink due to loss of gas through the foam skin, causing overall foam contraction. This indicates that the gas loss phenomena are a dominant factor that constrains the volume expansion when the melt temperature is high. This mechanism is schematically shown in Figure 3.

Another critical factor that affects the maximum expansion ratio in plastic foam processing is the crystallization behavior of semi-crystalline materials. Semi-crystalline polymer melt, such as PP, solidifies at the moment of crystallization during cooling. Therefore, the foam structure solidifies at the crystallization temperature during the foaming process. If the crystallization occurs in the primitive stage of foaming, i.e., before the dissolved blowing agent fully diffuses out of the plastic matrix and into the nucleated cells, then the foam cannot fully expand. Therefore, in order to achieve the maximum volume expansion ratio, the crystallization (or solidification) should not occur before all of the dissolved gas diffuses out into the nucleated cells. Upon exiting the die, the temperature of melt decreases due to external cooling outside the die and the cooling effect which is attributed to isentropic expansion of the blowing gases. Thus, the processing temperature at the die determines the time for the solidifying of the polymer melt. Therefore, in order to provide adequate time for the gas to diffuse into the polymer matrix, the processing temperature should be sufficiently high. It should be noted that if the processing

temperature is too close to the crystallization temperature, the polymer melt would solidify too quickly before the foam has expanded fully, as shown in the initial section of Figure 3.

This indicates that there is an optimum processing temperature for achieving maximum expansion as shown in the middle section of Figure 3. If the melt temperature is too high, then the maximum volume expansion ratio is governed by gas loss and it will increase as the processing temperature decreases. If the melt temperature is too low, then the volume expansion ratio is governed by the solidification (i.e., the crystallization) behavior and it will increase as the temperature increases.

2.4. Structural Characterization of Polymer Foams

Thermoplastic foams are generally classified in terms of foam density, volume expansion ratio, and cell morphology. Foam density is one of the structural parameters that directly represent the density reduction of the unfoamed material. The foam density (ρ_f) can be calculated as:

$$\rho_f = \frac{M}{V} \tag{2.16}$$

where

M = the mass of foam sample, g

V = the volume of foam sample, cm^3

The foam density also can be determined by water volume displacement of a known mass of foam. Volume expansion ratio is also used to describe the volume change of foams, and it has an inverse relationship with the foam density as shown in Equation 2.17.

$$\rho_f = \frac{\rho}{\Phi} \tag{2.17}$$

where

Φ = the volume expansion ratio,

ρ_f = the density of foam sample, g/cm^3

ρ = the density of unfoamed sample, g/cm^3

In addition to using the volume expansion ratio, researchers also use void fraction (V_f) to describe the amount of void in the foam, and it is defined as:

$$V_f = 1 - \frac{\rho_f}{\rho} \tag{2.18}$$

where

V_f = the void fraction

ρ_f = the density of foam sample, g/cm^3

ρ = the density of unfoamed sample, g/cm^3

The foam density, volume expansion ratio, and void fraction are related to each other, and all are directly related to the material savings that results from the void volume that replaces the original material. Apart from the foam density and the volume expansion ratio, the cell geometry, such as, open versus closed-cell, greatly affects the properties of foams. Closed-cell foams are most suitable for thermal insulation, while open-cell foams are the best for acoustical insulation [35].

The cell population density, N_0, is defined as the number of cells per cubic centimeter relative to the unfoamed material, and it is calculated by Equation (2.17) and (2.18).

$$N_0 = (\frac{NM^2}{a})^{3/2}(\frac{1}{1-V_f}) \tag{2.18}$$

where N is the number of bubbles in the micrograph, a and M are the area and the magnification factor of the micrograph, respectively.

The classification and application of thermoplastic foams are closely related to the structure of foams (cell size, cell density, foam density or volume expansion ratio, closed or open cell). This is why the structural characterization of foams is significant in foam processing.

2.5. Solubility of Blowing Agents in Polymer

When a blowing agent dissolves in a polymer, the weight of the polymer increases because of the weight of the impregnated blowing agent. Therefore weighing the polymer in pressurized gas can allow us to know the solubility and diffusion coefficient of gas. The magnetic suspension balance (MSB) makes it possible to weigh samples under the high pressure and temperatures. To perform measurements precisely in the MSB, the weight of dissolved gas has to be measured by taking the buoyancy effect into account (Figure 4). The balance weight read-out at each equilibrium condition [pressure (P) and temperature (T)], was recorded as W (P, T). Hence, the amount of gas dissolved in the polymer at each condition (P, T), Wg, was calculated by employing Equation 2.19, where ρ_{gas} is the density of the gas and can be measured in-situ by the function of MSB; V_B is the volume of the sample holder (including the sample container and the measuring load coupling device) and can be measured using the buoyancy method with high-pressure gas; and V_P is the volume of the pure polymer sample at pressure P and temperature T, which can be calculated by evaluating the pure polymer's PVT equations. V_S is the swollen volume of the polymer/ gas mixture due to the gas dissolution [36].

$$W_g = W(P, T) - W(0, T) + \rho_{gas} (V_B + V_P + V_S) \quad (2.19)$$

According to the previous study, the solubility of CO_2 and N_2 in PS is totally different as shown in the Figure 5 [37]. At the same pressure, CO_2 shows much higher solubility than N_2 in PS. Accordingly, it is easier to obtain larger volume expansion ratio using CO_2 than N_2. On this account, CO_2 is frequently used for low density foams, whereas N_2 is used for high density foams. Due to the greater solubility, CO_2 can better plasticize polymers, which is more favorable in batch foaming as well as extrusion foaming.

- Solubility Enhancing Effect of PDMS

As shown in Figure 6, since poly(dimethylsiloxane) (PDMS) has a number of siloxane linkages that are highly flexible, its Tg and Tm are as low as around -120°C and -50°C respectively. Recent researches discovered that PDMS has much higher solubility of CO_2 than other commodity polymers (Figure 7) and that blending PDMS with PP could substantially enhance the overall solubility [38-40]. It is believed that the increased solubility is favorable for polymer foaming due to wider processing window. In fact, it was reported that PDMS could improve cell population density and volume expansion ratio [41].

2.6. Expandable Polystyrene (EPS) Bead Foam

Expandable Polystyrene (EPS) beads are unexpanded bead materials used for the steam chest molding for PS bead foam products. It is manufactured in the form of very small polystyrene beads of weight-average molecular weight that ranges between 160,000 and 260,000, and contains 4 to 7% of a blowing agent, which is usually n-pentane. The bead diameter can vary between 0.007 inches (0.2 mm) to 0.12 inches (3.0 mm). Since introduced onto the market in the

1950s [42], EPS has been widely used in many applications due to many advantages such as low density, thermal and acoustic insulation, consistent performance and so on. EPS products have various density ranges. In the low-density range (0.008 to 0.016 g/cm^3), EPS is used on boats as floatation devices; in packaging as an energy absorber; in buildings as insulation; and in other applications as a moisture barrier. In the middle-density range (0.016 to 0.064 g/cm^3), the material is employed in packaging as a structural support as well as an energy absorber; in construction for applications such as concrete forms; in the foundry industry to create mold patterns; in various industries to manufacture insulated containers of all sizes and shapes; and in transportation as materials-handling pallets [43]. Figure 2.8 shows a variety of application areas of EPS bead foams.

A schematic of the production process of the conventional EPS beads and the bead foams is shown in Figure 2.9. The expandable polystyrene beads containing n-pentane are manufactured via a suspension polymerization process using styrene monomers. N-pentane is added as part of the polymerization process so that PS and the blowing agent can make homogeneous phase at the end of the polymerization reaction. After molding companies purchase the EPS beads whose bulk density is around 0.64 g/cm^3, the expandable beads are pre-expanded to become low-density pre-foams using steam in a pre-expander, stabilized in silo under atmospheric conditions from several to twenty-four hours (the maturing phase), and steam-molded into EPS foam products using a steam chest molding machine (Figure 2.10). After the mold cavity of steam chest molding machine is filled with pre-expanded PS beads, steam whose temperature is about 110°C should be injected into the mold. At this moment, the remnant n-pentane in the beads evaporates and further expands so that the PS beads can form strong bonding among beads by forming inter-penetrating networks.

2.7. Expanded Polypropylene (EPP) Bead Foam

Expanded polypropylene (EPP) beads are foamed plastic pellets that can be used for steam chest molding. Unlike expandable PS beads, EPP beads mean highly expanded PP beads literally. Therefore EPP doesn't contain any blowing agents in the beads. Moreover, the very low bulk density of EPP beads brings about high transportation cost. As a matter of fact, EPP beads are three times more expensive than EPS beads in industry. However, since EPP bead foam has many advantages such as excellent impact resistance, energy absorption, thermal insulation, recyclability, chemical and water resistance [44], it has been widely used in various industry areas; automotive parts, packaging, construction materials and toys as displayed in Figure 2.11. EPP bead foam can provide highly resilient property as well as diversified geometry with very low density. Conventional manufacturing process of EPP beads is a batch foaming process in which solid polypropylene (PP) pellets should be impregnated with a physical blowing agent for about 1 hour [45-49]. The low efficiency of the batch foaming process is one of the reasons why EPP beads are even more expensive than EPS beads. Figure 2.12 shows a typical impregnation batch process. In this process, PP resins and the required additives (nucleating agent, compatibilizer, plasticizer, etc.) are compounded in an extruder and are granulated into pellets. These pellets are then put into a stirred autoclave with a dispersion medium (e.g., water), dispersing agent (e.g., tricalcium phospate), surfactants (e.g., sodium dodecylarysulfonate) and a physical blowing agent at an elevated pressure and at a temperature above the melting temperature of PP. After appropriate processing time has elapsed to let the blowing agent impregnate and saturate the pellets, the pressure is released to expand the pellets. Then the expanded beads are cooled, washed and packed. These highly expanded EPP pellets are sold and

transported to steam-molding manufacturers. The steam chest molding machine (Figure 2.13) can be used to produce the final bead foams.

2.8. References

[1] S. T. Lee, *Foam Extrusion-Principles and Practice*, Technomic Publishing Company Inc., PA (2000)

[2] K. C. Frich, and J. H. Saunders, *Plastic Foams*, Part I, Marcel Dekker Inc., N.Y. (1972)

[3] R. A. Gorski, R. B. Ramsey, and K. T. Dishart, *J. Cell. Plast.,* 22, 21-52 (1986)

[4] F. J. Dwyer, L. M. Zwolinski, and K. M. Thrun, *Plas. Eng.,* May, 29-32 (1990)

[5] C. B. Park, and N. P. Suh, *Polym. Eng. Sci.* 36, 34 (1996)

[6] C. B. Park, A. H. Behravesh, and R. D. Venter, *Cell. Polym.* 17, 309 (1998)

[7] C. B. Park, D. F. Baldwin, and N. P. Suh, *ASME, Cellular and Microcellular Materials*, 53, 109-124 (1994)

[8] J. Crank, and G. S. Park, *Diffusion in Polymers*, Academic Press Inc., New York, N.Y. (1968)

[9] D. W. Van Krevelen, *Properties of Polymers*, Elsevier Scientific Publishers Company (1990)

[10] C. B. Park, and N. P. Suh, ASME Trans., *J. Manuf. Sci. Eng.,* 118, 639-645 (1996)

[11] J. S. Colton, and N. P. Suh, Polym. Eng. Sci., 27, 493-499 (1987)

[12] J. H. Han, and C. D. Han, J. Polym. Sci. Part B: Polymer Physics, 28, 743 (1990).

[13] C. B. Park, D. F. Baldwin, and N. P. Suh, *Polym. Eng. Sci.,* 35, 432-440 (1995)

[14] J. Throne, *Thermal plastic foams*, Chapter 6, Sherwood Publishers (1996)

[15] E. A. Columbo, *Sciece and Technology of Polymer Processing*, book edited by N. P. Suh and N. H. Sung, MIT press, 394 (1979)

[16] L. Chen, and H. Sheth, *Initial Stages of Bubble Growth During Foaming Process*, TREXEL INC.

[17] S. N. Leung, C. B. Park, and H. Li, *Plast Rubb Comp*, 35, 93 (2006)

[18] J. S. Colton, *Plast. Eng.,* 44, 53-55 (1988)

[19] A. H. Behravesh, C. B. Park, L. K. Cheung, and R. D. Venter, *J. Vinyl Addit. Technol,* 2, 349-357 (1996)

[20] C. Lee, S. H. Sheth, and R. Kim, *Polym. Eng. Sci.,* 41, 990 (2001)

[21] N. S. Ramesh, D. H. Rasmussen, and G. A. Campbell, *Polym. Eng. Sci.,* 34, 1685 (2001)

[22] D. Klempner, and K. C. Frisch, *Handbook of Polymeric Foams and Foam Technology*, Hanser, N. Y., 8 (1991)

[23] S. T. Lee, and N. S. Ramesh, *Cellular and Microcellular Materials,* edited by V. Kumar and K. A. Seeler, 76, 71-80 (1996)

[24] D. Klempner, and K. C. Frisch, *Handbook of Polymeric Foams and Foam Technology*, Hanser, N. Y., 5 (1991)

[25] C. B. Park, A.H. Behravesh and R. D. Venter, *Polymeric Foam: Science and Technology*, K. Khemani, ed., Chap. 8, ACS, Washington (1997)

[26] D. F. Baldwin, C. B. Park and N. S. Suh, *Polym. Eng. Sci.,* 36, 1446 (1996)

[27] K. C. Frisch and J. H. Saunders, *Plastic Foams,* Vol.1, Marcel Deckker, New York (1972)

[28] L. M. Matuana, R. Rachtanapun, and S. E. M. Selke, *J. Appl. Polym. Sci.* 88, 2842 (2003)

[29] C. B. Park, D. F. Baldwin, and N. P. Suh, *Polym. Eng. Sci.,* 35, 432-440 (1995)

[30] C. B. Park, A. H. Behravesh, and R. D. Venter, *Polym. Eng. Sci.,* 38, 1812 (1998)

[31] A. H. Behravesh, C. B. Park, and R. D. Venter, *Cellular Polymers,* 17, 309 (1998)

[32] X. Xu, C. B. Park, D. Xu, and R. Pop-Iliev, *Polym Eng Sci* 43, 1378 (2003)

[33] W. Michaeli, *Extrusion Dies for Plastics and Rubber*, Hanser, 52 (2003)

[34] H. E. Naguib, C. B. Park, P. C. Lee, and D. Xu, *J. Polym Eng* 26, 6 (2006)

[35] A. H. Landrock, *Handbook of Plastic Foams: Types, Properties, Manufacture, and Application*, Noyes Publications, 206 (1995)

[36] G. Li, H. Li, J. Wang, and C. B. Park, *Cellular Polymers*, 25, 4 (2006)

[37] G. Li, F. Gunkel, J. Wang, and C. B. Park, and Altstädt, V., *J. Appl. Polym. Sci*., 103, 5 (2007)

[38] L. J. Gerhardt, C. W. Manke, and E. J. Gulari, J. Polym. Sci. B: *Polym. Phy.*, 35, 523 (1997)

[39] T. A. Davidson, T. A. Jones, D. A. Canelas, and J. M. DeSimone, ACS *Polym. Prepr.*, 39, 463 (1998)

[40] P. Spitael , C.W. Macosko, and R. B. McClurg, *Macromol.* 37, 6874 (2004)

[41] Q. Wuh, C. B. Park, N. Zhou, *Annual Technical Conference - ANTEC,* Conference Proceedings 2, 837-843 (2009)

[42] F. Stastiny and R. Gaeth, U.S. Patent 2,681,321- Detailed description of the invention (1954)

[43] A. H. Landrock, Chap. 3 in "*Handbook of Plastic Foams*", edit by A.H. Landrock, 236-239, William Andrew Publishing: Noyes (1995)

[44] Modern Plastic Industry Co., Ltd., Korea (http://www.mpic.co.kr/eng/info/epp_1.asp)

[45] Fagerdala Deutschland GmbH, German (http://www.fagerdala.de)

[46] F. Braun, G. Gluck, K. Hahn, I. De Grave, and H. Tatzel, U.S. Patent 6,677,040 - Detailed description of the invention (2004)

[47] W. Kogel, I. De Grave, K. Hahn and J. Fischer, U.S. Patent 5,925,686 - Example 1 (1999)

[48] S. Yoshimura, T. Yamaguchi, M. Kanbe, and H. Kuwabara, U.S. Patent 4,704,239 – Example 1-3 (1987)

[49] H. Sasaki, M. Sakaguchi, M. Akiyama, and H. Tokoro, U.S. Patent 6,077,875 – Detailed Description of the Preferred Embodiments (2000)

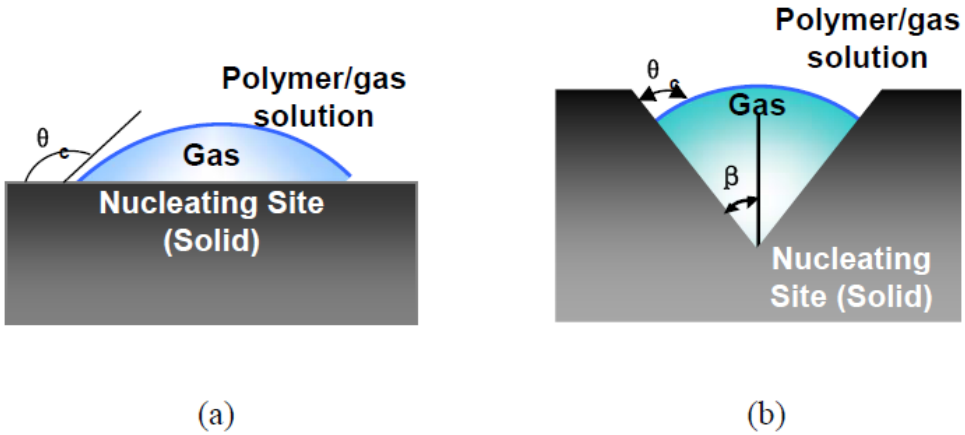

Figure 2.1. Cell nucleations on (a) smooth planar surface and (b) in a conical cavity [16].

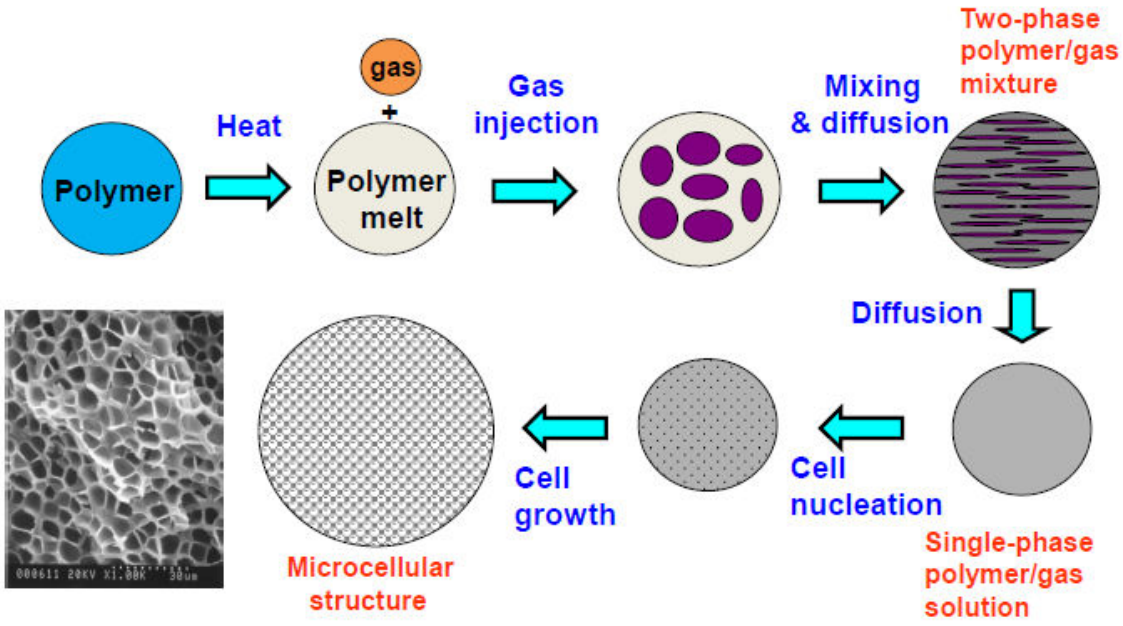

Figure 2.2. Steps of continuous extrusion foaming process.

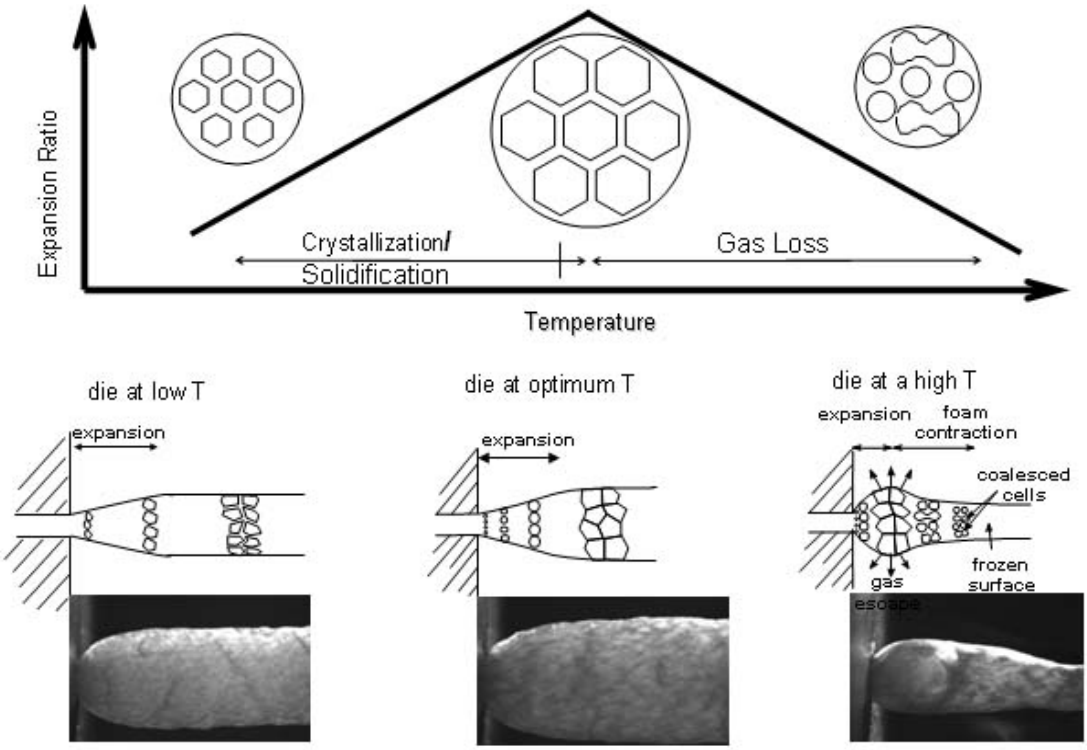

Figure 2.3. Effect of gas loss and crystallization on volume expansion [33].

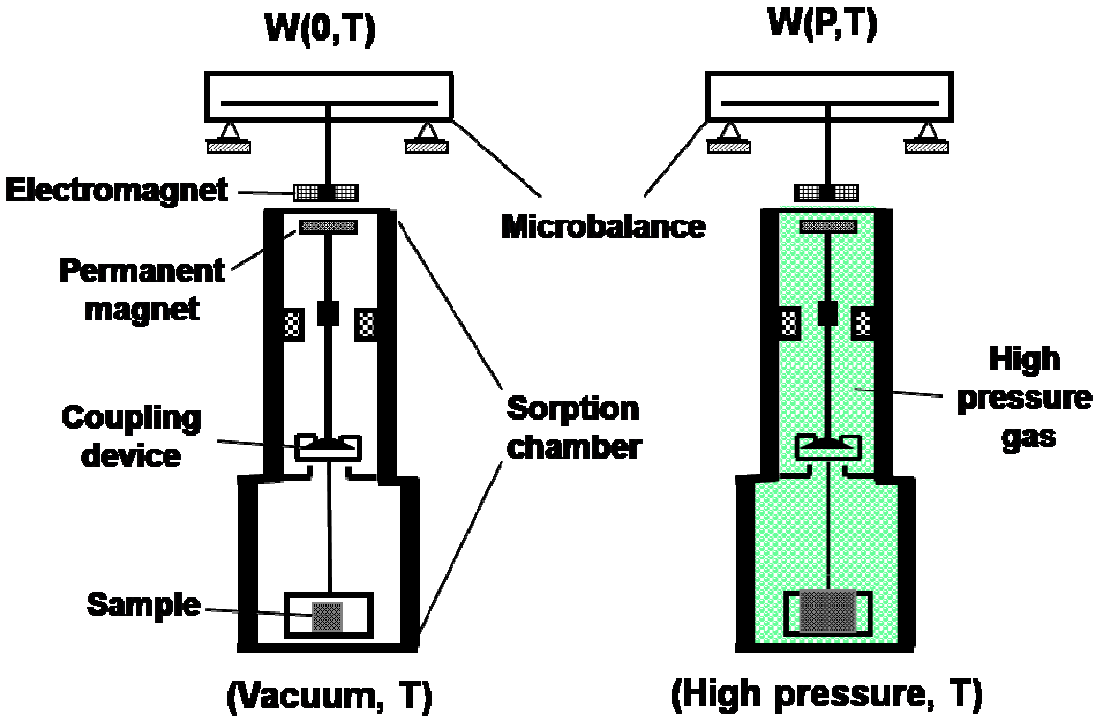

Figure 2.4. Schematic of magnetic suspension balance (MSB) [35].

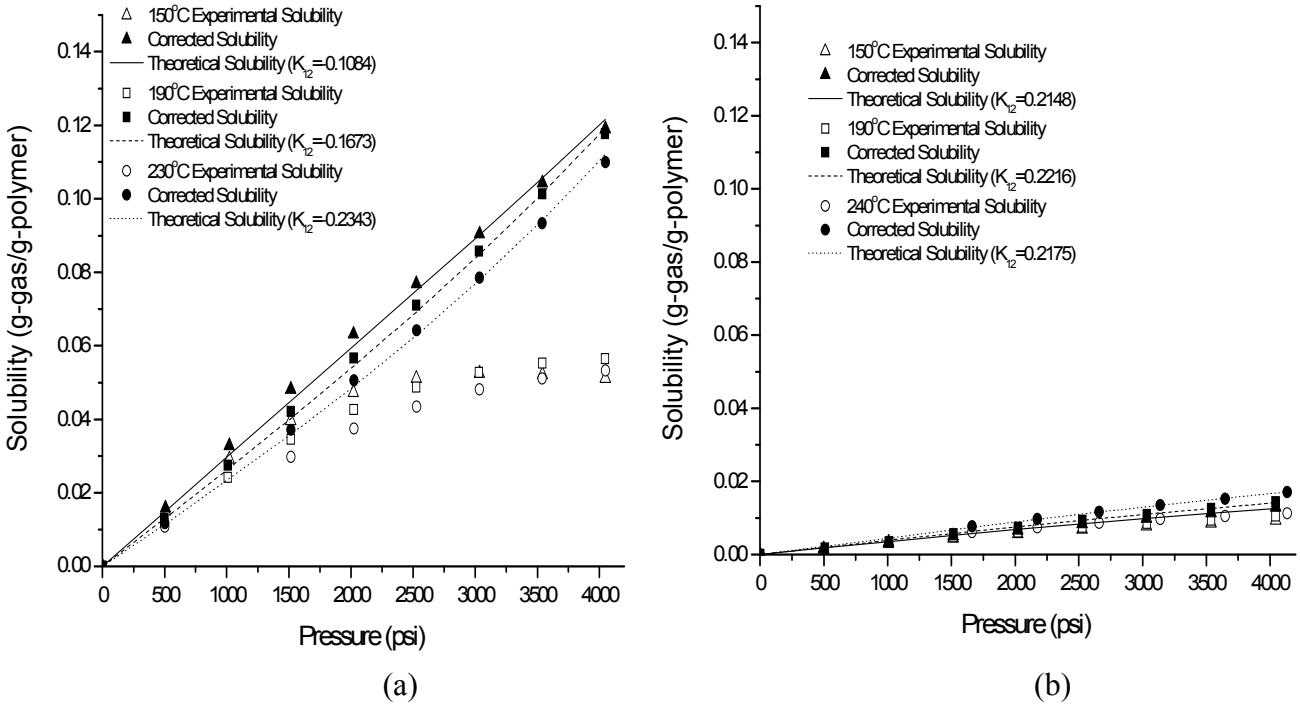

Figure 2.5. Solubility of (a) CO_2 and (b) N_2 in PS (Dow Chem Styron D685) [36].

$$(CH_3)_3SiO[Si(CH_3)_2O]_nSi(CH_3)_3$$

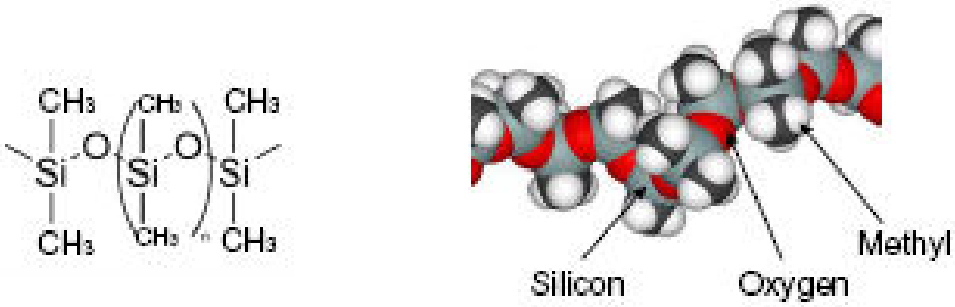

Figure 2.6. Chemical structure of poly(dimethylsiloxane) (PDMS).

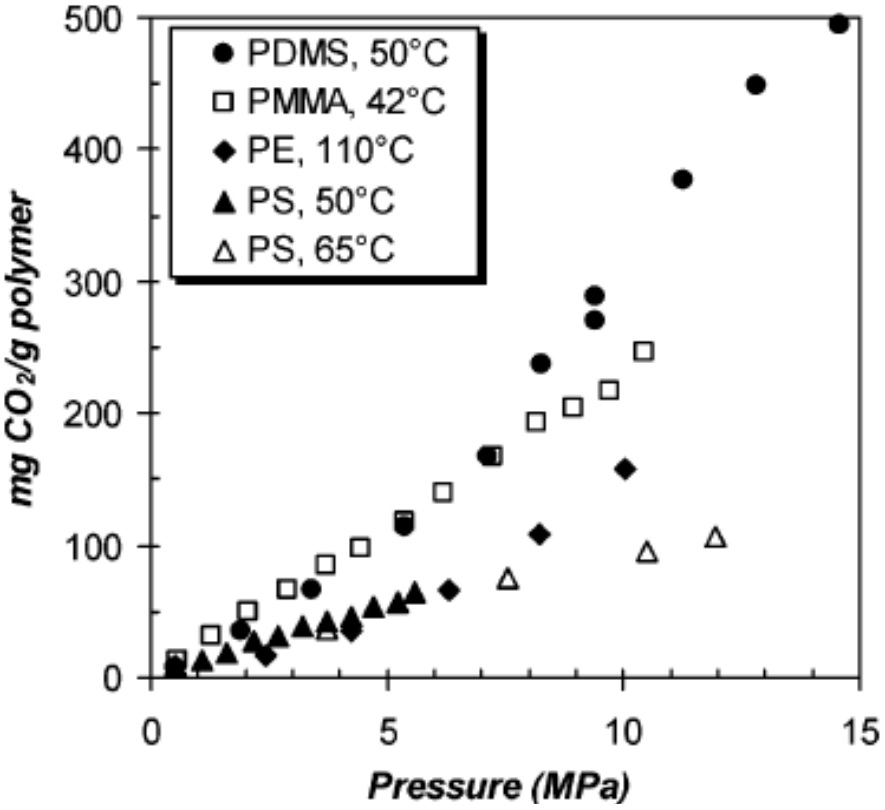

Figure 2.7. Solubility of CO2 for various polymers and PDMS [39].

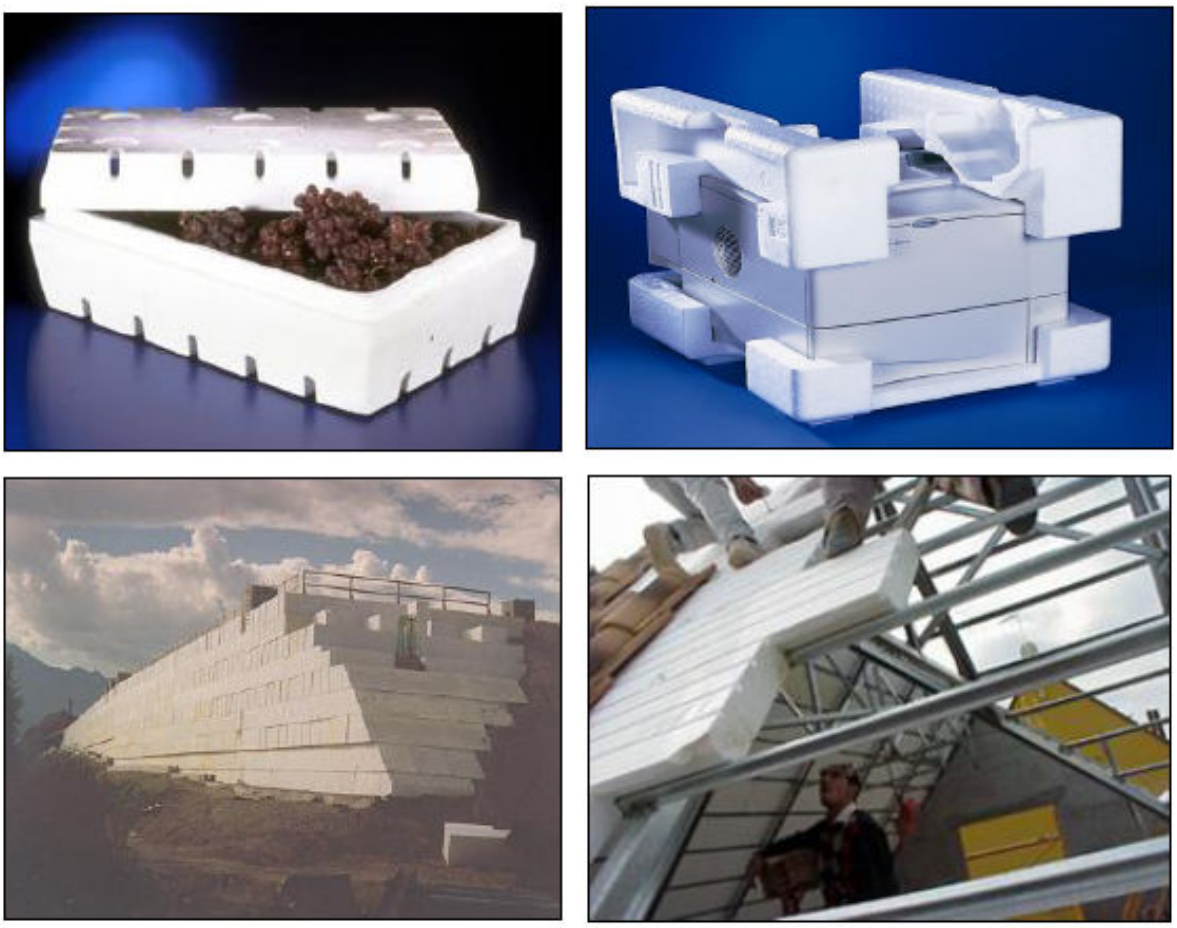

Figure. 2.8. Application areas of EPS bead foams.

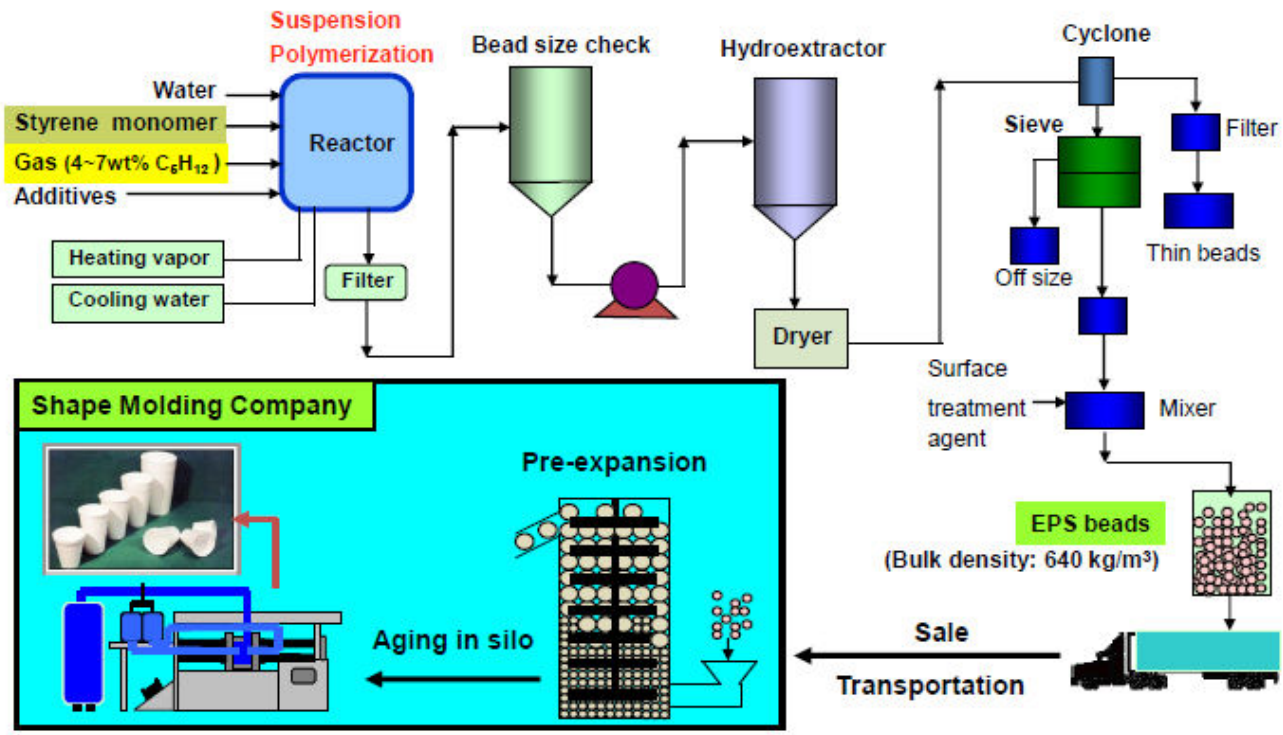

Figure 2.9. Conventional manufacturing process of EPS beads and EPS bead foams.

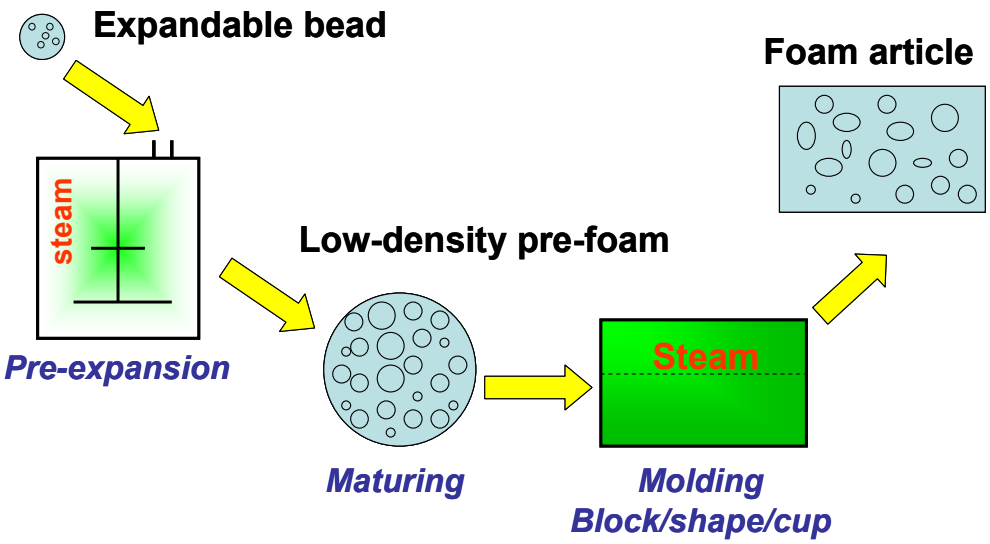

Figure 2.10. Pre-expansion of expandable PS beads, maturing and steam chest molding.

Figure 2.11. Application areas of EPP bead foams.

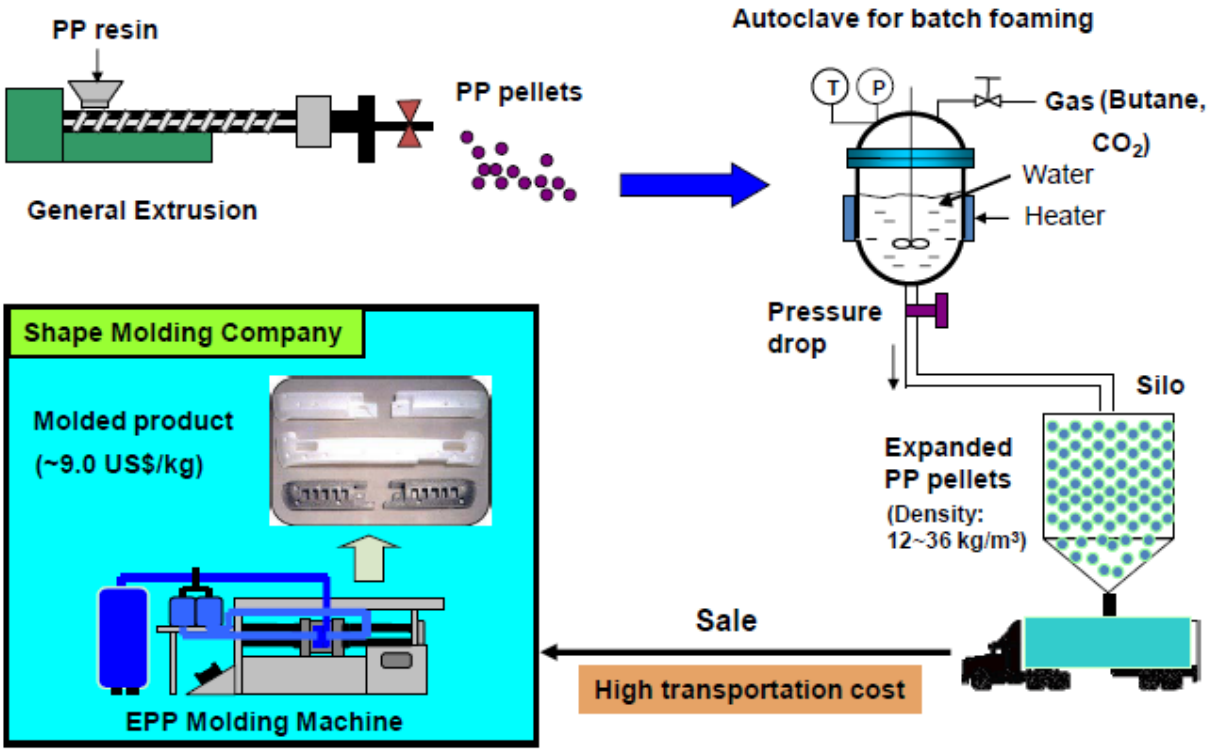

Figure 2.12. Conventional manufacturing process of EPP beads and EPP bead foams.

Figure 2.13. Steam chest molding machine (DABO Precision Ltd, Korea).

Chapter 3

Gas Transport Phenomenon of N-Pentane in Polystyrene and Polypropylene

3.1. Introduction

For more than 50 years, expandable polystyrene (EPS) bead foam has been widely used for structural foam molding products such as construction panels, food containers, packaging materials and so on. It is primarily because polystyrene has high melt strength in a wide temperature range as well as low diffusivity of blowing agent in PS. In particular the low gas diffusivity in PS is highly favorable for keeping a blowing agent, which is generally n-pentane, in PS beads for relatively longer time [1]. However, although PP foams have excellent properties such as high resilience, chemical resistance and recyclability, there have been no commercialized expandable polypropylene (EPP) beads that can keep any blowing agents in the solid PP matrix for a certain time needed for transportation as well as storage. It is believed that the primary reason is the high diffusion rate of blowing agents in the PP at ambient condition. The large mobility of n-pentane naturally can make it difficult for PP beads to maintain the blowing agent

for a certain period. Although in reality expanded polypropylene (EPP) beads for bead foam are commercially available, they are even more expensive than EPS beads due to the high transportation cost from their large volume-to-weight ratio. This is why it is meaningful to investigate sorption/desorption behaviors of a penetrant in polymers. It is true that those behaviors are related to several parameters such as diffusivity, solubility, temperature, and pressure [2].

When it comes to diffusivity, it has been claimed that only penetrants with very small molecules have concentration-independent diffusion coefficients. On the other hand, the diffusion behavior of large organic molecules can be characterized as concentration-dependent diffusivity [3-10]. Figure 3.1 shows the diffusivity of ethyl benzene in PS depending on the ethyl benzene concentration [4]. Similarly many studies on concentration dependency of diffusivity have been presented for a variety of polymer/penetrant systems [11-19]. However, little research has been conducted regarding sorption/desorption of n-pentane in polystyrene as well as polypropylene. This study commenced with the background story aiming at quantifying the concentration -dependent diffusivity and solubility of n-pentane in the two commodity polymers. In addition, computational modeling and numerical analysis were carried out.

3.2. Theoretical Background

Basically this study was based on the assumption that diffusion of n-pentane in PS and PP sheets would be one-dimensional, isothermal, free from chemical reactions, and independent of the effect of pressure on the total density of the system [7, 20]. Moreover the phase volume change caused by mass transfer was neglected. Therefore the sorption/desorption of n-pentane in

PS and PP can be governed by Fick's law of diffusion in the Cartesian coordinate system as follows:

$$\frac{\partial C}{\partial t} = \frac{\partial}{\partial x}(D\frac{\partial C}{\partial x}) \tag{3.1}$$

where *C(x, t)* stands for the concentration in the position of *x* apart from the centerline of the sample at time *t*; and *D(c, t)* represents the concentration-dependent diffusivity. Due to the symmetry of the sheet samples, the solution of Equation (3.1) is subjected to the following initial and boundary conditions:

$$C(x, t = 0) = C_m \tag{3.2}$$

$$\left.\frac{\partial C}{\partial x}\right|_{x=0,t} = 0 \tag{3.3}$$

$$C(x = L, t) = C_0 \tag{3.4}$$

where C_m and C_0 respectively represent the initial concentration and the saturation concentration which the sheet sample can finally reach. When the diffusivity is independent of the penetrant concentration, the concentration distribution can be analytically derived as the following equation [3]:

$$\frac{C - C_0}{C_m - C_0} = -\frac{4}{\pi}\sum_{n=1}^{\infty}\frac{\cos(n\pi)}{2n-1}e^{-((2n-1)\pi/2L)^2 Dt}\cos\frac{(2n-1)\pi x}{2L} \tag{3.5}$$

Transportation of penetrant amount in the samples will be understood accordingly. Specifically, the ratio of the penetrant increment at time *t* (M_t) to that at infinite time (M_∞) is given by [5]

$$\frac{M_t}{M_\infty} = 1 - \sum_{n=1}^{\infty}\frac{8}{(2n+1)^2\pi^2}\exp\left[\frac{-D(2n+1)^2\pi^2 t}{4L^2}\right] \tag{3.6}$$

Figures 3.2 and 3.3 illustrate the sorption and desorption process, respectively. For the sorption of penetrants, $C_m=0$. Thus, Equation (3.6) yields

$$\frac{M_t}{M_\infty} = 1 - e^{-(\pi/2L)^2 Dt} \tag{3.7}$$

For the desorption process, C_m is larger than C_0. By substituting M_∞ with M_0 and applying $C_0=0$ at the boundary, Equation (3.6) can be rearranged as

$$\frac{M_t}{M_0} = e^{-(\pi/2L)^2 Dt} \tag{3.8}$$

Numerical methods should be involved if diffusivity of penetrant in the polymer is related to the penetrant concentration. This is because the aforementioned analytic solution cannot be applied anymore. In this study, the Finite Different Method with an implicit scheme was employed to determine the concentration-dependent diffusivities.

3.3. Experimental

3.3.1. Materials

Polypropylene (WB-260) was supplied by Borealis. WB-260 was a branched propylene-ethylene random copolymer with a MFI of 2.5 g/10min at 230℃. Polystyrene (PS 1600) was donated by NOVA Chemicals. Its MFI was 5.5 g/10min at 230℃. N-pentane with a purity of 99.5%.was purchased from Sigma-Aldrich.

3.3.2. Sample Preparation

PS and PP were compression-molded to make thin films with a thickness of 0.30 ± 0.01mm using a hot-compressor at 200℃. The compression-molded films were cut into square pieces (4 cm x 4 cm) so that the sorption/desorption of n-pentane through side surfaces could be neglected.

3.3.3. Sorption and Desorption Experiment

The sorption experiments of PS and PP were conducted in different ways due to considerably different uptaking rates of the two polymers in liquid n-pentane. Since it took more than one month to saturate PS with n-pentane at ambient temperature and pressure, only five sheet samples were handled observing the weight gain. Specifically the weight of each PS sheet was measured by an electronic analytical balance at the beginning. The five PS sheets were then soaked into liquid n-pentane in a beaker. As time goes on, they were regularly taken out, weighed, and dropped back into n-pentane again.

When it comes to PP, since the uptaking speed was much faster than PS, 12 sheet samples were soaked into n-pentane at the same time after having been weighed. Subsequently the weight gain with time of each PP sheet was measured more frequently than PS. This experiment was put into practice with an assumption that diffusion and evaporation of n-pentane out of polymers could be effectively prevented while taking the samples out and dropping them back.

As to the desorption experiment, PS and PP sheet samples saturated with n-pentane were taken out of the liquid n-pentane and then put on a tray of an analytical balance to measure the weight loss of the samples along with time.

3.4. Results and Discussion

3.4.1. Sorption Profile and Solubility

The n-pentane sorption profiles of PS and PP in Figure 3.4 show that sorption rate of PP was much higher than that of PS as expected. Interestingly the beginning parts of the curves magnified in the embedded window reveal that the sorption profiles of the two polymers have typical S-shape curves in common, which is a characteristic of the sorption process with concentration-dependent diffusivity. At the very beginning of the sorption, the diffusivity and the sorption rate are very low. It is believed that the swelling effect of penetrants dissolved in polymers can more enhance the diffusivity therefore the sorption is consequently self-accelerated. As the penetrant concentration increases, the sorption force, *i.e.*, the difference between the saturation concentration and the current concentration, is getting smaller. Accordingly, the sorption rate becomes substantially lower as the concentration gets closer to the saturation concentration. In the case of amorphous polymers, it is known that the overshoot of sorption can occur due to the development of small microvoids in the unrelaxed glassy core [4, 8, 21-23]. However, PS in this work did not display the overshoot phenomenon, which is probably because the room-temperature sorption took such a long period (about a month) that all residual relaxation could be accomplished prior to the saturation. In contrast, a clear overshoot was observed in the PP sorption, which may be caused by additional crystallization during sorption process [9, 24-29].

At the end of the sorption, the solubilities of n-pentane in PS and PP were determined from the final weight gain. Results are summarized in Table 3.1. The solubility difference between the two polymers is not concerned because no more than 3 weight percents of blowing agents can make the polymer well foamed.

3.4.2. Desorption Profile

Desorption is a process of the evaporation of the penetrant from the polymer. Figure 3.5 illustrates the desorption curves using the square root of the time as the x-coordinate. Obviously, a considerable difference between the desorption results of PS and PP gradually appears, although the desorption rates of the penetrant are very high for both PS and PP in the first couple of days. The penetrant concentration in PP approaches zero after 3 days whereas PS stills maintains nearly 2% of n-pentane after 3 months. These desorption experiments at an ambient condition clearly demonstrated that it was impossible to manufacture expandable PP beads that could retain n-pentane for a while for transportation and storage as the conventional expandable PS beads could.

3.4.3. Computational Modeling

Since the desorption experiments were more accurate, the desorption profiles were selected for validation of computational modeling. While Equation (3.8) is utilized, the desorption curves are plotted in Figure 3.6, where 2L equals 0.03cm under a variety of diffusivities from 10^{-6} to 10^{-12} cm^2/s. Apparently, the experimental curves could not be well predicted through Equation (3.8) using the concentration-independent diffusivity. On this account, two diffusivity values, D_0 and D_1, were adopted in the analysis. They respectively correspond to the innate diffusivity and the diffusivity at saturation concentration. In detail D_0 and D_1 represent the diffusivities of the penetrant when the concentration in the polymer is 0% and 100% apiece. Based on the results of Kruger [2] and Ni [3] where linear relationship between diffusivity and penetrant concentration in a wide range of concentration was claimed,

this research formulated the diffusivity corresponding to the concentration fraction from 0 to 1 as follows:

$$D = D_1^c D_0^{1-c} \tag{3.9}$$

As diagrammed in Figure 3.7, this diffusivity has linear relationship with the concentration. Using this concentration-dependent diffusivity, the profile of M_t/M_0 with time could be solved numerically. During the programming, the layer number was selected as 20 in order to ensure sufficient accuracy. Since high diffusivity demands a small time step for good convergence, time steps for PS and PP were 0.01s and 0.001s, respectively. Through numerous trials, a compatible pair of D_0 and D_1 was eventually acquired. Figure 3.8 shows that the simulated profiles well corresponded to the experimental data especially when the penetrant concentration was greater than 30%. The calculated D_0 and D_1 for PS and PP are summarized in Table 3.2. Evidently, this approach is favorable to understand the relationship between diffusivity and concentration. Nevertheless, considerable deviation took place at the region of lower concentration than around 30%. This deviation is attributed to an error of the presumed diffusivity or unknown mechanisms related to the desorption process.

3.5. Summary

For the purpose of quantitatively analyzing the solubility and diffusivity of n-pentane for PS and PP at room temperature and atmospheric pressure, a series of sorption and desorption experiments were systematically executed. The resultant data demonstrated that n-pentane had high solubility in both PS and PP even though sorption and desorption of n-pentane in PP were

much faster than in PS. In this sense, it was clearly proven why expandable PP beads could not be commercialized in spite of the fact that expanded PP beads are even more expensive than expandable PS beads due to costly transportation and storage. Consequently it is believed that the traditional EPS technology can not directly apply to PP bead foams due to much inferior blowing agents-keeping capability of PP compared to PS.

The concentration-dependent diffusivities of n-pentane in PS and PP were numerically calculated. The simulated desorption profiles well accorded with the experimental data to a certain degree, because some deviation was shown when the concentration was less than about 30%.

3.6. References

[1] D. Klempner, and K. C. Frisch, *Handbook of Polymeric Foams and Foam Technology*; Hanser Verlag (1991)

[2] J. Crank, and G. S. Park, Diffusion in Polymers, Academic Press: London and New York (1968)

[3] K. M. Kruger, and G. Sadowski, *Macromolecules*, 38, 8408 (2005)

[4] J. L. Duda, Y. C. Ni, J. S. Vrentas, *J. Appl. Polym. Sci.*, 22: 3, 689 (1978)

[5] S. Areerat, et al. *Polym. Eng. Sci.*, 44:10, 1915 (2004)

[6] M. Tsige, and G. S. Grest, *J. Chemical Physics*, 120:6 2989 (2004)

[7] J. L. Duda, and J. S. Vrendas, *J. Polym Sci*.: Part A-2, 6, 675 (1968)

[8] B. R. Baird, H. B. Hopfenberg, V. T. Stannett, *Polym. Eng. Sci*., 11:4 274 (1971)

[9] C. J. Durning, W. R. Russel, *Polymer*, 26:1 131 (1985)

[10] S. Prager, E. Bagley, F. A. Long, *J. Am. Chem. Soc*., 75:5 1255 (1953)

[11] S.T. Ju, et al. *J. Appl. Polym. Sci*., 26, 3735 (1981)

[12] J. S. Vrentas, et al. *Macromolecules*, 19, 1718 (1986)

[13] S. K. Kailasam, et al. *Metall. Mater. Trans.* A, 30A:10 2605 (1996)

[14] N. Divinis, et al. AIChE J., 52:9 3029 (2006)

[15] W. R. Vieth, and K. J. Sladek, *J. Colloid Sci*. 20, 1014 (1965)

[16] W. J. Koros, and D. R. Paul. *J. Polym. Sci., Polym. Phys*. Ed. 14, 1903 (1976)

[17] S. A. Stern, and A. H. Meringo, D. *J. Polym. Sci., Polym. Phys*. Ed. 16, 735 (1978)

[18] Y. Sato, M. Yurugi, K. Fujiwara, S. Takishima, and H. Masuoka, *Fluid Phase Equilib.* 125, 129 (1996)

[19] O. Pfohl, C. Riesesell, R. Dohrn, *Fluid Phase Equilib.* 202, 289 (2002)

[20] R. F. Boyer, *Rubber Chem. Technol*. 36, 1303 (1963)

[21] E. W. Russell *Nature*, 165, 91 (1950)

[22] A. Peterlin. *Makromol. Chem.* 124, 136 (1969)

[23] T. Alfrey, E.F. Gurnee, and W. G. Lloyd, *J. Polym. Sci.* 12, 249 (1966)

[24] W. V. Titow, M. Braden, B. R. Currel, and R. J. Loneragen, *J. Appl. Polym. Sci.* 18, 867 (1974)

[25] E. Turska, W. Benecki, *J. Appl. Polym. Sci.* 23, 3489 (1979)

[26] R. Ware, S. Tirtowidjojo, and C. J. Cohen, *J. Appl. Polym. Sci.* 26, 2975 (1981)

[27] N. Overbergh, H. Berghmans, and G.Smets, *Polymer.* 16, 703 (1975)

[28] E. Turska, and W. Benecki, *J. Polym. Sci.* Symp. 44, 59 (1974)

[29] C. J. Durning, M. G. Scott, and H.D. Weigmann, *J. Appl. Polym. Sci*. 27, 3597 (1982)

Table 3.1. Solubility of n-pentane in PS and PP at ambient temperature and pressure.

Polymer	**Solubility, wt%**
PS	24.8 ± 0.3*
PP	17.1 ± 0.4*

* All the errors here and hereafter are the SE errors calculated by ORIGIN 7.0.

Table 3.2. The diffusivity pairs fitting to the experimental data.

Polymer	**D_0, cm^2/s**	**D_1, cm^2/s**
PS	$8.1 \pm 0.7 \times 10^{-10}$	$8.0 \pm 0.5 \times 10^{-9}$
PP	$2.1 \pm 0.2 \times 10^{-8}$	$3.0 \pm 0.3 \times 10^{-6}$

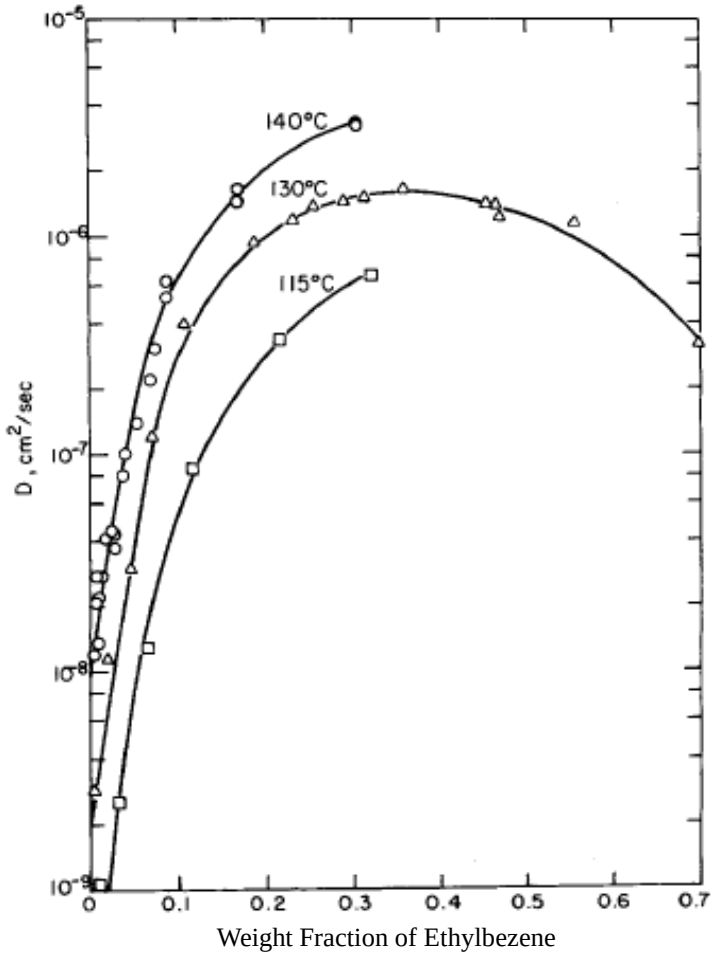

Figure 3.1. Diffusivity of ethyl benzene in PS at different concentrations [4].

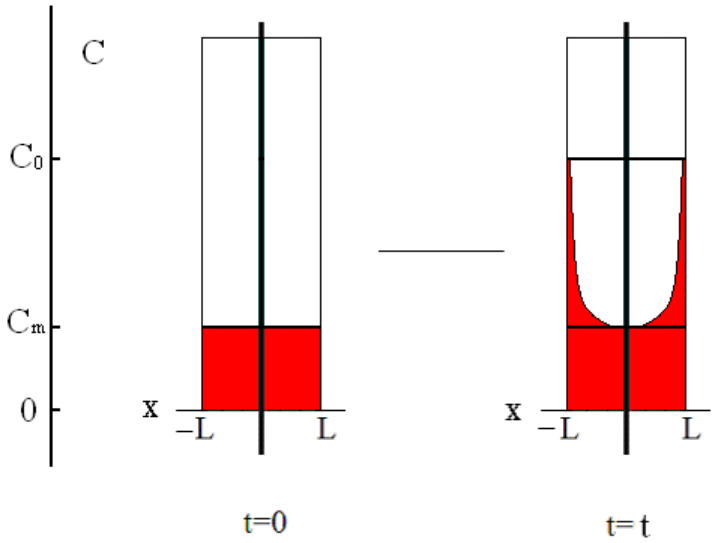

Figure 3.2. Illustration of the sorption process.

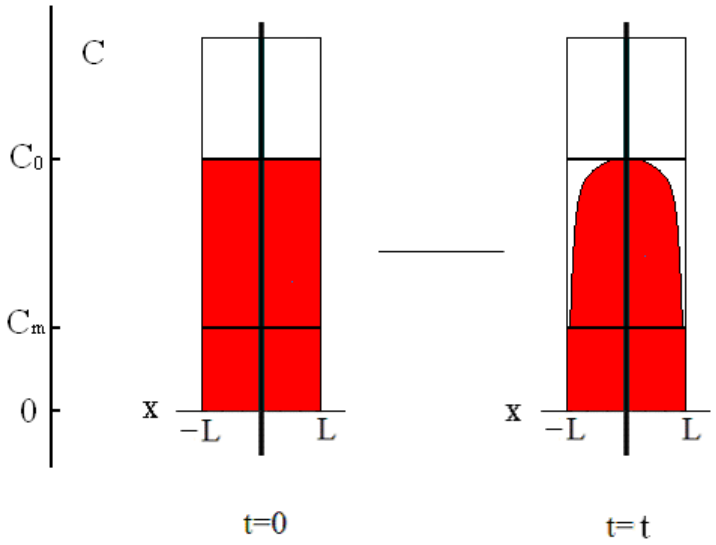

Figure 3.3. Illustration of the desorption process.

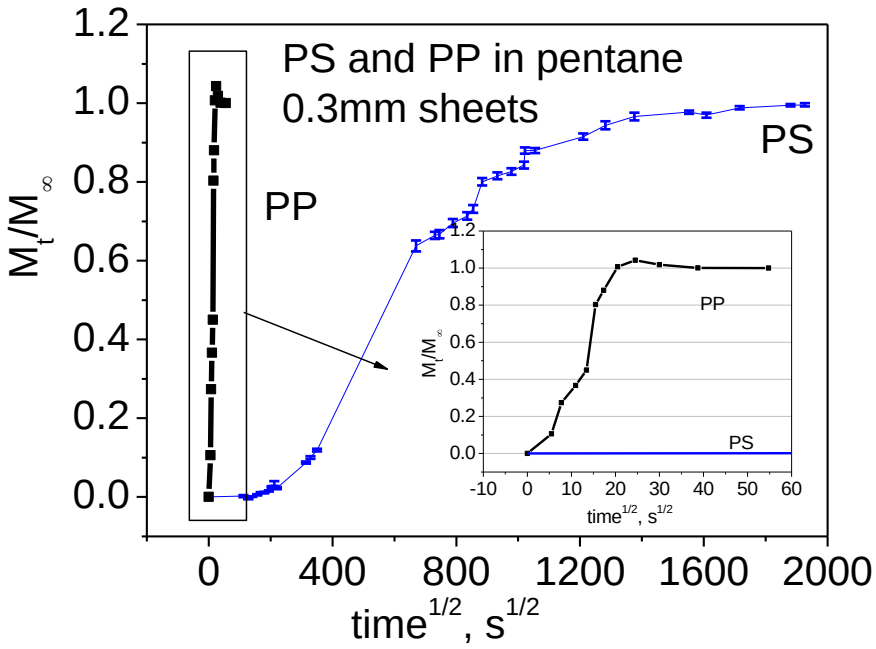

Figure 3.4. The n-pentane uptaking of PS and PP vs square root of sorption time.

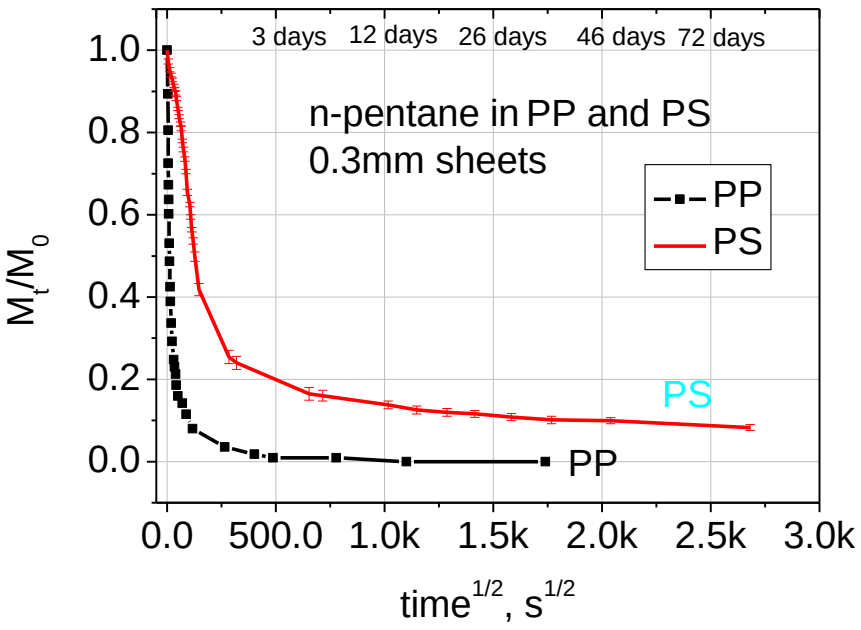

Figure 3.5. Desorption curves of n-pentane in PS and PP.

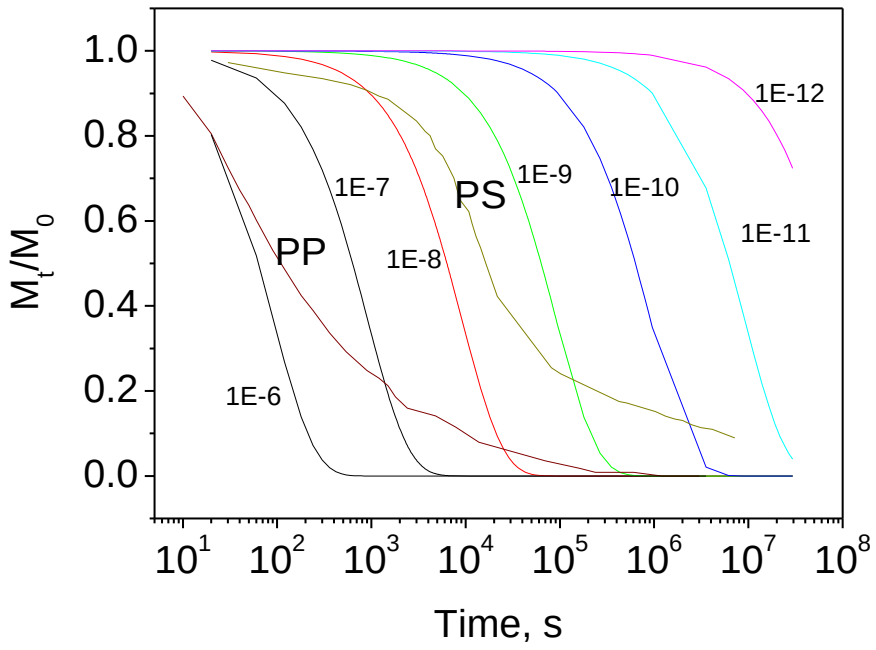

Figure 3.6. Desorption curves of Equation (3-8) and experimental curves of PS and PP.

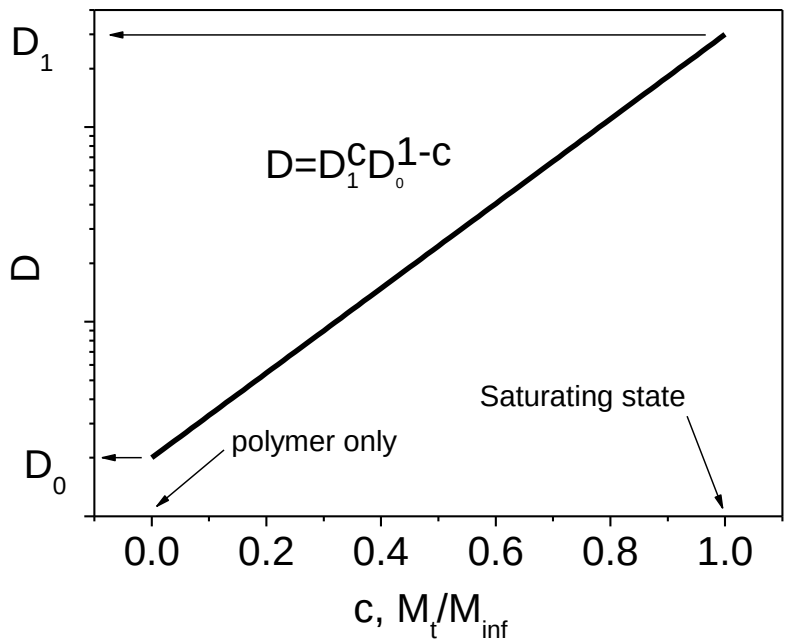

Figure 3.7. Concentration-dependent diffusivity.

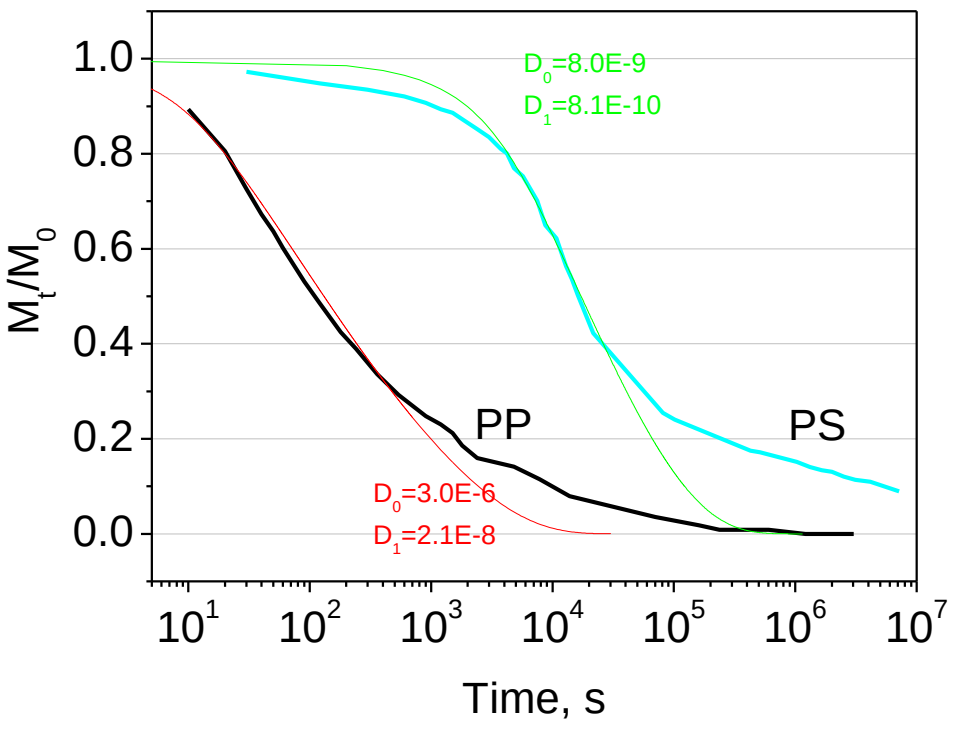

Figure 3.8. Validation of the simulated profiles.

Chapter 4

Development of VOC-Free Polystyrene Bead Foam Process

The research motivation in this chapter is from the issue of the VOC, n-pentane, used as a blowing agent in the conventional EPS bead foam process. Research procedure and results will be displayed to demonstrate the feasibility of the VOC-free EPS bead foam process. Two issues of the new EPS process will be addressed in this chapter; 1) development of efficient process for preparation of nucleated PS beads; 2) Optimum processing conditions for the pressurization of nucleated beads and the re-pressurization of pre-expanded beads.

4.1. Introduction

Since n-pentane is the most commonly used blowing agent in the conventional EPS bead foam process, there are some drawbacks related to the flammable VOC. When the expandable beads are heated with steam, the n-pentane vaporizes and contributes to the volume expansion. Some of the gas state of n-pentane can diffuse out of the beads. The n-pentane that is accumulated on the ground due to the higher density than air can have the serious risk of fire

around the expansion system. Aside from the safety issue, the product shelf life is also a challenging factor in handling the VOC-containing polymer beads, because the low boiling point of n-pentane leads to product deterioration over time depending on the packaging and storage conditions [1,2]. In general the shelf life of the EPS beads is just about a month. There have been many research efforts to develop alternative EPS technology without VOC emissions. Several technologies have been developed based on using blowing agents other than the conventional C4-C5 hydrocarbons [3-15]. A couple of companies tried to develop technologies that use water as a physical blowing agent [7-12]. There are several disadvantages inherent to the use of water as a blowing agent instead of pentane [13-15]. The glass transition temperature of PS is very close to the boiling point of water. When the foam has expanded and is being cooled down, the water condenses before or at the same time, as the foam gets rigid. This often leads to the foam collapse and limits sufficient volume expansion.

Recently Nova Chemical Ltd. proposed a prototype technology for VOC-free EPS foam process [9, 10]. The new EPS technology contains a foaming concept that allows expanding and molding polystyrene without the use of VOC blowing agent. Nucleation of beads is achieved by slightly expanding them to a bulk density about 400 kg/m^3. The increase of bulk density in this process is minimal so that transportation of the material is still economical. To elaborate on the processes of the technology, it basically consists of three stages; (a) preparation of nucleated beads from PS resin, (b) pressurization and pre-expansion of the nucleated beads, and (c) molding of pre-expanded beads. (Figure 4.1)

The cell-nucleated PS beads can be manufactured from the conventional suspension polymerization with a small amount of n-pentane and the subsequent mild expansion in a pre-expander. Unlike the existing EPS technology requiring large amount of n-pentane, much smaller

content (1-2 wt%) of n-pentane in the new process makes it possible to create fine cell structure in PS beads with relatively high bulk density, which is approximately 400 kg/m^3. Figure 4.2 shows a SEM picture of a cell-nucleated PS bead that was manufactured based on the new process. The cell morphology in the Figure 4.2 reveals that cell population density is about 3 x 10^7 cell/cm^3 and closed-cells are obviously dominant in the bead. As mentioned earlier, the cell-nucleated beads should have a bulk density greater than 200 kg/m^3 (ideally around 400 kg/m^3), which would allow for the economical storage and transportation (Table 4.2).

The second process in the VOC-free EPS process is the pressurization of nucleated PS beads for the purpose of increasing the cell pressure that is internal pressure of each cell in the nucleated PS bead. The increased cell pressure is supposed to contribute to further expansion of beads in the following pre-expansion step. In detail the pressurized beads will get in a pre-expander machine, where injected steam can soften the PS beads and induce the expansion of beads thanks to the internal cell pressure. As a result, the pre-expanded beads can be obtained for final steam chest molding. Since there is no remaining blowing agent in the beads, further pressurization just prior to molding is needed for the sake of successful steam chest molding. However, unlike the nucleated beads, it is challenging to pressurize the pre-expanded PS beads, because the high pressure could easily crush the foamed PS beads.

4.2. Preparation of Nucleated PS Beads through Batch Foaming

A series of batching foaming experiments were performed using a batch foaming system, where the temperature and the pressure can be varied to find the optimum condition of making nucleated PS that have ideal cell structure for the VOC-free EPS process. The effects of talc and PDMS on batch-foaming behaviors of PS were studied as well.

4.2.1. Experimental

The polystyrene used in all experiments was Styron 685D provided by Dow Chemical Company with the weight-average molecular weight of 315,000 g/mol. Table 4.3 shows the physical properties of Styron 685D in detail. As a nucleating agent, talc (Cimpact CB7, Luzenac) whose average size is 1.7μm was used. In order to achieve uniform dispersion of particles, a 20 wt% of talc masterbatch of PS was prepared using a C.W. Brabender 3-piece mixer. Subsequently, the master batch was diluted with pure PS using the same batch mixer to produce PS-talc compounds with various talc contents. PDMS (MB50-004, Dow Corning Company) was also blended into PS using the same Brabender mixer so that 1, 2, 5, 10 wt% of PDMS could be obtained for batch foaming. The physical blowing agents used for the foaming experiments were 99% pure CO_2 and N_2 (Linde Gas). A compression molding machine (Carver Inc.) equipped with a digital temperature controller was used to prepare film samples of the PS and the PS-talc compounds. PS resins or PS-talc compounds were hot compression-molded into 120 μm thick films using the press. The PS and PS-talc films were then punched into disc-shaped samples of about 6 mm in diameter for the batch foaming as well as in-situ visualization experiments.

- In-situ Foaming Visualization

The setup of the batch foaming visualization system [16], as shown in Figure 4.3, was used to observe the *in-situ* foaming behaviors of the aforementioned polymer-blowing agent system. The system consists of a high-pressure, high-temperature chamber, a pressure-drop rate control system, a data acquisition system for pressure measurement (i.e., a data acquisition board and a computer), a gas supply system (i.e., a gas tank, a syringe pump, and valves), and an

optical system (i.e., objective lens, a light source, and a high-speed CMOS camera). With a maximum frame rate of 120,000 frames per second, the CMOS camera is capable of capturing any fast foaming processes.

- Experimental Procedures

The foaming chamber loaded with a PS or PS-talc sample was charged with a blowing agent at the pre-determined saturation pressure, while the chamber temperature was controlled using a thermostat. The pressure and temperature of the chamber were maintained at the set points for 3 hours to allow the sample to be saturated with the blowing agent. Finally the blowing agent was released by opening the solenoid valve that can control the pressure drop rate. The pressure transducer and the CMOS camera captured the pressure decay data and *in-situ* foaming data, respectively.

- Foam Characterization

The foamed samples were characterized by measuring the foam density and conducting SEM experiments to observe the cell morphology of the foamed samples. Therefore the effects of each parameter on foaming behaviors were systematically investigated.

4.2.2 Results and Discussion

- Effect of Foaming Temperature and Blowing Agents

Batch foaming was conducted with pure PS film at different temperatures of 60°C, 65°C and 70°C. The reason why low temperature was selected here was not only because it is known

that high temperature is not favorable to create small cells, but also because the glass transition temperature of PS is about 105°C. The images from the visualization system in Figure 4.4 show that cell nucleation can occur at as low as 60°C with 1,500 psi of saturation pressure.

In order to see the effect of nitrogen as a blowing agent for batch foaming, foaming was carried out changing the foaming temperature from 70°C to 90°C at the same pressure of 2,000 psi. As exhibited in Figure 4.5, cell nucleation and growth did not occur at these conditions at all, which is most likely because the solubility of N_2 in PS is much lower than that of CO_2. It is believed that the dissolved gas content at 2,000 psi was not enough to plasticize PS for foaming. It is safe to say that CO_2 is preferable to N_2 in that the foaming temperature and pressure can be reduced and accordingly it is more cost-effective.

- Effect of Saturation Pressure

Basically saturation pressure can determine the dissolved gas content at certain temperature. Furthermore the degree of plasticization of polymer depends on the gas content dissolved in the polymer. In this aspect, saturation pressure is a critical factor in the batch foaming. Figure 4.6 shows SEM pictures of foam samples that were expanded at different saturation pressures with fixed temperature of 65°C. All the cell sizes of these foam samples are less than 10 μm regardless of saturation pressure. It is believed that foaming temperature of 65°C was not high enough for cells to grow further. Since the target cell size of nucleated PS bead is around 30μm, higher foaming temperature were experimented in order to boost the cell size. Figure 4.7 indicates that regardless of saturation pressure, foaming at 90°C was quite effective to generate ideal cell size in PS film .

- Effect of PDMS Blending

Taking the mass-production of nucleated beads into account, the saturation pressure has to be reduced as low as possible because building high pressure in the actual large chamber is costly as well as at risk of explosion. On this account, foaming of PDMS-blended PS was carried out at fixed pressure of 1,000 psi of CO_2 changing temperature from 60 ^oC to 90^oC. The pressure drop rate was fixed at -22 MPa/sec. It is well known that PDMS has much higher solubility, which may be conducive to lower-pressure batch foaming [17, 18]. However, it was thought that low content of PDMS should be introduced to PS, because PDMS might deteriorate the mechanical properties of the final foam products [19-22] and its cost is very high as well. In this study 1 wt% and 2 wt% PDMS were compounded with PS 685D at 180^oC using a Brabender batch mixer. Table 4.4 shows the formulation for compounding of PDMS for foaming.

SEM analysis was executed to observe the cell morphology of PS/PDMS foam. Figure 4.8, 4.9, 4.10 and 4.11 show the cross-sections of foam samples. It is remarkable that the average cell size increases with foaming temperature. PDMS appears to be effective as a cell nucleating agent when it is blended with PS just like talc. What is very interesting here is that 2 wt% PDMS generates larger cells and lower cell population density than 1 wt% PDMS (Figure 4.12). To see the relationship between foaming temperature and void fraction in the Figure 4.13, it shows that void fraction is less than 60% for all the foam samples. Besides the void fraction increased proportionally with foaming temperature, which is probably because cell growth can proceed more at higher temperature. Considering the ideal cell size and cell population density, foaming at 80^oC with composition of 1 wt% PDMS and no talc provided desirable cell morphology for VOC-free EPS process.

4.3. Preparation of Nucleated PS Bead Using Extrusion Foaming

4.3.1. Experimental

Extrusion foaming can be utilized as another method to manufacture nucleated PS beads. In an attempt to create fine cells in PS, highly hydrophilic silica particles (320DS, Degussa) and water were introduced as a water carrier and a blowing agent respectively. The basic purpose of using these materials for extrusion foaming is that numerous micro-pores on the surface of the precipitated silica are expected to actively absorb water and then to put it out after being dispersed in the matrix of PS [23]. Figure 4.14 shows the SEM pictures of the precipitated silica. In addition, SDS (Sodium Dodecyl Sulfate, Aldrich) was used as a surfactant to help water disperse better in PS melt. Experimental compositions were tabulated in Table 4.5.

For the foaming extrusion experiment, a single screw extruder was used in this study. Water was consistently injected and mixed with the PS (PS 685D) melt as a blowing agent using a syringe pump. Since solubility of water in PS is very low, the precipitated silica particles were expected to work as a carrier of water while dispersing in PS melt. Die temperature was fixed at 180°C because the plasticization effect of water is negligible due to very low solubility.

4.3.2. Results and Discussion

As exhibited in Figure 4.15, fine cells as small as 30 μm in diameter could not be obtained from any of the conditions. The smallest cell size was 120-180 μm in diameter at the condition #3. Most of the cells were greater than 200 μm in other conditions regardless of the contents of water, silica and SDS. Consequently it was difficult to make high cell density and fine cells in PS using water as a blowing agent for the extrusion foaming method. The

precipitated silica particles could work not just as a carrier of water but also as a cell nucleating agent. As the content of silica increases, the cell population density was enhanced as well. However SDS content did not make significant effect on cell size and cell population density in the experiment.

4.4. Pre-expansion of Nucleated Beads and Steam Chest Molding

After the preparation of nucleated PS beads, pre-expansion and steam chest molding should be conducted to manufacture EPS bead foams. Since the nucleated PS beads do not have any blowing agent, pressurization is required in order to give expandability to the nucleated PS beads. The expandability comes from increased internal pressure in each cell of the nucleated PS beads. It is possible to expand the pressurized beads in a pre-expander by injecting steam which is about 110 ^{o}C. The following step is the steam chest molding for producing three-dimensional PS bead foams. Unlike the conventional EPS beads, the pre-expanded beads just before steam chest molding do not have any blowing agents. Therefore pressurization is needed one more time for enough expansion and good adhesion between beads in the stage of steam chest molding. Figure 4.16 is illustrating the overall procedure from pressurization to steam chest molding.

4.4.1. Pressurization of Nucleated PS Beads

In an attempt to find optimum time and pressure for pressurization of nucleated PS beads, the weight gain and loss were investigated with time at different pressures. The nucleated PS beads were manufactured and supplied by Nova Chemical. Figure 4.17 shows the pressurization chamber and air compressor for these experiments. Figure 4.18 (a) shows the weight gain of nucleated PS beads with pressurization time at three different pressures; 100, 200, and 360psi. It

turned out that it took about 2 hours to saturate the nucleated beads with 360psi at room temperature. It is because of low diffusion rate of air through thick cell wall of the PS bead. Moreover room temperature for preventing sintering among beads was not favorable for process time for pressurization, because gas diffusivity through a polymer decreases at lower temperature. The weight loss in the air of the nucleated beads that were already pressurized and saturated with 3 different pressures was also monitored in Figure 4.18 (b).

4.4.2. Re-pressurization of Pre-expanded Beads for Steam Chest Molding

As shown in Figure 4.16, prior to steam chest molding, re-pressurization is required for the pre-expanded PS beads to expand enough and form good sintering in the mold. However, it is very challenging to pressurize the pre-expanded PS beads, because it can easily crush the soft pre-expanded beads and deteriorate the mechanical properties of final foams. Therefore the optimum condition for re-pressurization of the pre-expanded beads needs to be determined.

- Determination of Saturation Pressure

In order to find the optimum pressure for re-pressurization step, weight gain and volume change depending on saturation pressure were monitored with time. For this experiment, the pre-expanded PS beads whose bulk density was 16 kg/m^3 were supplied by Nova Chemical. A pressure chamber was used to impose various pressures of nitrogen gas on the beads.

Figure 4.19 exhibits that the maximum weight gain of beads is proportional to the pressure applied to beads. The weight gain of beads increased and finally saturated after certain pressurization time. Besides, the higher pressure was, the faster it reached the maximum weight

gain. It took 16 minutes to reach the saturation under the pressure of 30 psi. Figure 4.20 shows the trend of the decreasing weight of saturated beads with time when they were exposed in the air.

Table 4.6 indicates that the bulk density of expanded beads increased after re-pressurization. It is because of crushed PS beads by high pressure. However it is remarkable that 30 psi as re-pressurization pressure did not change the bulk density of the pre-expanded beads. It is inferred that most of PS beads could recover the original volume because 30 psi was not too high to endure. It is meaningful to determine the condition for re-pressurization without crushing the PS beads even though it took about 16 minutes which is somewhat long process time. It is thought that the process time issue can be overcome through continuous pressurization and feeding of the beads in a large chamber.

4.5. Summary

Given that the existing EPS bead foam technology has the VOC issues, it is valuable to develop new EPS foaming process that does not need and emit VOC at all. In this study, research efforts have been made regarding how to manufacture nucleated PS beads that have desired cell characteristics as well as how to pre-expand them before the final steam chest molding process.

In attempts to develop the best process of producing nucleated PS beads, batch foaming and extrusion foaming were executed changing compositions and processing parameters. It was successful to obtain ideal cell structure from batch foaming below glass transition temperature of PS thanks to both plasticization effect of carbon dioxide and solubility-enhancing effect of PDMS. It turned out that addition of just 1 wt% PDMS to PS gave rise to ideal cell morphology in terms of cell size and cell population density. On the other hand, the extrusion foaming method was also conducted to manufacture the nucleated PS beads using water as a blowing agent as well as

precipitated silica as water dispersing media. Unfortunately, it was difficult to obtain small cells and high cell population density despite the effort of blending hydrophilic porous silica in PS matrix. However more experimental efforts on extrusion foaming will be valuable by using various blowing agents and nucleating agents in the aspect of reducing cost through a continuous process. In an effort to determine optimum conditions for pressurization and pre-expansion of nucleated beads as well as re-pressurization of pre-expanded beads for steam chest molding, pressurization time and the level of pressure were investigated considering the effect of high pressure on PS beads. It was remarkable that 30 psi was enough for re-pressurization without crushing pre-expanded beads.

It is believed that in order to develop commercially viable VOC free EPS technology, mechanical systems also have to be studied regarding the connections of pressurizing chamber, continuous pressurizing chamber, and so on.

4.6. References

[1] D. Klempner, and K.C. Frisch, *Handbook of Polymeric Foams and Foam Technology;* Hanser Verlag: Munich (1991)

[2] A. H. Landrock, Chap. 3 in "*Handbook of Plastic Foams*", edit by A.H. Landrock, William Andrew Publishing: Noyes, 236 (1995)

[3] J. Fischer, J. Rieger, K. Hahn, I. De Grave, and W. Kogel, U.S. Patent 5,773,481-Detailed description of the invention (1998)

[4] B. H. Meyer and J. C. Kingslow, U.S. Patent 5,049,328-Detailed description of the invention (1991)

[5] B. H. Meyer and J. C. Kingslow, U.S. Patent 4,911,869 (1990)

[6] W. Collom, D. Fuller, J. C. Kingslow, B. H. Meyer and R. H. Immel, U.S. Patent 5,271,886-Detailed description of the invention (1993)

[7] J. J. Crevecoeur, E. Neijman, L. Nelissen and J. M. Zijderveld, U.S. Patent 6,242,540 (WO 98/01488)-Detailed description of the invention (2001)

[8] J. J. Crevecoeur, E. Neijman, L. Nelissen and J. M. Zijderveld, U.S. Patent 6,160,027 (WO 98/01489)-Detailed description of the invention (2000)

[9] H. Berghmans, I. Chorvath, P. Kelemen, E. Neijman and J. M. Zijderveld, U.S. Patent 6,127,439 (WO 98/01501)-Detailed description of the invention (2000)

[10] M. Berghmans, C. Mesters, A. Metsaars, E. Neijman and J. Pallay, U.S. Patent 6,528,570 (EPC 99202459.6)-Detailed description of the invention (2003)

[11] G. Guiscard, H. Klaus and G. Roland, WO 99 48936-Detailed description of the invention (1999)

[12] G. Guiscard, H. Klaus and G. Roland, WO 99 48958-Detailed description of the invention (1999)

[13] J. J. Crevecoeur, L. Nelissen and P. J. Lemstra, *Polymer*, 40(13), 3685-3689 (1999)

[14] J. Pallay, P. Kelemen, H. Berghmans and D. Van Dommelen, *Macromolecular Materials and Engineering*, 275(2), 18-25 (2000)

[15] J. Pallay and H. Berghmans, *Cellular Polymers*, 21(1), 19-33 (2002)

[16] Q. Guo, J. Wang, C. B. Park, and M. Ohshima, *Industrial & Engineering Chemistry Research*, 45, 18, 6153 (2006)

[17] L. J. Gerhardt, C.W. Manke and E. J. Gulari, *J. Polym. Sci. B: Polym. Phy.* 35, 523 (1997)

[18] P. Spitael, C.W. Macosko, and R. B. McClurg, *Macromol.* 37, 6874 (2004)

[19] R. N. Jana, G. B. Nando, *J. Appl. Polym. Sci*., 88, 2810 (2003)

[20] E. Yilgor, T. Sinmazcelik,I. Yilgor, *J. Appl. Polym. Sci*., 84, 535 (2002)

[21] R. N. Jana, G. B. Nando, *J. Elastomers Plast.*, 37, 149 (2005)

[22] P. M. P. Mun˜oz, M. M. Werlang, I. V. P. Yoshida, R. S. Mauler, *J. Appl. Polym. Sci.*, 83, 2347 (2002)

[23] K. M. Lee, E. K. Lee, S. G. Kim, C. B. Park, and H. E. Naguib, *J. Cell. Plast.*, 45, 539 (2009)

Table 4.1. Characteristics of nucleated PS bead

Characteristics	**Data**
Bulk density	400 kg/ m^3
Cell density	3×10^7 cells/cc
Average cell diameter	30 μm

Table 4.2. Desirable densities of PS beads in each stage

Density	Solid PS bead	Nucleated PS bead	Pre-expanded PS bead
Bulk density	650 kg/m^3	400 kg/m^3	15~25 kg/m^3
Bead density	1,050 kg/m^3	600 kg/m^3	25~40 kg/m^3

Table 4.3. Physical properties of polystyrene

Property	**Styron 685D**
MFI (ASTM D1238)	1.5g/10 min
M_n	120,000
M_w/M_n	2.6
Specific gravity	1.04
Glass transition temperature (T_g)	108℃

Table 4.4. Compounding formulation for blending PDMS

No.	**PS (wt%)**	**PDMS (wt%)**	**Talc (phr)**	**Remark**
#1	99	1	0	• Brabender Batch Mixer (50 RPM, 5min at 180°C) • PDMS (Dow Corning) • Talc (Cimpact CB7, Luzenac)
#2	98	2	0	
#3	99	1	3	
#4	98	2	3	

Table 4.5. Experimental scheme of extrusion foaming for manufacturing nucleated PS beads.

Materials	#1	#2	#3	#4	#5	#6
Water (wt% of PS)	**0.35**	**0.35**	**0.35**	**0.5**	**0.5**	**1**
SiO_2 (wt% of PS)	**1**	**1**	**3**	**1**	**3**	**3**
SDS (wt% of water)	**0**	**1**	**1**	**5**	**5**	**5**

Table 4.6. Final bulk density of pre-expanded PS beads after the re-pressurization.

Pressure	Final Bulk Density
30 psi (1.9 atm)	**16 kg/m^3**
50 psi (3.4 atm)	20 kg/m^3
70 psi (4.8 atm)	21 kg/m^3
100 psi (6.8 atm)	23 kg/m^3
150 psi (10.2 atm)	25 kg/m^3

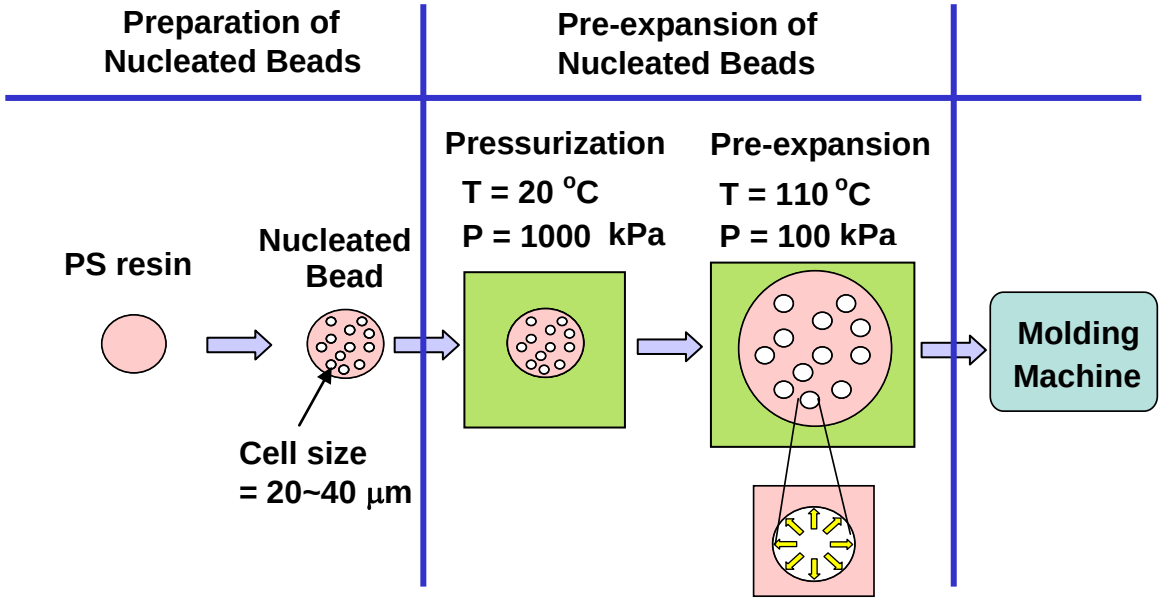

Figure 4.1. Research outline of VOC free EPS technology [9, 10].

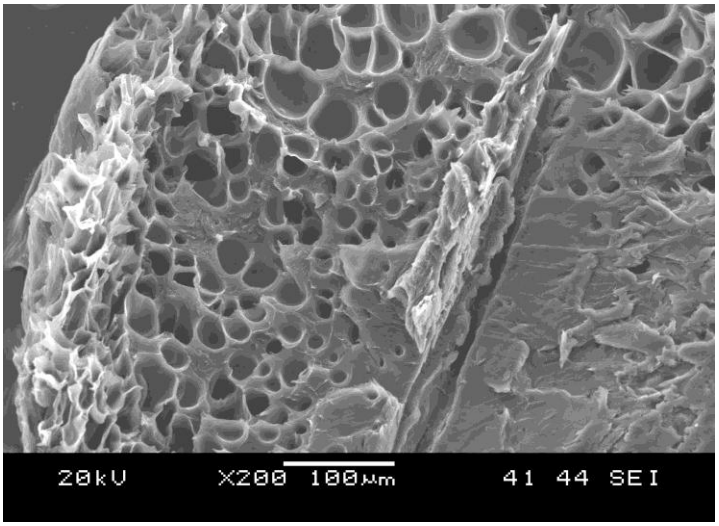

Figure 4.2. SEM picture of the cross-section of a nucleated PS bead.

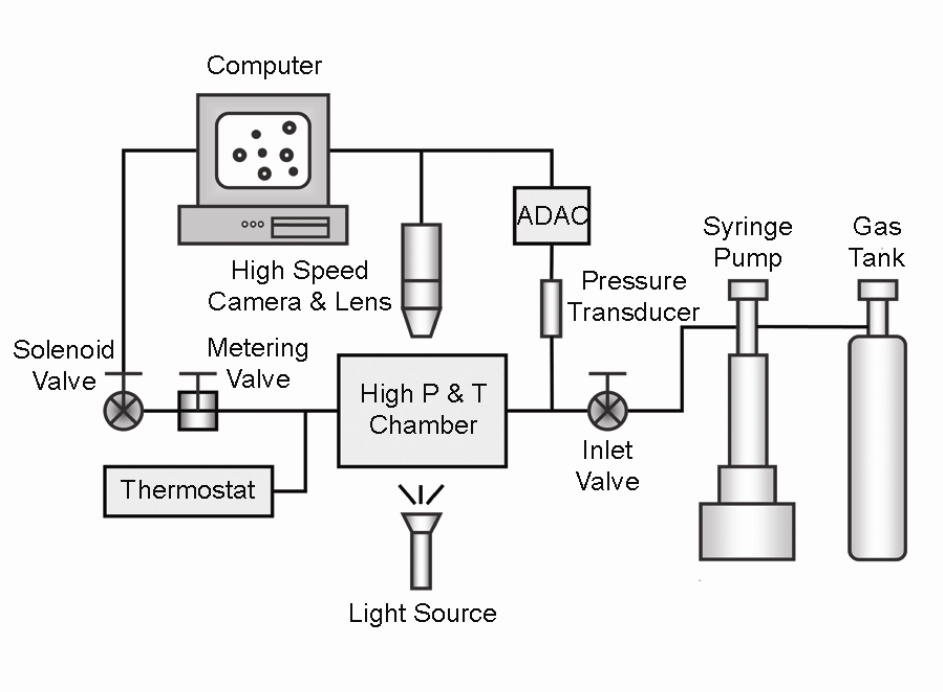

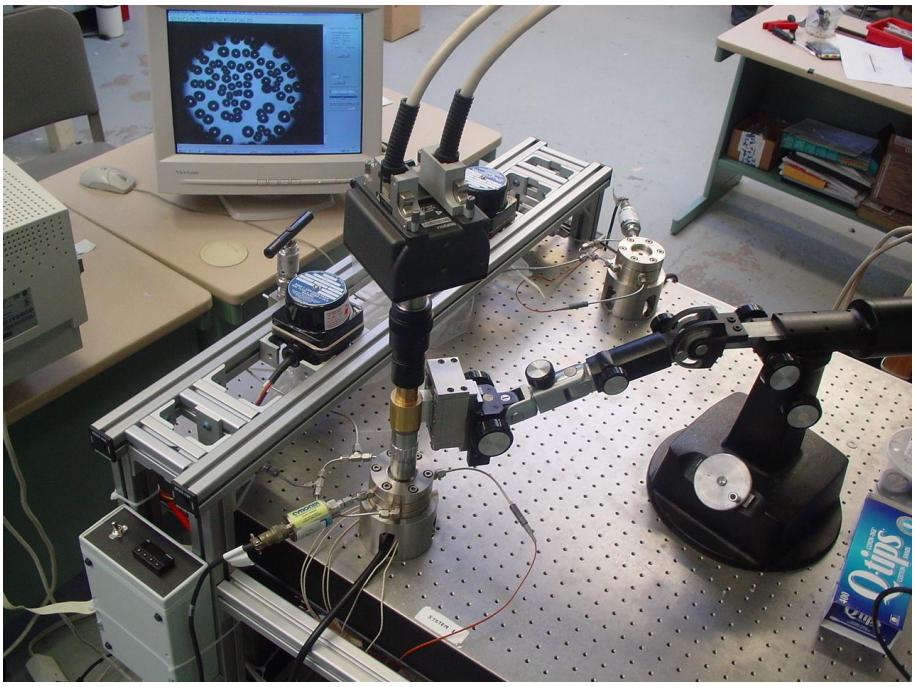

Figure 4.3. Batch foaming visualization system [22]

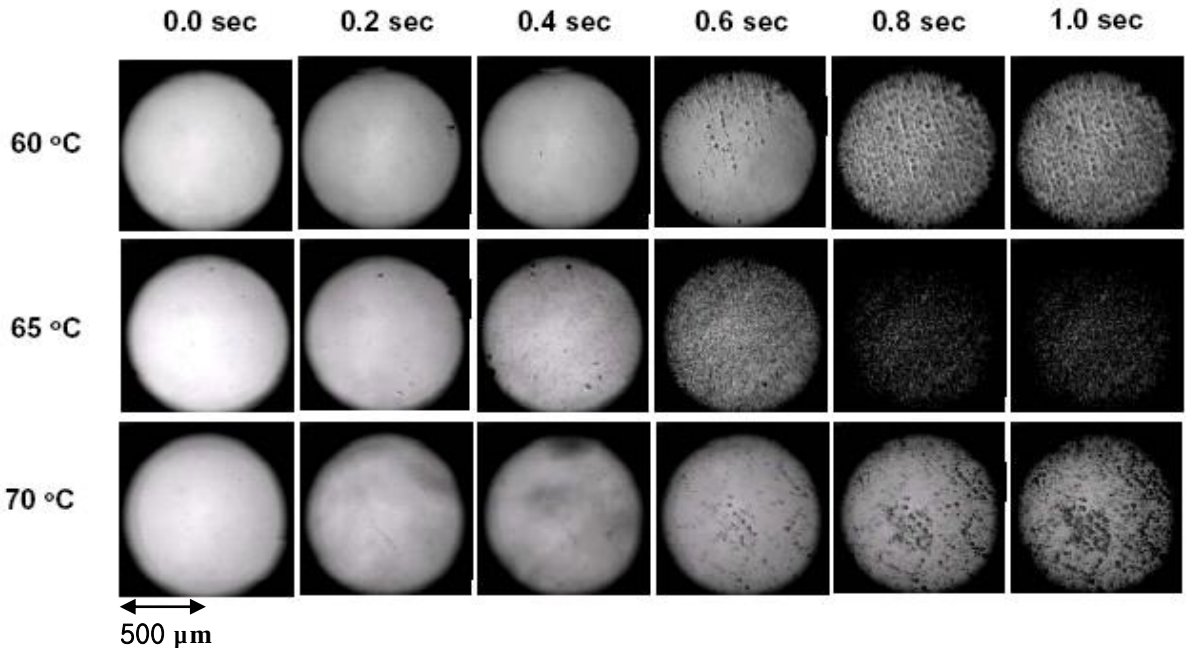

Figure 4.4. Images from visualization system during the batch foaming of PS film with 1,500 psi CO_2 at different temperatures.

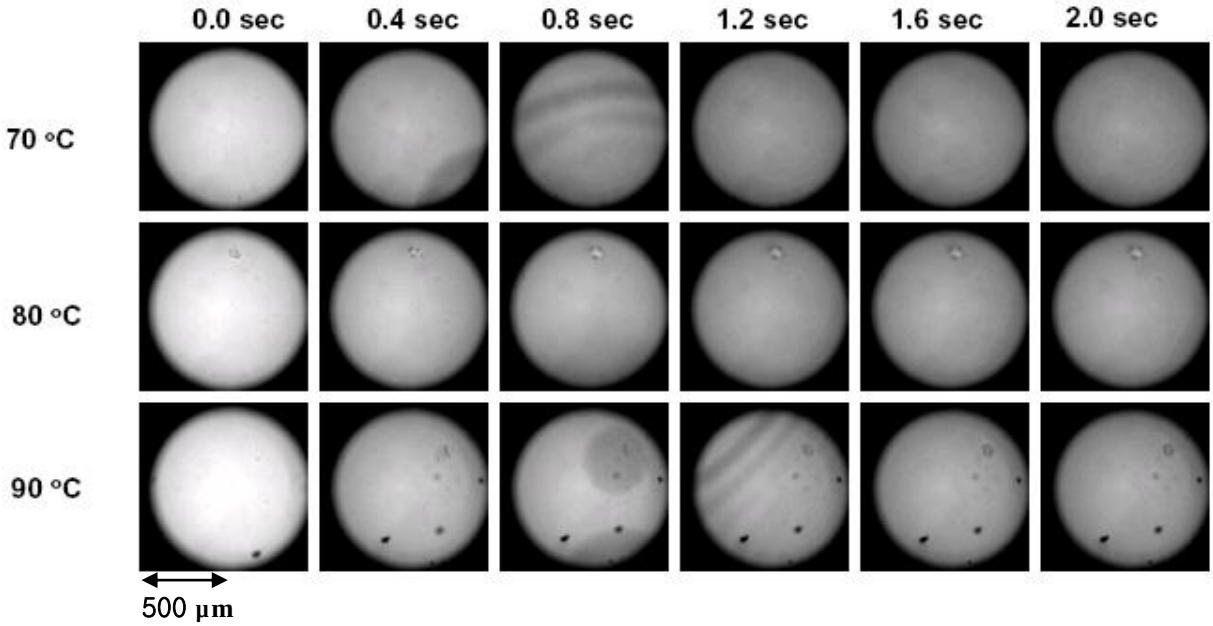

Figure 4.5. Images from the visualization system during foaming with 2,000 psi N_2 at different temperatures.

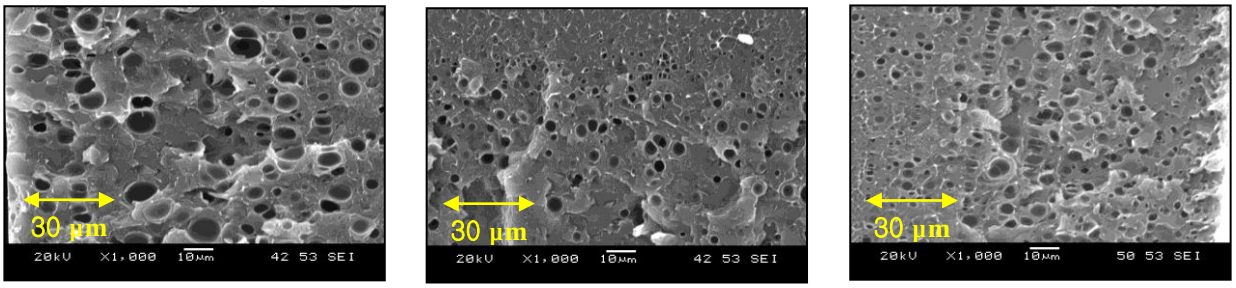

(a) (b) (c)

Figure 4.6. SEM pictures of final foam samples at 65°C with different pressure; (a) 1,500psi, (b) 2,000psi, and (c) 2,500psi.

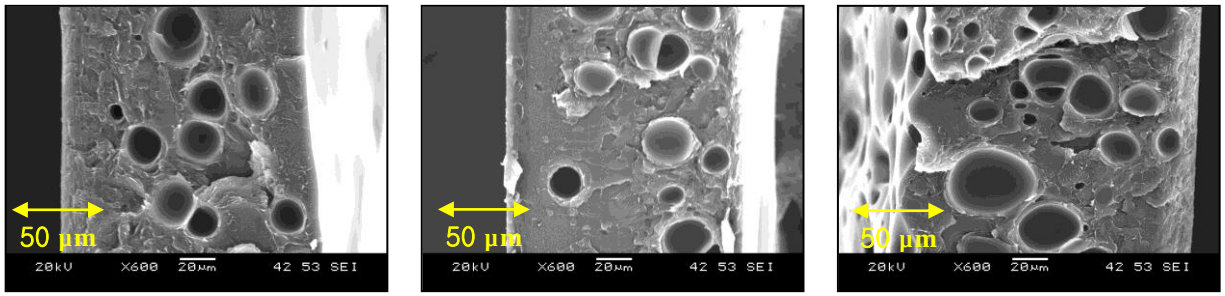

(a) (b) (c)

Figure 4.7. SEM pictures of final foam samples at 90°C with different pressure; (a) 1,000psi, (b) 1,200psi, and (c) 1,500psi.

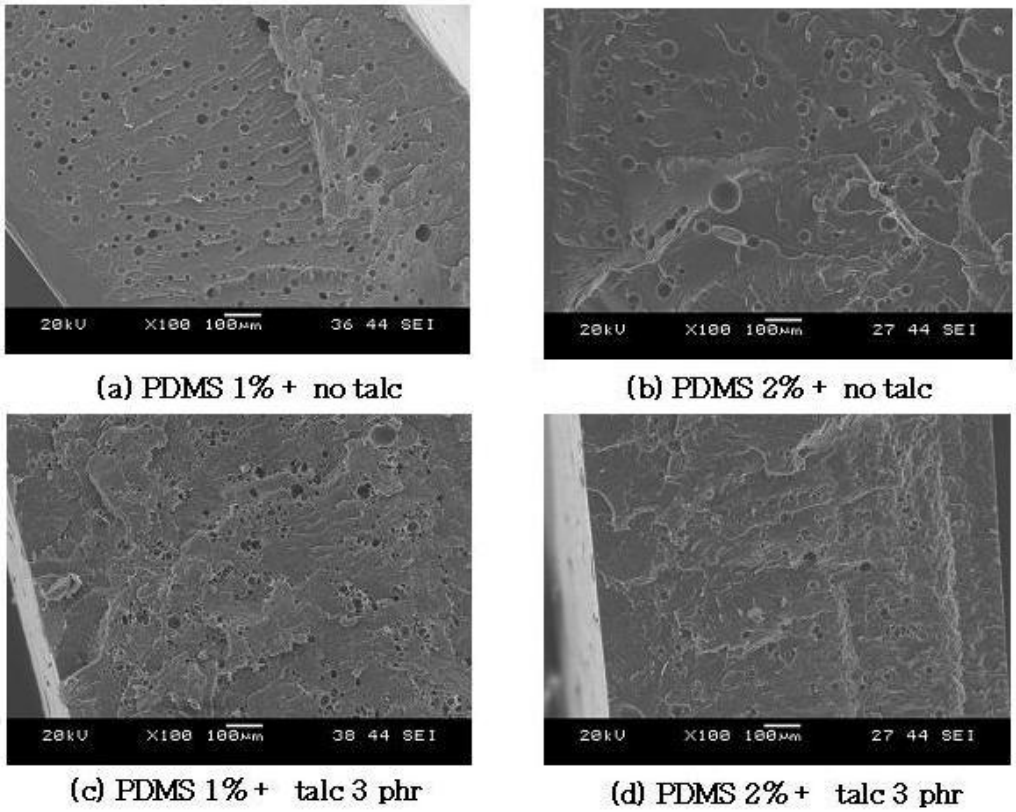

Figure 4.8. SEM pictures of PS film foamed with different formulations at 60°C and 1,000 psi ; (a) PDMS 1 wt% and no talc, (b) PDMS 2 wt% and no talc, (c) PDMS 1 wt% and 3 phr talc, and (d) PDMS 2 wt% and 3 phr talc.

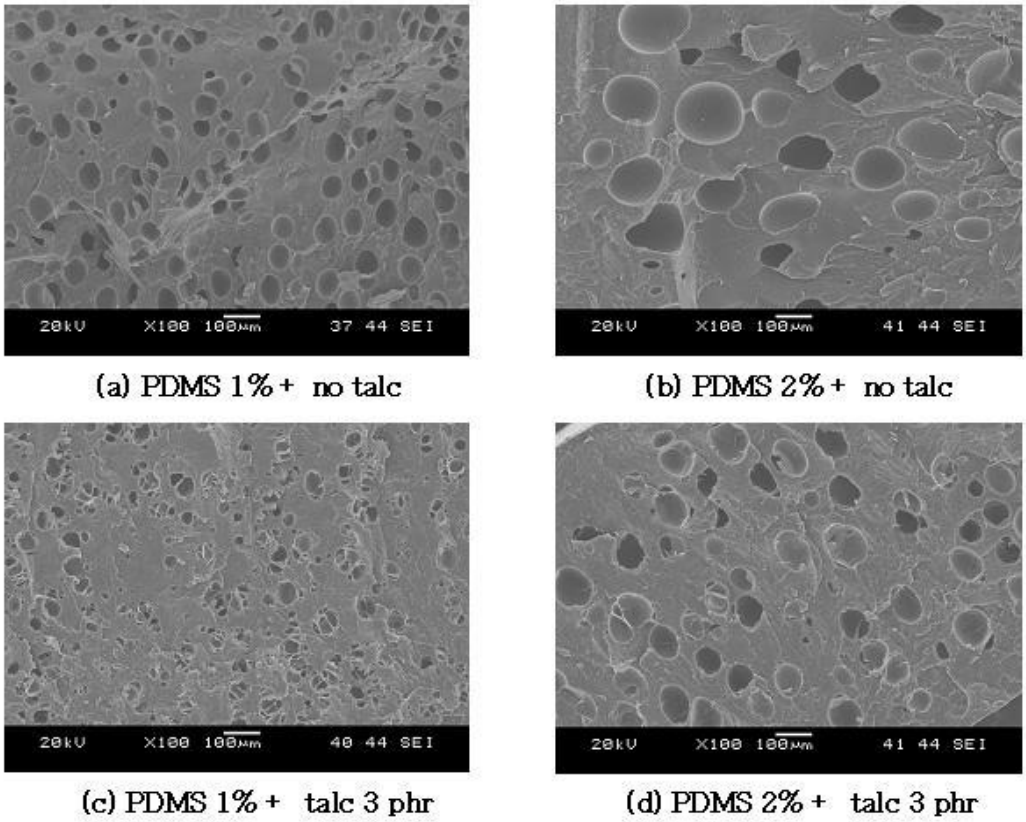

Figure 4.9. SEM pictures of PS film foamed with different formulations at 70 ^{o}C and 1,000 psi ; (a) PDMS 1 wt% and no talc, (b) PDMS 2 wt% and no talc, (c) PDMS 1 wt% and 3 phr talc, and (d) PDMS 2 wt% and 3 phr talc.

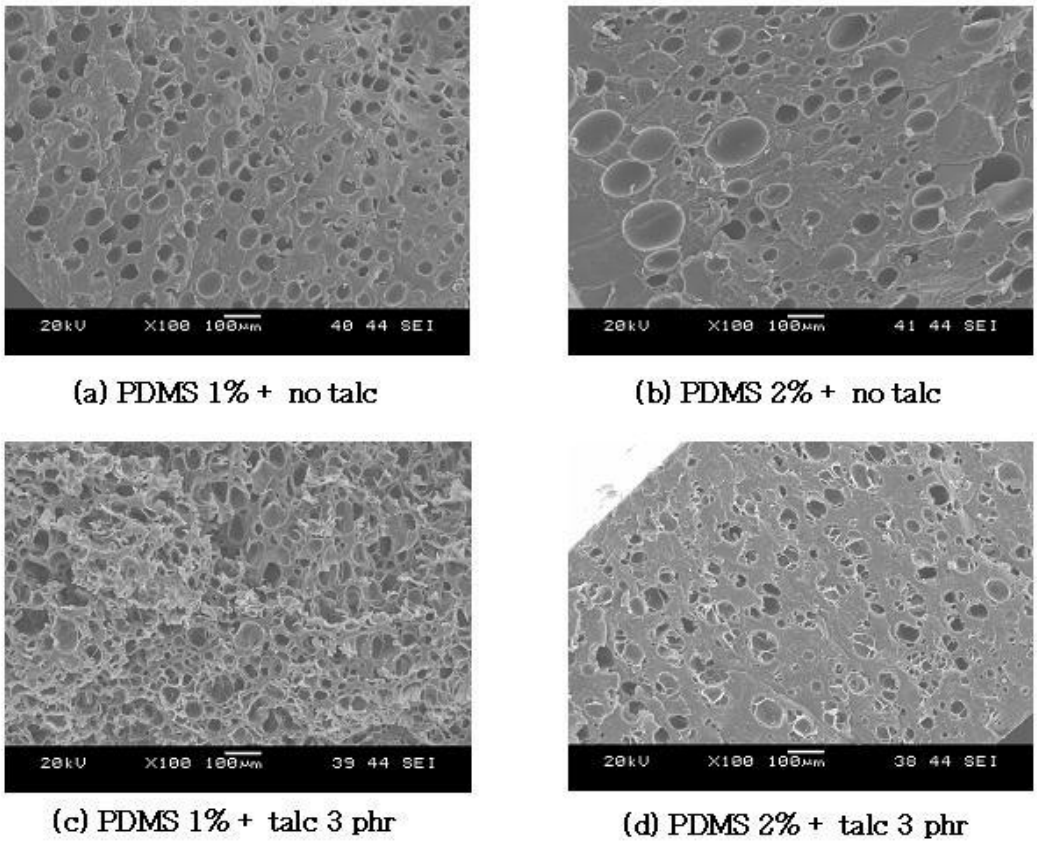

Figure 4.10. SEM pictures of PS film foamed with different formulations at 80 ^{o}C and 1,000 psi; (a) PDMS 1 wt% and no talc, (b) PDMS 2 wt% and no talc, (c) PDMS 1 wt% and 3 phr talc, and (d) PDMS 2 wt% and 3 phr talc.

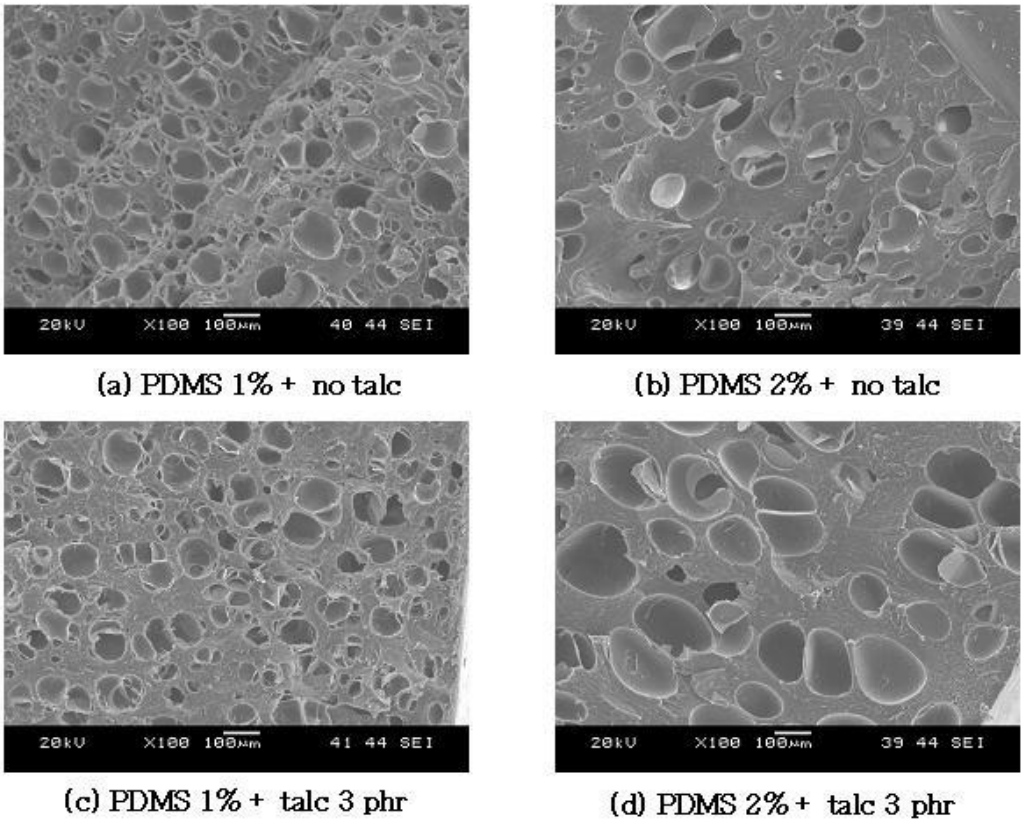

Figure 4.11. SEM pictures of PS film foamed with different formulations at 90 ^{o}C and 1,000 psi; (a) PDMS 1 wt% and no talc, (b) PDMS 2 wt% and no talc, (c) PDMS 1 wt% and 3 phr talc, and (d) PDMS 2 wt% and 3 phr talc.

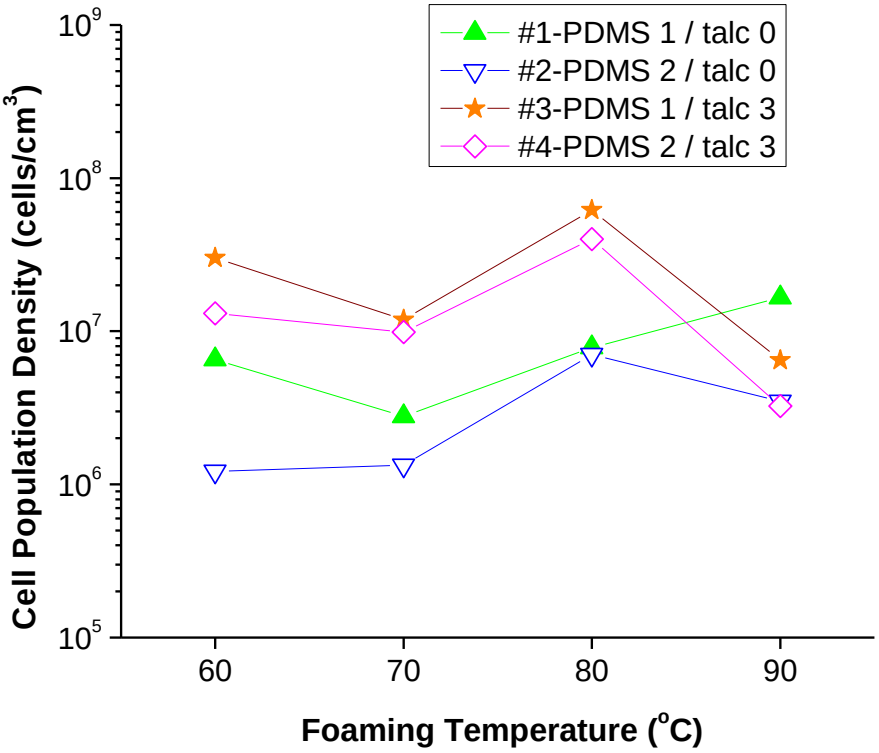

Figure 4.12. Cell population density of PS foams

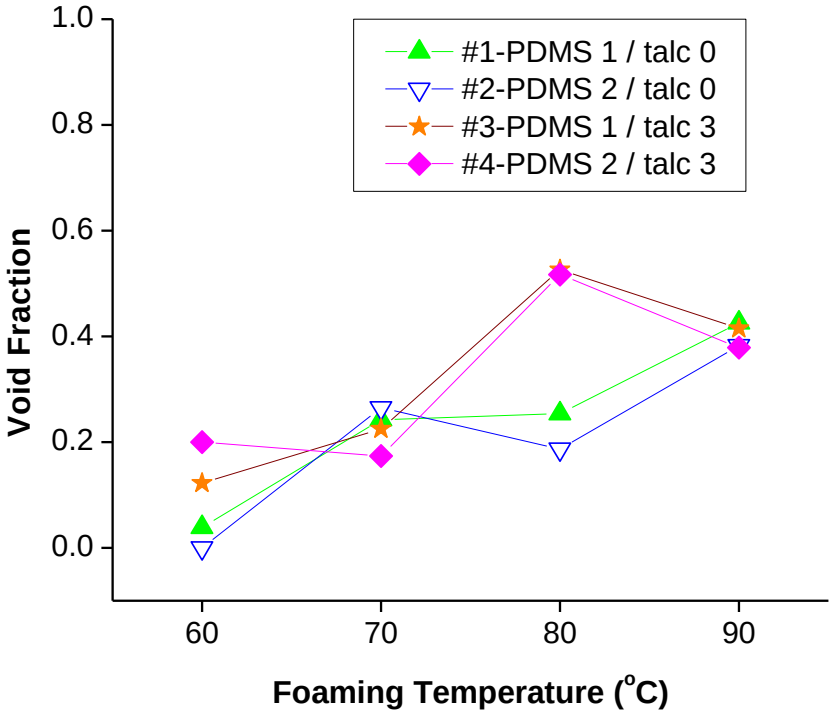

Figure 4.13. Void fraction depending on foaming temperature.

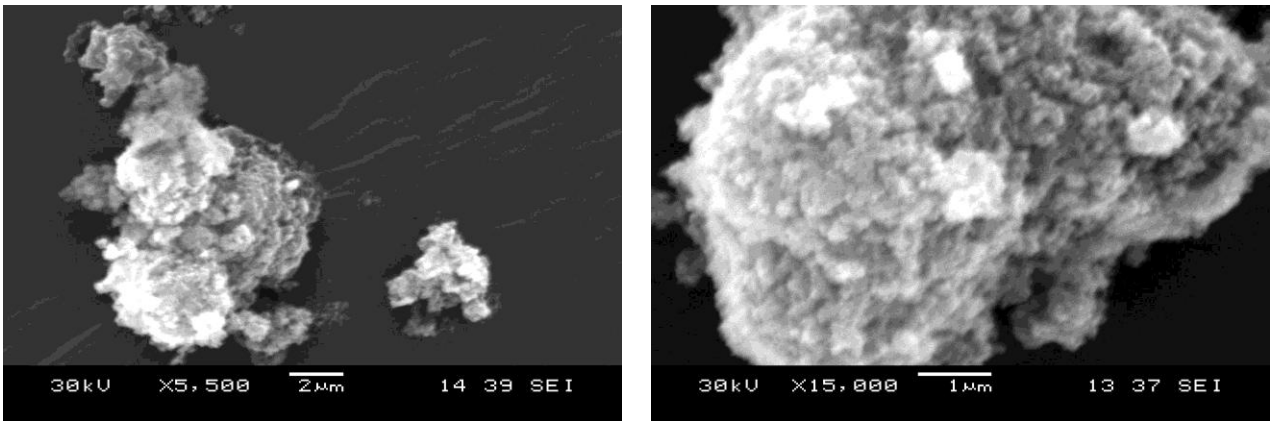

Figure 4.14. SEM pictures of precipitated silica particles from .

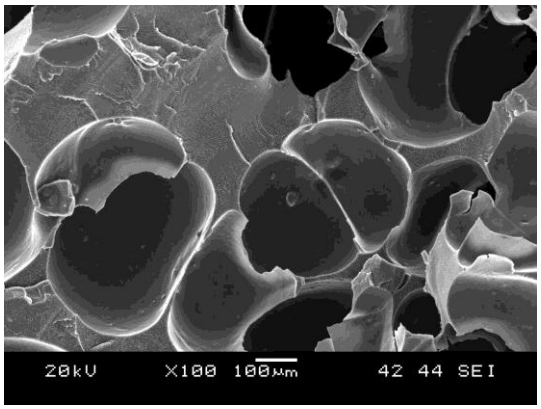

#1

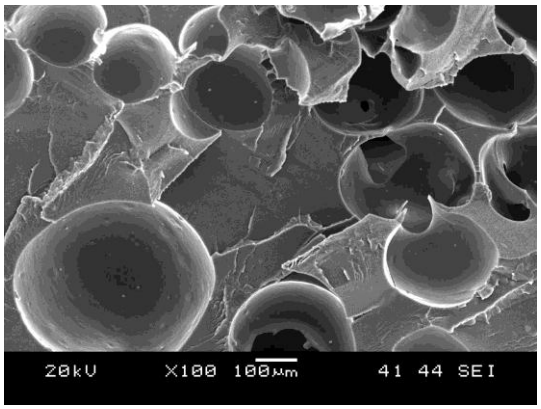

#2

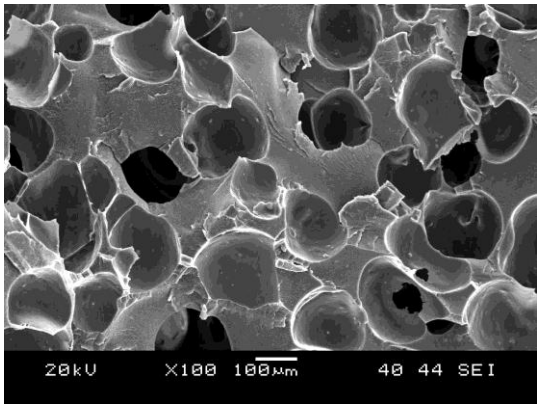

#3

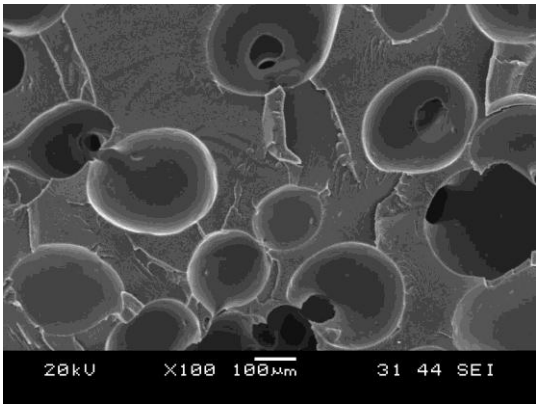

#4

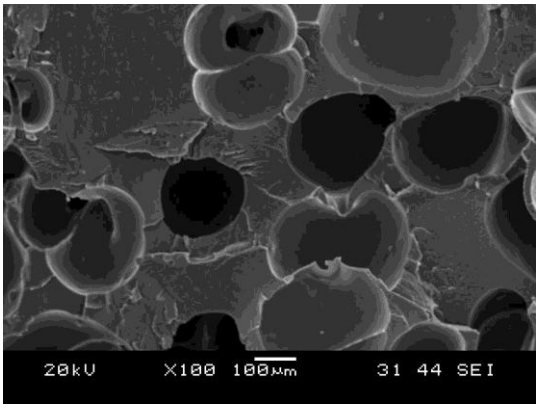

#5

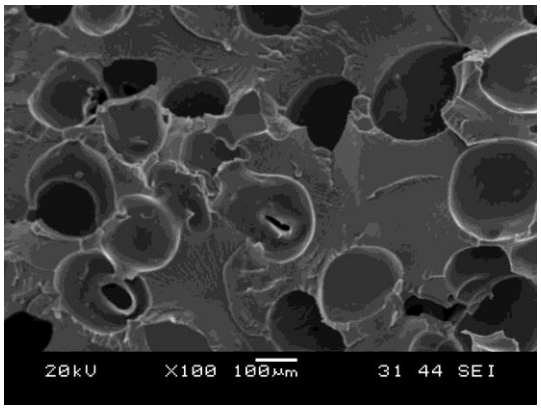

#6

Figuew 4.15. SEM pictures of extrusion-foamed PS samples for making nucleated PS bead;

Each condition (#1 ~ #6) is described in the Table 4.5.

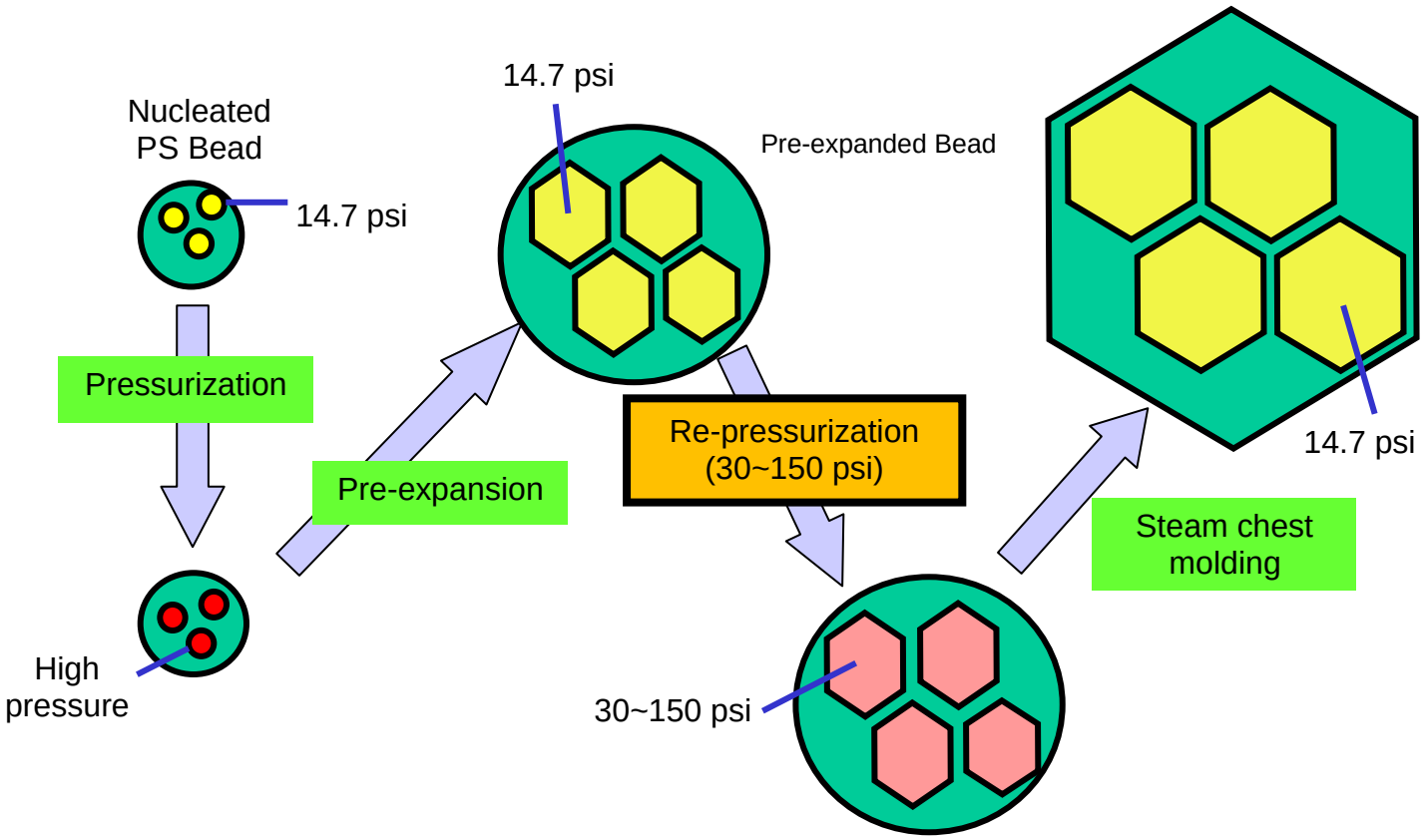

Figure 4.16. Schematic of pre-expansion and steam chest molding.

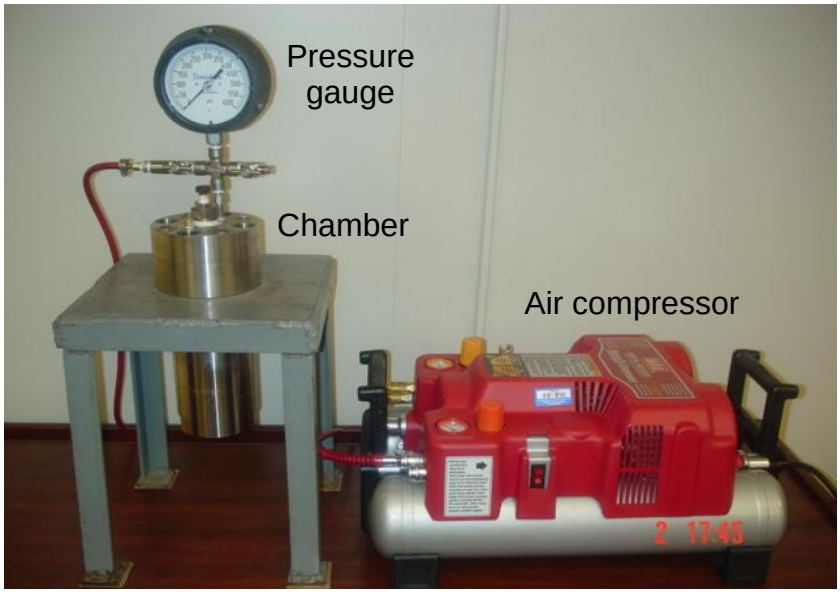

Figure 4.17. Pressure chamber and air compressor for pressurization of nucleated PS beads.

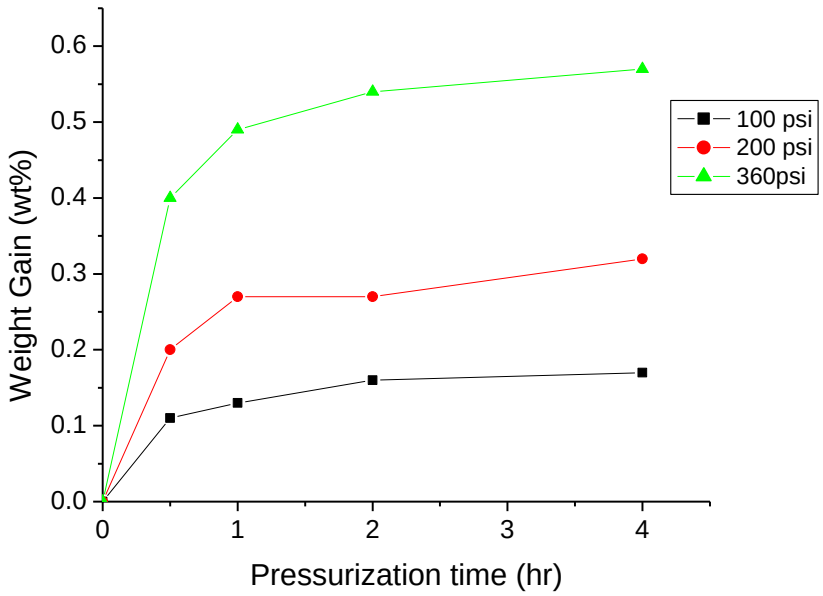

(a)

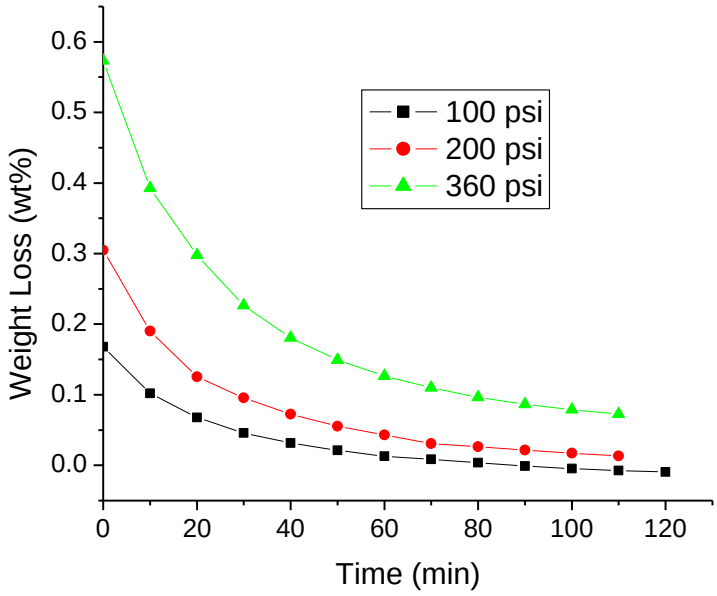

(b)

Figure 4.18. Weight gain (a) and loss (b) of nucleated PS beads.

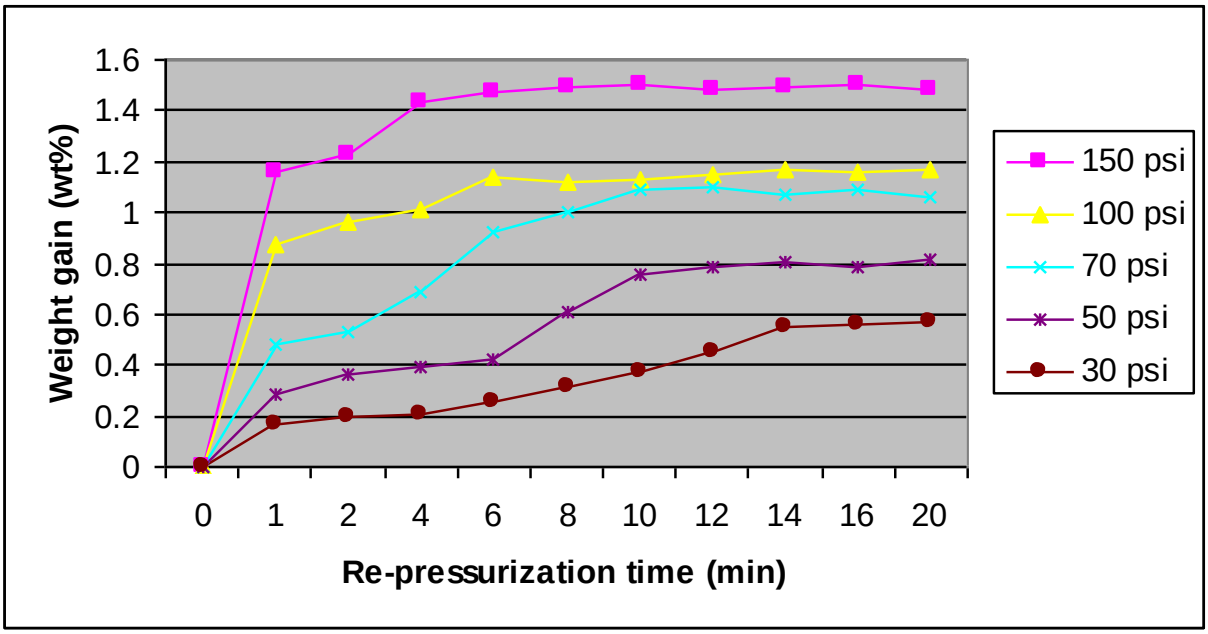

Figure 4.19. Weight gain of pre-expanded PS beads with re-pressurization time.

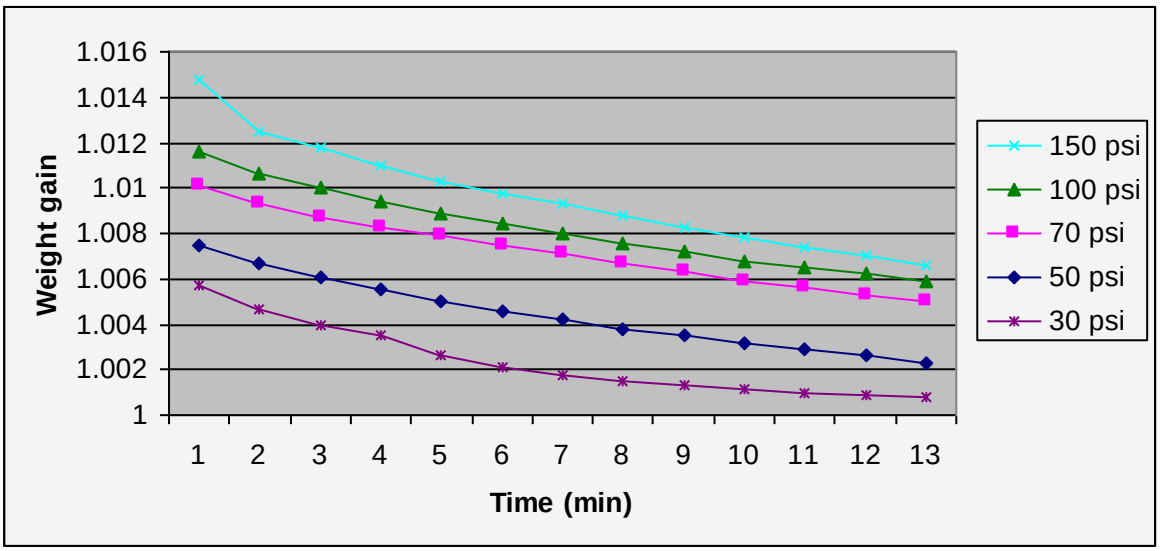

Figure 4.20. Weight loss of pre-expanded PS beads in the air which were re-pressurized and saturated at various pressures.

Chapter 5

Bi-Cellular Polystyrene Foam

5.1. Introduction

Since expanded PS bead foam has a high thermal insulation property, it has been widely used in many application areas. In addition to PS foam, researchers have been working to further enhance the insulating capability of a variety of other polymers. In an attempt to maximize thermal insulation property, hydrofluorocarbons (HFCs) used to be introduced as an insulating physical blowing agent [1-5]. However, HFCs had a disadvantage of serious green house effect as well as high cost issue [6]. Alternative approach to achieve higher thermal insulation was the modification of cellular structure without using HFCs as blowing agents. In particular Dow Chemical Company proved that the bi-cellular foam structure had superior thermal insulation property compared to conventional mono-cellular foams [7-12]. The bi-cellular foam structure has two types of cells, relatively larger foam cells and relatively smaller cells as shown in Figure 5.1. The definition of these two types of cells differs in the literature, but in general, the larger

cell size ranges from 0.1 to 1.2 mm and the smaller cell size ranges from 5 percent to about 50 percent of the average larger cell size; The two kinds of cells should constitute more than 90 percent of the total cell volume. In an effort to produce the bi-cellular foam structure, a combination of two different blowing agents is often used to induce two different nucleating mechanisms instead of using a single blowing agent. In fact, there have been various researches on the water foaming method because water is environmentally benign as well as inexpensive [8, 13-23]. However, since the solubility of water in polymers is very low, it is generally believed to be very difficult to obtain a fine and uniform cell morphology using water as a blowing agent. To overcome the problem of poor solubility, other materials, such as water-absorbing polymers and inorganic particles, could be employed to carry and disperse the water in the polymer melt [16, 21-23].

The purpose of this chapter is to optimize the material composition and processing condition for achieving bi-cellular foam structure using PS with an ultimate hope that this technology will be able to evolve to develop the EPS bead foam with excellent thermal insulation property. Water and n-butane are incorporated as a mixture of blowing agents in polystyrene in order to achieve a bi-cellular foam structure. In addition, precipitated silica particles are introduced in the polystyrene to help disperse the water by absorbing water on the hydrophilic and porous surface of the silica. It was expected that investigation of cell nucleation and growth behaviors would eventually enhance understanding of the bi-cellular foaming mechanisms.

5.2. Experimental

5.2.1. Materials

Polystyrene resin (Styron 685D) supplied by Dow Chemical Inc. was used in this study, with the following properties: melt flow index (MFI) 1.5 g/10min; weight average molecular weight (Mw) 300 kg/mol; and number average molecular weight (Mn) 120 kg/mol. As physical blowing agents, n-butane (Matheson, 99.0% Purity) and pure water (EMD chemicals, HPLC grade) were used. Precipitated silica particles (320DS, supplied by Degussa) were used as a nucleating agent and for absorbing water. Its characteristics were as follows: a specific surface area of 175 m^2/g; a mean particle size of 5 μm; and 98% SiO_2 content. The precipitated silica was dried at 80˚C for 24 hours prior to compounding.

5.2.2. Experimental Setup

A schematic of the experimental extrusion setup used in this study is shown in Figure 5.2. The setup consisted of a single screw extruder (Brabender, 05-25-000) with a mixing screw (Brabender, 05-00-144) of 30:1 L/D ratio and 3/4” diameter, which was used for plasticizing the polymer pellets and dispersing the injected blowing gas throughout the melt. A positive displacement syringe pump (manufactured by ISCO Inc.) was used to inject the physical blowing agents in the polymer melt. A static mixer (omega, FMX-84441-S) was installed after the extruder to improve the dissolution of the physical blowing agent. A gear pump (Zenith, PEP-II 1.2cc/rev) is included where the volumetric displacement was properly controlled by the motor, a heat exchanger for cooling the polymer that contained the homogenizing static mixer (Labcore Model H-04669-12), and a cooling sleeve for the precise control of die temperature. A filamentary die with L/D 1.16”/0.06” was used in this foaming experiment.

5.2.3. Experimental Procedure

In order to verify the relationship among material composition, processing condition and cell morphology, eighteen sets of experimental condition were schemed in total. The experiments were carried out with 5 wt% and 7 wt% of n-butane changing the die temperature. The water content was varied from 0%, 0.25%, 0.5%, 1%, 2%, and 4%, while silica contents of 0, 1, and 3 wt% were used.

The silica-PS mixed pellets were first fed into the barrel through the hopper and then completely melted by the screw rotation and shear force; mixing and melting occurred before the two injection ports. Metered amounts of the physical blowing agents (n-butane and water) were subsequently injected into the extrusion barrel using the positive displacement pump and mixed intensively with the polymer melt stream at the same time. When the gas was injected into the extrusion barrel, the screw generated shear fields to dissolve the gas completely in the polymer melt via mixing and diffusion. Moreover, the static mixer was used to enhance the dissolution of the gas in the polymer melt. Ideally a single-phase polymer/gas solution was generated, and this solution was funneled through the gear pump and fed into the heat exchanger where it was cooled down to a designated temperature. The cooled polymer/gas solution entered the die, and foaming occurred at the die exit through a process of thermodynamic instability, induced by a rapid pressure drop. While optimizing all the parameters, the melt and die temperatures were lowered gradually from 160˚C to 120˚C, in decrements of 10˚C. As the temperature was decreased, the pressures were recorded once the steady state of each set of processing conditions was achieved. Samples were collected randomly at each designated temperature when no further change was observed at each pressure.

The temperature of the heat exchanger and the die were decreased from 160˚C to 120˚C. The flow rate of the polymer melt was maintained at 14.7 g/min, and the volumetric flow rate was set to 2.3×10^{-7} m^3s^{-1}, which was maintained for the extrusion system throughout the course of the experiment. Finally, the calculated pressure-drop rate was 60~120 $MPa.s^{-1}$. Based on the results of the first experiments, the contents of the additives and temperature were optimized in order to achieve a bi-cellular foam structure.

5.2.4. Characterization of Foams

The foam samples were characterized in terms of volume expansion ratio, cell population density and cell size. The expansion ratio of the bi-cellular foam was determined by measuring the weight and volume expansion of the sample. The volume of the foam sample was determined using the water displacement method (ASTM D792). The volume expansion ratio (Φ) was calculated on the basis of the ratio of the bulk density of the pure PS material (ρ_p) to the bulk density of the foam sample (ρ_f) [24]:

$$\Phi = \frac{\rho_p}{\rho_f} \tag{5.1}$$

The cell population density (n) was calculated as the number of cells per unit volume with respect to the unfoamed polymer. First, the number of cells (n_b) in a defined area (L x L) was determined and then the total number of cells per cubic centimeter was calculated as follows [25]:

$$n = \left(\frac{n_b}{L^2}\right)^{3/2} \times 10^3 \times \Phi \tag{5.2}$$

where L is the side length in mm. Three samples were characterized for each set of processing conditions, and the average value for each processing condition was reported.

It may be noted that we used the cell population density defined with respect to the unfoamed polymer volume in this processing paper to better describe the processing-to-structure relationships, since this parameter indicates how well cell nucleation was controlled during foam processing [26].

5.3. Results and Discussion

5.3.1. Processing of Bi-cellular Foam Structure

In order to obtain the bi-cellular structure in the foamed PS, material composition and die temperature were varied in the extrusion foaming. The cell morphology was analyzed through scanning electron microscope (SEM). Table 5.1 shows various processing conditions for bi-cellular foam structure and the quantitative data of the foam manufactured in this study. It is remarkable to note that silica content should be more than 3 wt% for forming bi-cellular structure. We also noted that the appropriate amount of water ranged from 1 wt% to 2 wt%. There may be an ideal ratio of water to silica to be able to make a bi-cellular structure in that silica has a function of dispersing water in PS melt by absorbing the water in the pore. In addition, relatively low temperature is more favorable for a bi-cellular structure. Figure 5.3 shows the SEM pictures of foams extruded at different processing conditions and compositions. The n-butane and temperature were set to 5% and 120˚C, respectively. Depending on the conditions, the structures varied slightly in terms of the cell size ratio between large cells and small cells. It is noticeable that excessive water leads to serious cell deterioration. Unlike other blowing agents, water has a very low solubility (~0.5 wt%) [27], so it is impossible to expect

water to be dissolved into the polymer melt. Instead, the liquid water droplets will be mechanically dispersed as gas pockets in polymer melt.

Figure 5.4 exhibits a typical bi-cellular structure, which was formed under the condition; 5% n-butane, 1% water, 3% silica, and 110˚C. It is well known that precipitated silica is highly hydrophilic and has numerous micro pores on the surface. Therefore it is no wonder that the silica can absorb part of water actively and function as a water carrier in the polymer melt. Meanwhile some of water can remain as water droplets in the molten polymer. Since polymer melt is under high pressure and temperature, the water droplets are believed to be superheated state. Accordingly the superheated water will explosively vaporize and form relatively large cells as the polymer melt comes out of the die. At this moment, the dissolved n-butane can help make large cells in association with water droplets. Subsequently, water trapped in the pore of silica is believed to form the small cells surrounding the large cells. In addition, when water vapor is condensed in the large cells, n-butane can maintain the bubble structure until PS is solidified.

5.3.2. Effect of Die Temperature on the Cell Morphology of Bi-cellular Foam

In an effort to observe the effect of die temperature on the cell morphology, the die temperature was varied in the range of 120˚C to 160˚C. The cell density in Figure 5.5 shows the sums of the cell densities for the large and small cells, but we noted that the cell density was governed by the number of the smaller cells. On that account, these results appear different from what is observed in the SEM images. It turns out that die temperature does not affect the cell density significantly regardless of compositions. It is possible to obtain more than 10^6 cells/cc of cell density with 3wt% silica regardless of die temperature. Figure 5.6 shows the volume expansion ratio at different temperatures. However no remarkable effects of temperature on

expansion were detected for the 1 wt% and 3 wt% silica contents. In the absence of silica, the expansion ratio was more significantly affected by the die temperature with 1.5 wt% and 2.0 wt% water contents.

5.3.3. Effect of Silica Content on the Cell Morphology of Bi-cellular Foam

For 0 wt% and 1 wt% silica, the cell density tends to be proportional to the water content up to 2% of water. It means that dispersed water through the silica particles contributes to the increase of cell density. A larger amount of water than 2 wt% didn't make enhancement of cell density. On the other hand, the effect of water content on cell nucleation was not prominent for 3 wt% of silica. Since it is likely that silica particles absorb water and then contributes to cell nucleation, cell nucleation tends to be governed by the distribution of the silica particles. It is inferred that finely dispersed water drop can form cells at low silica content in PS below 2% and the silica particles may have serious aggregation from 3% because of the strong silica-silica interaction. With regard to the expansion ratio, a similar behavior was observed for all the silica contents.

5.3.4. Effect of Blowing Agent

Generally one of the most critical factors affecting the foaming behavior of polymer is the amount of injected blowing agent. In this study, two blowing agents of water and n-butane were injected into the PS melt in the barrel of the extruder. It should be noted that n-butane has a much higher plasticizating effect than water due to the even higher solubility. Table 5.1 shows that 5wt% and 7wt% of n-butane did not make substantial difference in terms of the expansion ratio. As far as the effect of water content on cell density is concerned, dispersed water droplets

appear to contribute to increasing the cell density particularly at low contents of silica. In case of 3wt% silica, the cell density is not affected by the water content, which is most likely because the dispersion of the silica particles is limited at the high silica contents. As shown in Figure 5.6, expansion ratio was proportionally enhanced with increasing water content, but this trend disappears when water content is higher than 2 wt%. It is inferred that surplus water no longer contributes to the expansion ratio because the excessive water that was not absorbed by the silica particles may easily escape to the environment through cell coalescence or rupture.

5.4. Summary

In this study, bi-cellular PS foam was successfully fabricated using co-blowing agents of water and n-butane along with precipitated silica. It was found out that the bi-cellular structure can be controlled by changing the ratio of n-butane/water/silica content as well as die temperature in the extrusion foaming process. The experimental study conducted in this research led to a few conclusions. It is inferred that water trapped in the pore of silica contributed to the formation of the smaller cells, whereas both the excessive water that was not absorbed by silica and n-butane primarily resulted in the larger cells. The precipitated silica particles seemed to function as a water carrier in the PS melt, which must have contributed to dispersion of water despite its low solubility. Cell nucleation behavior was insensitive to the die temperature. However, in the absence of silica, volume expansion of PS foam was more significantly affected by die temperature with 1.5 wt% and 2.0 wt% of water content. It is safe to say that the bi-cellular PS foam could be manufactured only when the appropriate ratio of water and silica content was satisfied.

5.5. References

[1] A. Biedermann, C. Kudoke, A. Merten, E. Minogue, U. Rotermund, H.-P. Ebert, U. Heinemann, and H. Seifert, *Journal of Cellular Plastics*, 37 (6) 467 (2001)

[2] R. Perkins, L. Cusco, J. Howley, A. Laesecke, S. Matthes, and M.L.V. Ramires, *J Chem. Eng. Data*, 46, 428 (2001)

[3] R. G. Richard and I. R. Shankland, A Transient Hot-Wire Method for Measuring the Thermal Conductivity of Gases and Liquids, *International Journal of Thermophysics*, 10(3), 673 (1989)

[4] C. V. Vo, and A. N. Paquet, An evaluation of the thermal conductivity of extruded polystyrene foam blown with HFC-134a or HCFC-142b, *Journal of Cellular Plastics*, 40 (3), 205 (2004)

[5] L. Glicksman, M. Schuetz, and M. Schuetz, Radition, Heat transfer in foam insulation, *International Journal of Heat and Mass Transfer*, 30 (1), 187 (1987)

[6] Montreal Protocol on Substances that Deplete the Ozone Layer, Montreal (1987)

[7] K. Suh, and A. N. Paquet, In: Scheirs, J. and Priddy, D. (eds), *Polystyrene Foams*, Chap. 10. Modern Styrenic Polymers: Polystyrene and Related Polymers, John Wiley & Sons, Chichester, UK (2003)

[8] K. Suh, and G. Killingbeck, GB Patent, 1,537,421 (1978)

[9] R. Gendron, M. Huneault, J. Tatibouet, and C. Vachon, Foam extrusion of polystyrene blown with HFC-134a, *Cellular Polymers*, 21, 315 (2002)

[10] P. Dournel, and L. Zipfel, HFC blends for the production of high performance XPS insulating foams, In: Blowing agents and foaming process, *Foams Conference 2001*, 24, 1 (2001)

[11] F. Buttler, and J. Radlinsky, The change of thermal conductivity with time of extruded polystyrene skinboards, *International Foamed Plastic Symposium* (1979)

[12] J. Kuhn, H.-P. Ebert, M. C. Arduini-Schuster, D. Buettner, and J. Fricke, Thermal transport in polystyrene and polyurethane foam insulations, *International Journal of Heat and Mass Transfer*, 35 (7), 1795 (1992).

[13] S. Motani, T. Saito, and T. Itho, U.S. Patent 5,064,874-Detailed description of the invention (1991)

[14] A. N. Paquet, and K. Suh, U.S. Patent 5,240,968-Examples (1993)

[15] K. Suh, and A. N. Paquet, U.S. Patent 5,380,767-Detailed description (1995)

[16] H. Berghmans, I. Chorvath, P. Kelemen, E. Neijman, and J. Zijderveld, U.S. Patent 6,127,439-Detailed description of the invention (2000)

[17] J. C. Schubert, and E. C. Leduc, U.S. Patent 5,380,767-Detailed description of the invention (1984)

[18] R. L. Hurps, and K. Suh, U.S. Patent 4,559,367-Detailed description of the invention (1985)

[19] A. N. Paquet, and K. Suh, U.S. Patent 5,369,137-Detailed description of the invention (1994)

[20] T. Hayashi, K. Tanaka, H. Kobayashi, J. Fukuzawa, and S. Kurihara, U.S. Patent 6,841,581-Detailed description (2005)

[21] J. Pallay, P. Kelemen, H. Berghmans, and D. Van Dommelen, *Macromol. Mater. Eng.*, 275, 18 (2000)

[22] J. Pallay, and H. Berghmans, *Cellular Polymers*, 21, 1 (2002)

[23] J. Pallay, and H. Berghmans, *Cellular Polymers*, 21 19 (2002)

[24] H. E. Naguib, C. B. Park, and N. Reichelt, J. Appl. Polym. Sci, 91, 2661 (2004)

[25] D. W. van Krevelen, Properties of polymers, 3rd edition, Elsevier science publishers, Amsterdam, Oxford, New York (1990)

[26] X. Xu, C. B. Park, D. Xu, and R. Pop-Iliev, *Polym. Eng. and Sci.*, 43 (7), 1378 (2003)

[27] J.W. Gibbs, The scientific papers of willard gibbs, Vol.1, Dover publication, New York (1961)

Table 5.1. Experimental conditions to achieve bi-cellular structure

n-Butane (wt%)	Water (wt%)	Silica (wt%)	Die Temperature (^oC)	Expansion Ratio	Cell Density (cells/cc)	Cell Size Ratio (large/small)
5	1	3	100	22.8	3.67E+06	5.43
5	1	3	110	28.1	1.59E+07	9.58
5	1.5	3	130	33.2	4.21E+06	2.65
5	2	3	120	34.5	9.50E+06	4.17
7	1	3	90	26.0	8.13E+06	3.22
7	1	3	100	30.1	9.95E+06	1.92
7	1	4	100	30.6	1.82E+07	8.36
7	1	4	110	30.1	2.20E+07	6.17
7	2	3	90	31.9	1.30E+08	10.09
7	2	3	100	33.6	2.12E+07	9.80

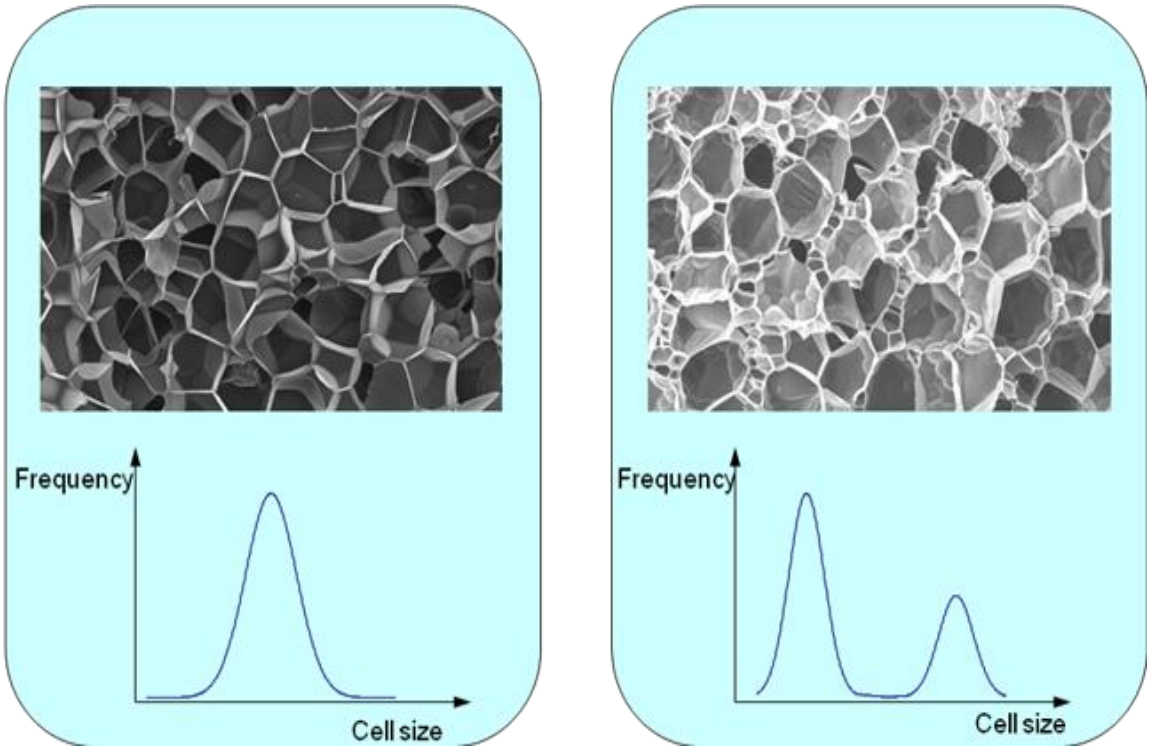

a) Conventional form b) Bi-cellular form

Figure 5.1. Conventional cell structure and bi-cellular cell structure

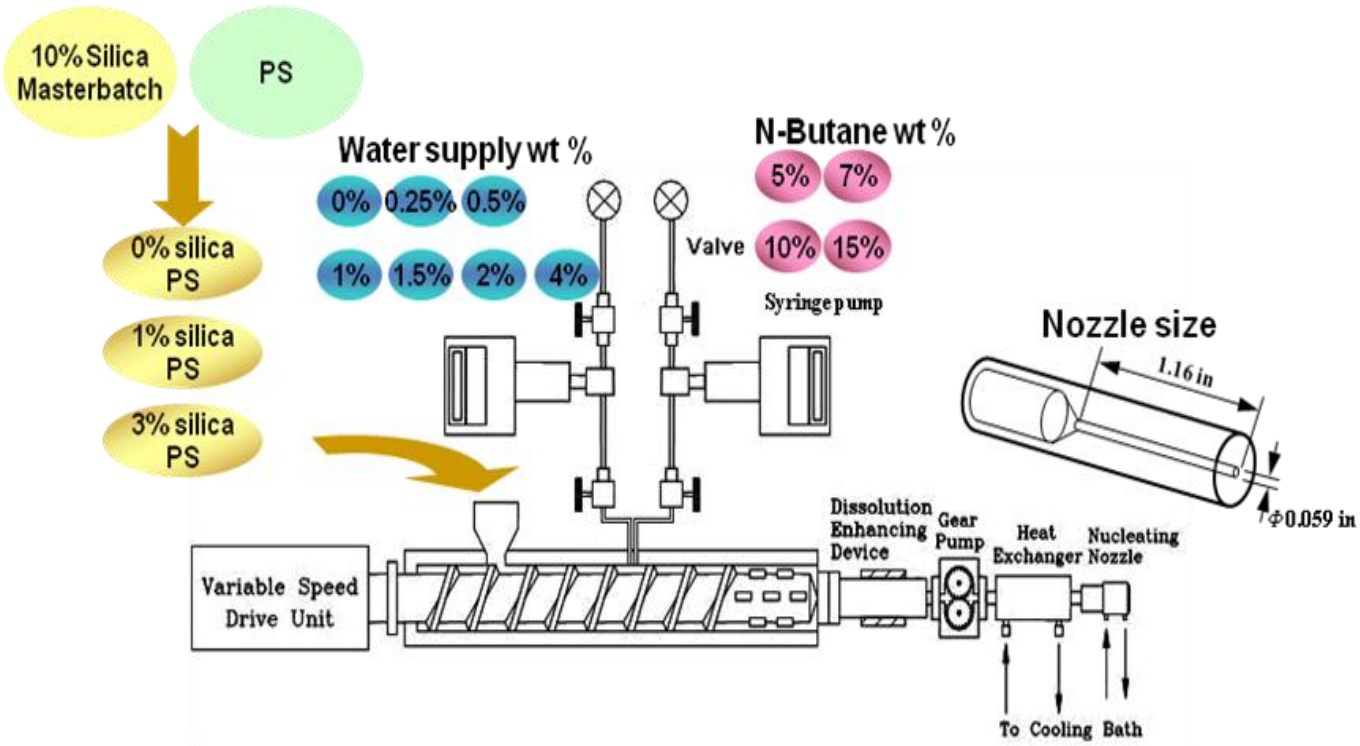

Figure 5.2. Experimental schematic of extrusion foaming with single-screw extruder.

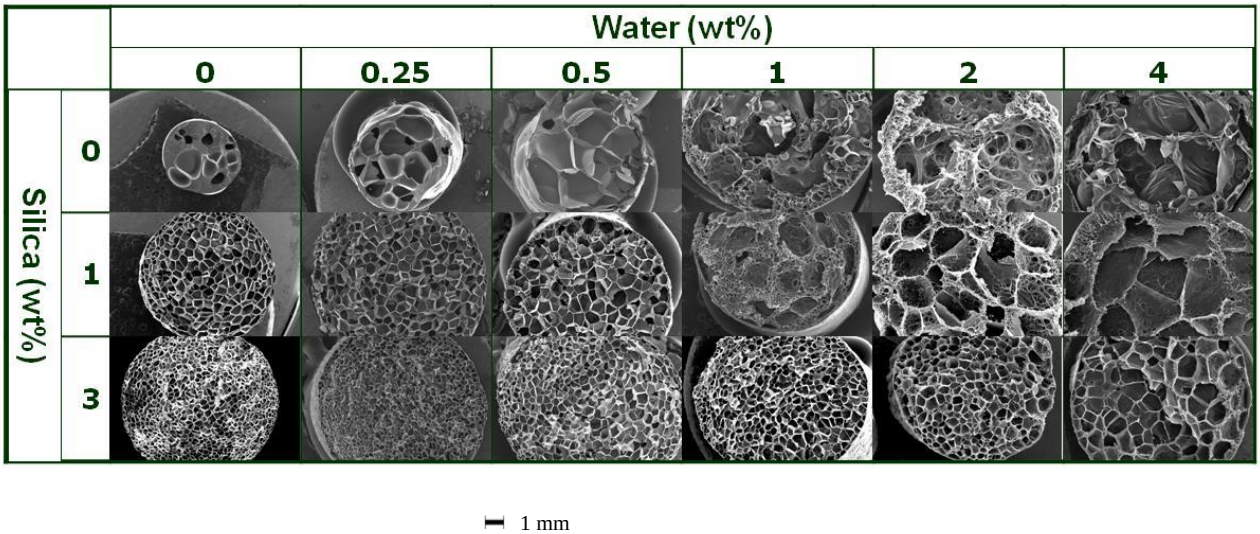

Figure 5.3. SEM micrograph of foamed PS (butane 5% and 120˚C).

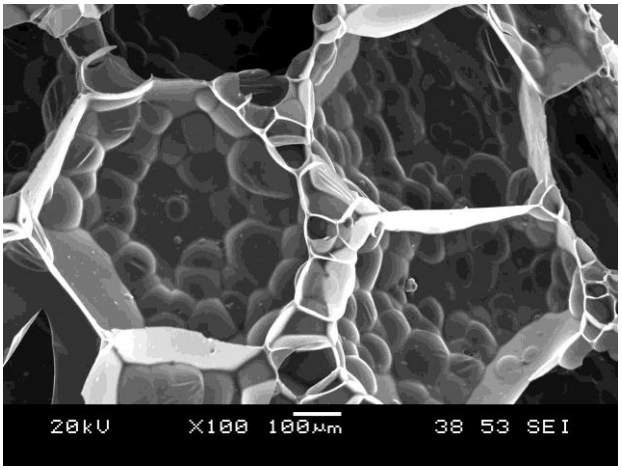

Figure 5.4. SEM micrograph of a foam sample (5% n-butane, 1% water, 3% silica, and 110˚C).

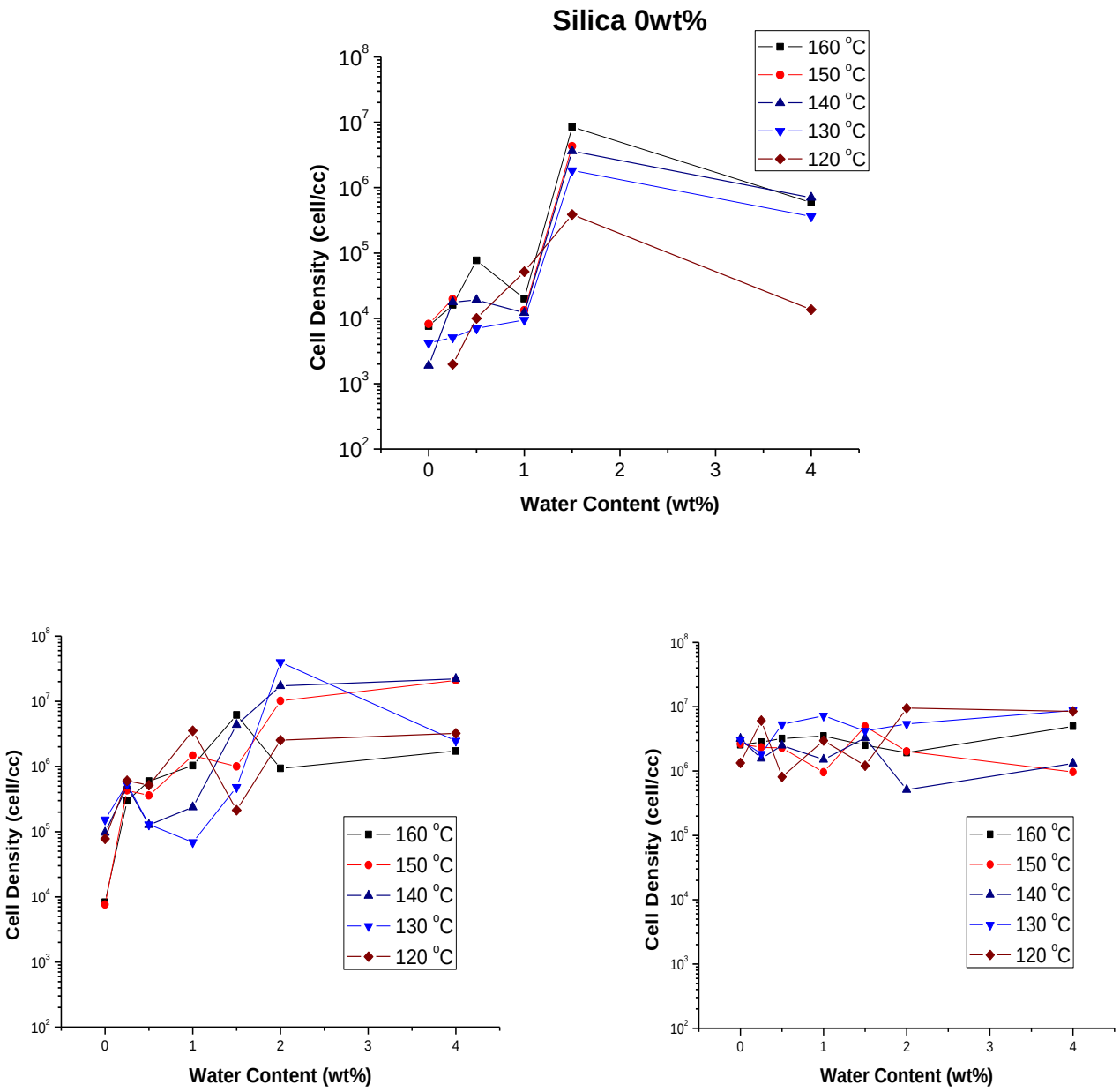

Figure 5.5. Cell density of PS foam depending on die temperature and water content.

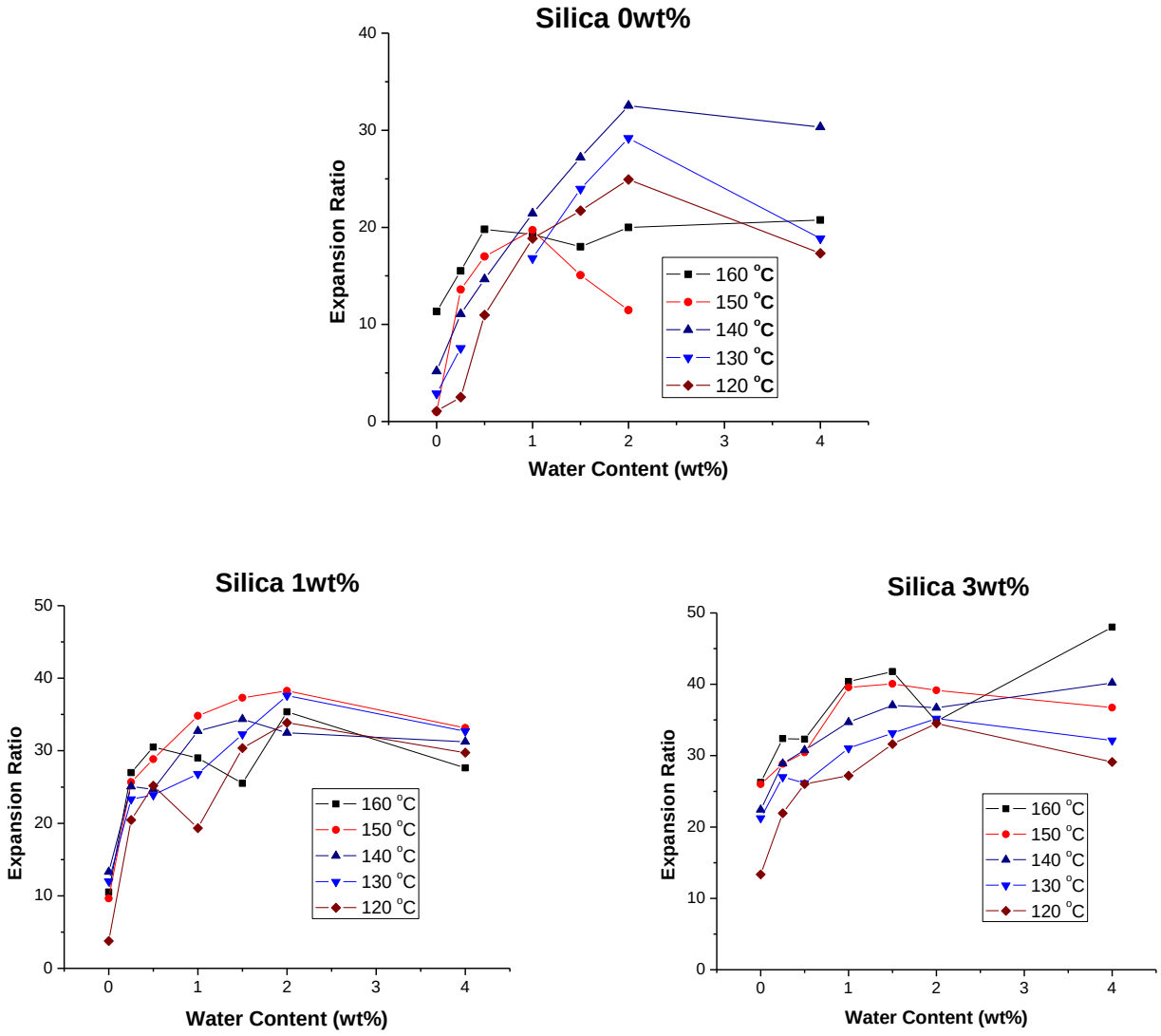

Figure 5.6. Volume expansion ratios of PS foams depending on die temperature and water content.

Chapter 6

Analysis of EPP in an Autoclave Process

This chapter aims at the scientific comprehension of the existing EPP bead manufacturing process. The conventional process features a batch foaming process using an autoclave chamber. In particular, the mechanism of beta crystal formation in PP is studied through literature review as well as the DSC analysis method.

6.1. Manufacturing Procedure of Conventional EPP Beads

The first step of the existing EPP bead manufacturing process is to prepare the unfoamed PP mini-pellets whose diameters are about 1-2 mm using an extruder and a subsequent micro-pelletizer system. In general, random propylene copolymers are utilized as a base resin in the EPP process. Propylene copolymers should be copolymers of propylene containing at least 60 mol % of the propylene monomer, and another co-monomers. Examples of other co-monomers which can be copolymerized with propylene include alpha-olefins other than propylene, such as

1-butene, 1-pentene, and 1-hexene. The propylene copolymer may be a binary copolymer such as a propylene-ethylene copolymer or a propylene-butene copolymer, or a ternary copolymer such as propylene-ethylene-butene copolymer. As cell-nucleating agents, talc or graphite powder is commonly used. Besides the cell-nucleating agent, other functional additives such as UV stabilizers, lubricants, and anti-oxidants should be blended. Depending on their applications, various pigments can be introduced in the mini PP pellets [1, 2].

Following the production of the PP pellets, the next step is the autoclave foaming process. The pellets are mixed with suspension stabilizers and water in a pressure vessel. Frequently sodium dodecylbezene sulfonate or aluminum sulfate is used as a suspension stabilizer to prevent the agglomeration of PP beads in the foaming chamber. The chamber is pressurized with CO_2 or n-butane in order to impregnate the PP pellets floating in the water for about an hour at about 150°C. It is during the impregnation time that another crystal peak whose melting temperature is higher than the impregnation temperature is created in the mini PP pellets in the autoclave. After the saturation of gas in the pellets, the pellets are released from the pressure vessel so that they can expand due to the thermodynamic instability. Typically the bulk density of the foamed PP beads ranges from 14 g/L to 70 g/L. The highly expanded PP beads have to be transferred to another vessel for washing, because there remains a great deal of suspension stabilizers on the surface of PP beads. It is known that the remnant suspension stabilizers can deteriorate the bonding between the PP beads during the steam chest molding process. Therefore the bead washing step is very significant for the ultimate physical properties of PP bead foams [3, 4].

Once the beads have been washed, they are transferred to a flash-drying transfer line to complete the drying process. Subsequently the dried beads are sent into a batch silo and stored until the internal cell pressure reaches the atmospheric pressure [5]. Finally these EPP beads are

sold and transported to bead foam molding manufacturers. Since the bulk density of the EPP beads is extremely low, the transportation cost is quite high.

6.2. Cell Morphology of Conventional EPP Beads

The cellular structure of the current EPP beads features the high closed-cell content which is normally higher than 90% as shown in Figure 6.1. The closed-cell content of the foamed beads can be measured using a pycnometer in accordance to ASTM D6226. The closed-cell structure is imperative in that the sufficient expansion and the strong bonding of EPP beads during the steam chest molding highly depend on the closed-cell content. There is no expecting the high expansion force of the beads without the closed-cell structure. The cell diameters of the EPP beads range from 200-500 μm depending on the bulk density of beads. The cell population density could be 10^5-10^6 cells/cm^3. Cell wall thickness of the commercialized EPP bead could be analyzed using SEM. Several cell wall thicknesses (mainly the middle parts between struts) in a cross-section of a bead were measured. Figure 6.2 revealed that the cell wall thicknesses were 2-4 μm (for 45 fold bead), 4-8 μm (for 30 fold bead), and 12-20 μm (for 15 fold bead), depending upon the volume expansion ratio.

In the batch foaming process, it is relatively more straightforward to achieve the high closed-cell content, because the melt strength is much higher at no shear-force circumstance unlike the case of extrusion foaming. The polymer chain entanglements, which is the fundamental cause of the high viscosity of polymer melt, provides enormous melt strength so that the cell wall can be bi-axially extended without being broken during the drastic cell growth. However, in the case of extrusion foaming, the melt strength is substantially reduced due to the

release of the large number of chain entanglements at the high-shear rate condition. Accordingly it is by far more difficult to obtain the high closed-cell content through the extrusion foaming process. In addition to that, since part of the PP crystals are not melted in the batch foam process, these remnant crystals can behave as cross-linking points that can considerably enhance the overall melt strength of the gas-impregnated mini PP pellets. It implies that there is no superior process to the batch foaming process in terms of acquiring such high closed-cell contents and avoiding cell opening during cell growth.

6.3. Crystallization Characteristics of Conventional EPP Beads

In the conventional EPP process, it is known that a new crystal peak is generated in the PP pellets during the gas impregnation time. Figure 6.3 shows the typical DSC thermograms of the EPP beads manufactured based on batch foaming process using an autoclave [6].

T1 represents the original melting peak of the ethylene-propylene copolymer, whereas the T2 peak was created by impregnating the PP pellets at around 150°C. The newly formed high-temperature crystal peak is inferred to be a kind of beta PP crystals, which is important for maintaining the cellular structure of EPP beads when the beads are steam-chest-molded using high steam temperature. Thus the steam temperature in the steam molding machine should be between the original melting temperature and the beta crystal peak temperature in order to obtain excellent bead foam products. DSC thermograms in Figure 6.4 indicate that the crystal peaks in conventional EPP beads have very similar patterns regardless of the different volume expansion ratios. It is also shown in Figure 6.4 (b) that EPP has only one intrinsic crystal peak around 145 ^{o}C, judging from the fact that the higher temperature peak disappeared when the thermal history

was removed.

6.4. Crystallization Behavior of PP with Additives

6.4.1. Characteristics of Crystals of PP

PP is a semi-crystalline polymer that forms a few kinds of crystals when the molten resin cools down. The most common crystal form of isotactic polypropylene is the alpha, or monoclinic form, which melts around 167 ^{o}C. In an injection molded or extruded part, over 95% of the PP crystals are typically the alpha type [7]. A less common form, known as the beta or hexagonal crystal form, generally accounts for less than 5% of the crystals (Figure 6.5). The beta crystals have a melting point that is typically about 150 ^{o}C (Table 1). One of unique properties of the beta crystalline phase is the fact that when a polypropylene part is deformed past its yield point, the beta crystals undergo a solid state transformation into alpha crystals [8-13]. During this transformation microvoids develop in the deformed region, and the density of the polypropylene part decreases. If a PP sheet having a high level of beta crystallinity is stretched, it turns an opaque white, since the microvoids scatter and reflect most of the light. It is generally believed that the improved impact strength of a beta nucleated molded part is due to both the higher ductility of the beta crystal phase and the additional energy absorption that accompanies the formation of the microvoids [14-16].

6.4.2. Experimental

6.4.2.1. Material and Compounding

Two propylene-ethylene copolymers were utilized in the research. The first polymer was Daploy WB260HMS with a MFI of 2.5 g/10min (ASTM D1238. 230℃/2.16kg) donated by Borealis. The second polymer was a propylene-ethylene copolymer (denoted as J-A) with a MFI of 7.0 g/10min (ASTM D1238. 230℃/2.16kg). As a special additive, T-5 (abbreviated grade name) was compounded with the two copolymers using a Brabender batch mixer at 50 rpm and 180℃ for 5 minutes.

6.4.2.2. DSC Analysis

The crystallization characteristics of all the specimens were investigated using a DSC. Calorimeter model DSC Q2000 from TA Instruments was utilized. Samples for the DSC experiments were taken from the compressed films with a sample size of 10.0~15.0 mg. The samples were heated from room temperature to 180℃ at a ramp of 10℃/min under a nitrogen purge and were kept at this condition for 10 min to remove the thermal history. Then the samples were cooled down to 40℃ at a cooling rate of 10℃/min. Finally, the samples were reheated at 10℃/min to 180℃. During the cooling and heating process, the enthalpy changes during the crystallization and the melting of the samples were recorded. Especially while cooling down the samples, isothermal crystallization was investigated at different temperature and keeping time.

6.4.3. Results and Discussion

6.4.3.1. Beta Crystallization in Pure PP Copolymers

The effect of cooling rate on the formation of beta crystals in pure WB260 and J-A was investigated. Figure 6.6 shows the second heating scans of two copolymers right after cooling

step at various cooling rates in DSC. It is obvious that the change of cooling rates did not lead to the significant formation of beta crystals in the two copolymers. WB260 alone was observed to form a small beta crystal peak around 135℃ at the very low cooling rate of -1℃/min. Therefore it turned out that the two copolymers tend to preferably form the alpha crystals at all cooling conditions without any additives.

6.4.3.2. Effect of T-5 Content on Beta Crystallization

T-5 as an additive was compounded to make different compositions of 0.1, 0.3, 0.5 and 1.0 phr in the two copolymers. Figure 6.7 represents that there was no significant effects of the addition of T-5 on the beta crystal formation in WB260 regardless of the T-5 contents. On the other hand, J-A showed quite different crystallization behaviors fromWB260. The formation of beta crystals was linearly proportional to the T-5 content as displayed in Figure 6.8. The reason why the two copolymers resulted in the different crystallization behaviors is presumably due to the fact that WB260 is a branched polypropylene. The branched molecular structure may be unfavorable to generate the beta crystals in PP.

6.4.3.3. Effect of Cooling Rate on Beta Crystallization

Generally the cooling rate is crucial for the crystallization characteristics of polymers. Therefore the cooling rate was changed at -1℃/min, -10℃/min, -20℃/min, -30℃/min, and -50℃/min. After the cooling at different cooling ramps, the second heat scans were recorded as shown in Figure 6.7 and Figure 6.8. WB260 did not make remarkable effects of cooling rates. It is notable that the slowest cooling (-1℃/min) of WB260 containing varied T-5 contents exhibited a small peak of beta crystals just as the pure WB260 did. However J-A showed obvious

dependence of beta crystallization on the cooling rate at the same T-5 contents. The area of the beta crystal peak increased at all compositions of J-A, as the cooling ramp decreased. The much higher viscosity of WB260 seems to retard the beta crystal formation, whereas the low viscosity of J-A is believed to be favorable for it. It is interesting that the formation of beta crystals gets relatively more dominant at slower cooling conditions of J-A. It means that the lower cooling rate can provide more time for the growth of beta crystals in J-A. It is believed that the longer time is needed for the growth of beta crystals presumably due to the slow epitaxial crystallization effect of T-5.

6.5. Summary

The characteristics of the existing EPP bead were analyzed in the aspect of the cellular structure and crystallization behaviors. Since the high closed-cell content is critical for EPP beads, it is of importance that the melt strength should be high enough to prevent the cell opening during the cell growth. It is true that extrusion foaming is very difficult to get high closed-cell contents due to the severely high shear forces in the extruder. The batch process can easily make closed-cell foams because the newly formed crystals behave like a long-chain branching or cross-linking points to increase the melt strength.

When it comes to the formation of beta crystals in the conventional EPP bead, it is attributed to the gas impregnation period at an elevated temperature in the autoclave process. The effect of blending a functional additive in two PP copolymers on the beta crystallization behaviors was investigated.

6.6. References

[1] J. Schweinzer, J. Fischer and W. Kogel, U.S. Patent 5,703,135–Detailed description (1997)

[2] F. Braun, U.S. Patent 6,723,760 (WO 01/772139)- Description of Preferred Embodiments (2004)

[3] H. Sasaki, M. Sakaguchi, and M. Akiyama, U.S. Patent 6,313,184-Detailed description of the invention (2001)

[4] F. Braun, G. Gluck, K. Hahn and H. Tatzel, U.S. Patent 6,677,040-Detailed description of the invention (2004)

[5] H. Sasaki, K. Ogiyama, A. Hira, K. Hashimoto and H. Tokoro, U.S. Patent 6,838,488-Description of Preferred Embodiments (2005)

[6] H. Sasaki, A, Hira and H. Tokoro, U.S. Patent 2003/0162012 A1 – Description (2003)

[7] J. Varga, I Mudra, and G. W. Ehrenstein, *J. Appl. Polym. Sci.*, 74, 2357-2368 (1999)

[8] J. Varga, *J. Macromolecular Science, Part B, Physics*, 41, 1121 (2002)

[9] Y. F. Zhang, Z. Xin, *J. Polymer Science, Part B, Physics*, 45, 590 (2007)

[10] A. Marcincin, A. Ujhelyiova, K. Marcincin and P. Alexy, *J. Thermal Analysis*, 46, 581-595 (1996)

[11] A. J. Lovinger, J. Chua, and C. C. Gryte, *J. Polymer Science: Polymer Physics Edition*, 15, 641-656 (1977)

[12] P. Jacoby, B. H. Bersted, W. J. Kissel, and C. E. Smith, *J. Polymer Science: Part B. Polymer Physics*, 24, 461-491 (1986)

[13] W. P. Zhu, G. P. Zhang, J. Y. Yu, and G. Dai, *J. Applied Polymer Science*, 91, 431–438

(2004)

[14] J. Weng, R. H. Olley, D. C. Bassett, and P. Jaaskelainen, *J. Polymer Science: Part B: Polymer Physics*, 42, 3318–3332 (2004)

[15] J. T Xu, P. J. Ding, Z. S. Fu and Z. Q. Fan, *Polymer International*, 53, 1314–1320 (2004)

[16] A. T. Es, J. M. Aizlewooda, and D. R. Beckett, *Makromolecular Chemistry*, 75, 134-158 (1964)

Table 6.1. Characteristics of α and β crystals in isotactic polypropylene

Crystal	Form	Crystallization temperature	Melting temperature	Density（g/cm^3）
α	Monoclinic	112 ^oC	162~ 168 ^oC	0.936
β	Hexagonal	130 ^oC	148~ 152 ^oC	0.921

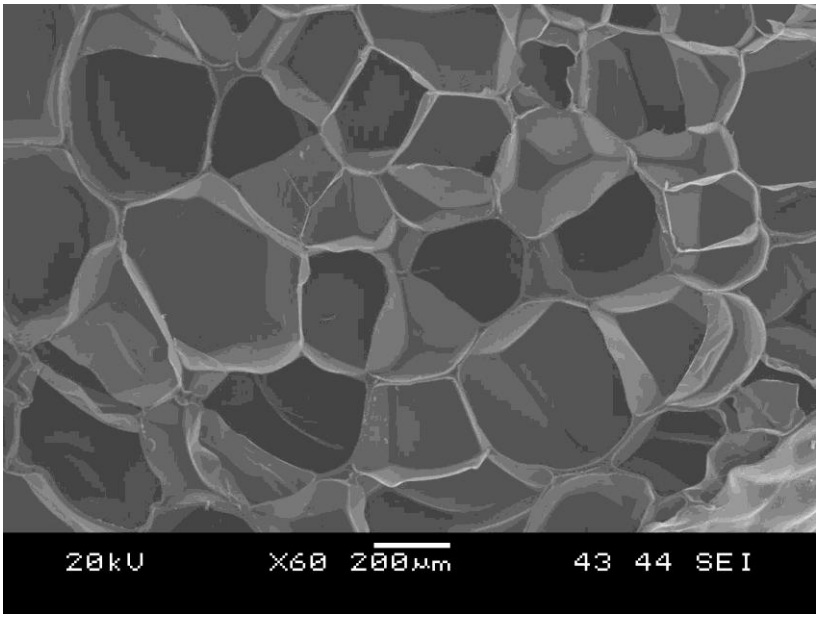

Figure 6.1. SEM micrograph of a cross-section of an EPP bead made from the autoclave foaming process.

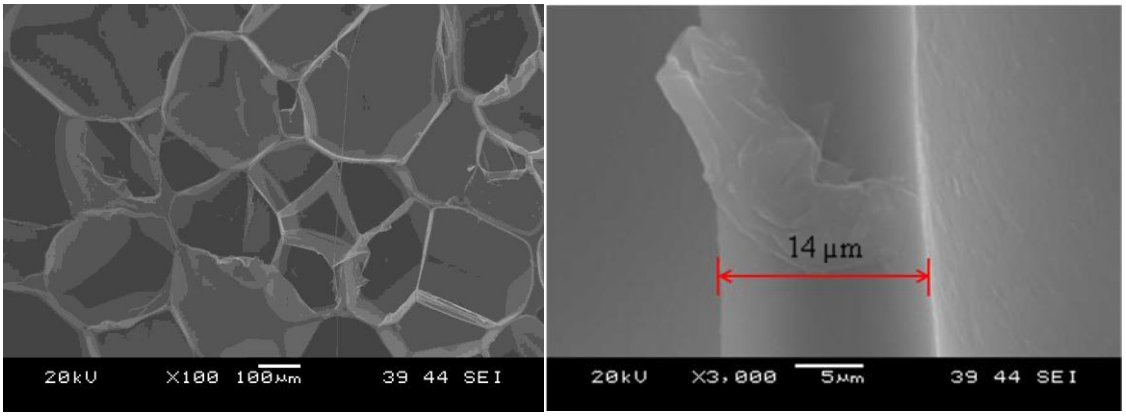

(a) 15 fold bead

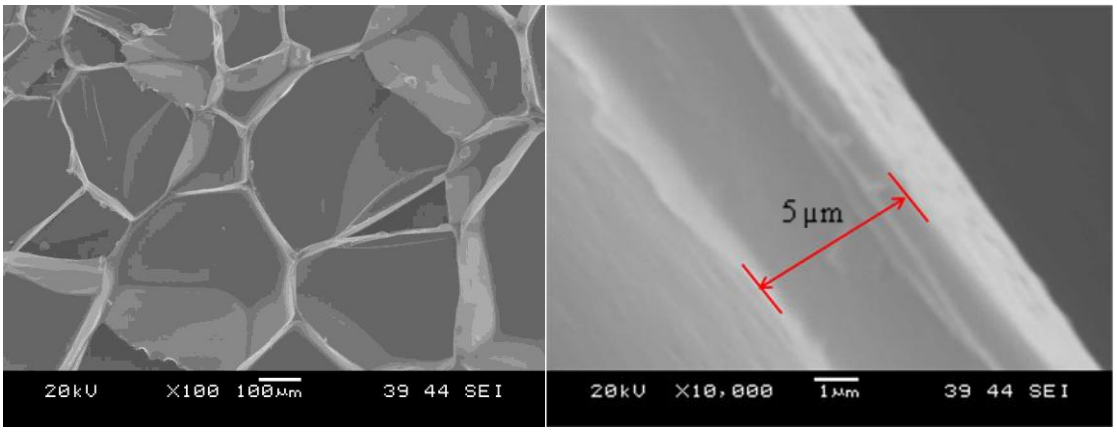

(b) 30 fold bead

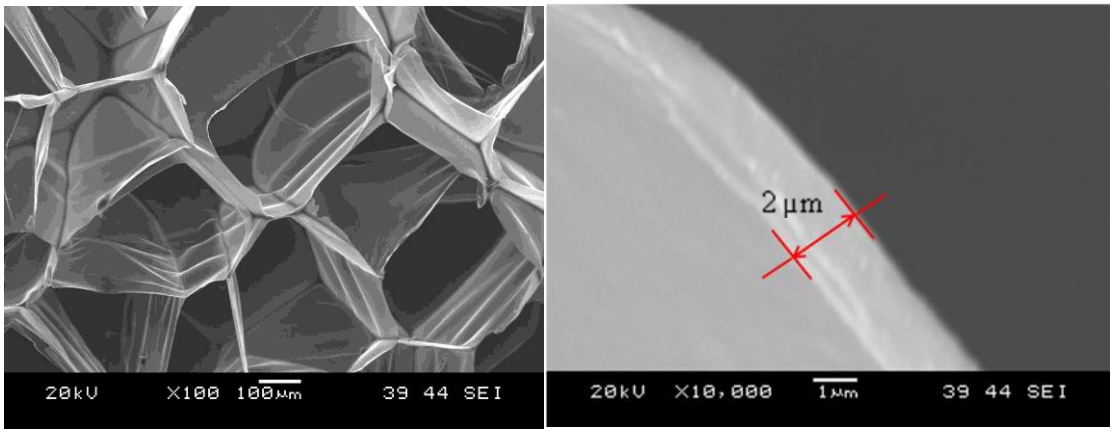

(c) 45 fold bead

Figure 6.2. Cell wall thicknesses of EPP beads with different volume expansion ratios; (a) 15, (b) 30, and (c) 45 fold beads.

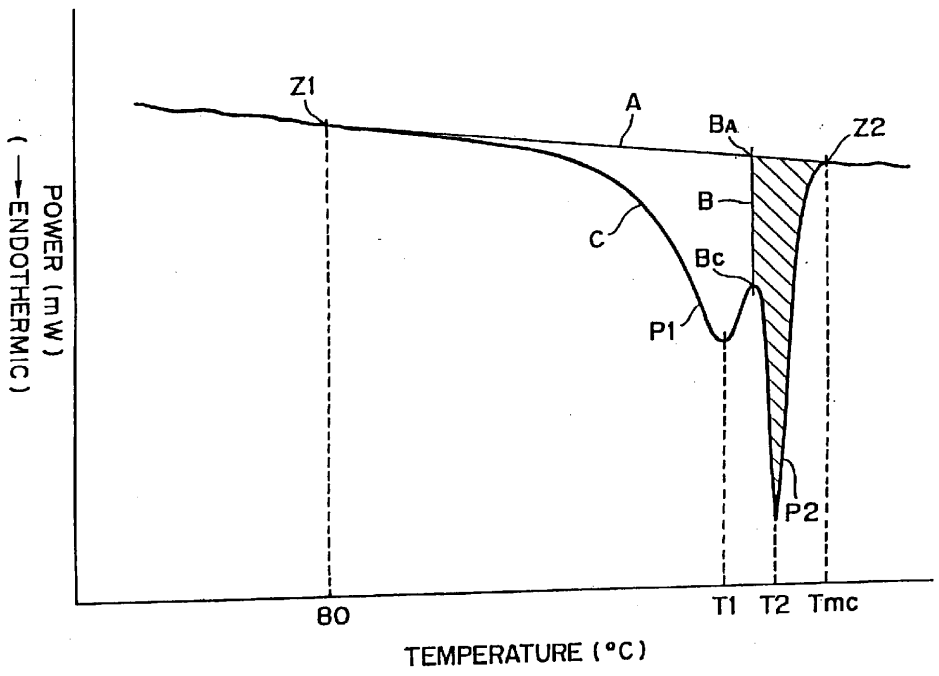

Figure 6.3. Crystallization in EPP beads during the gas impregnation in an autoclave process [6].

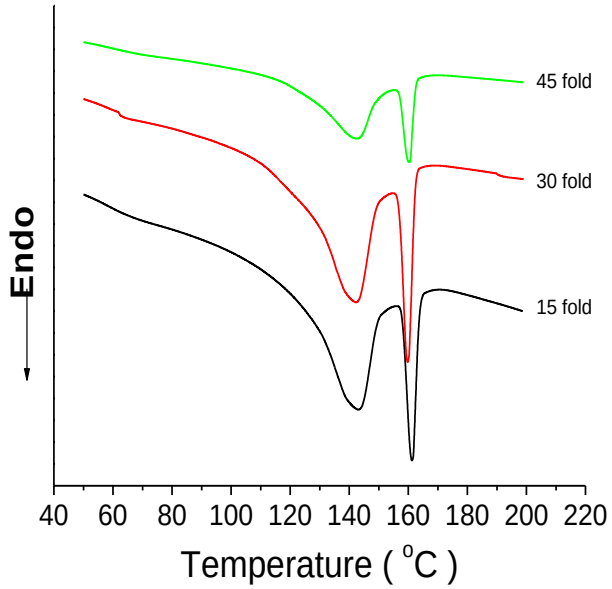

(a)

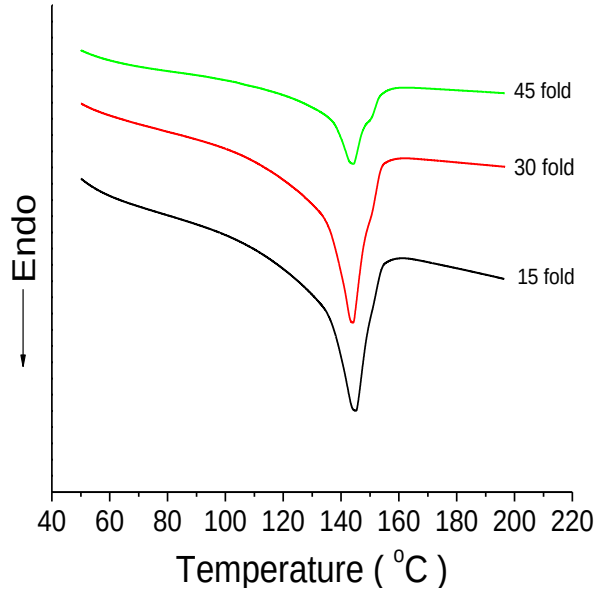

(b)

Figure 6.4. DSC thermograms of conventional EPP beads made from an autoclave process; (a) first heating scan, and (b) second heating scan (5°C/min for both scans).

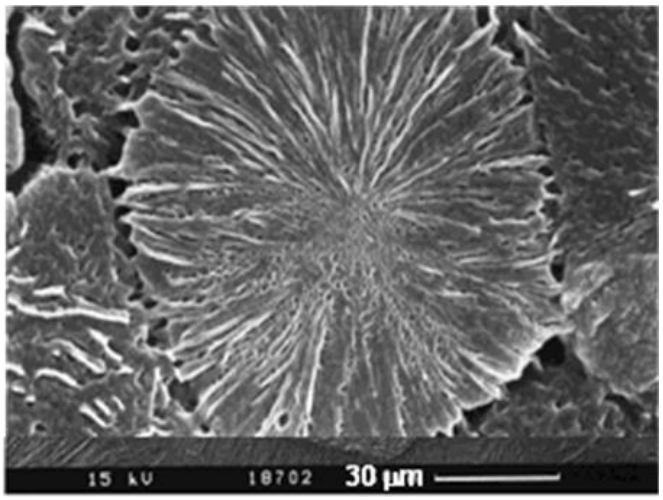

(a) α crystal

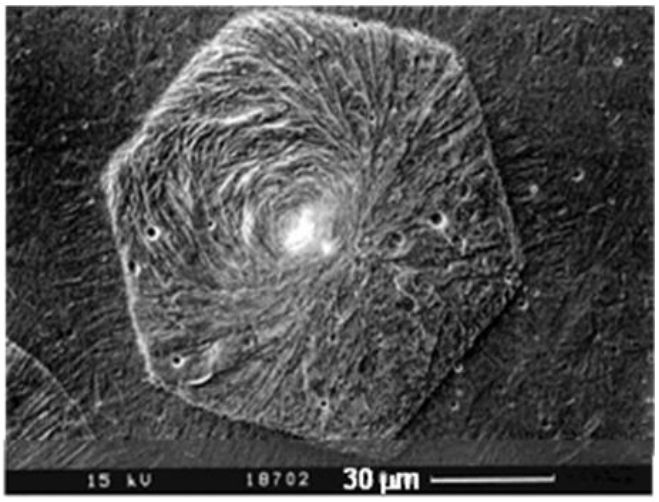

(b) β crystal

Figure 6.5. SEM micrographs of α and β crystals of PP [7].

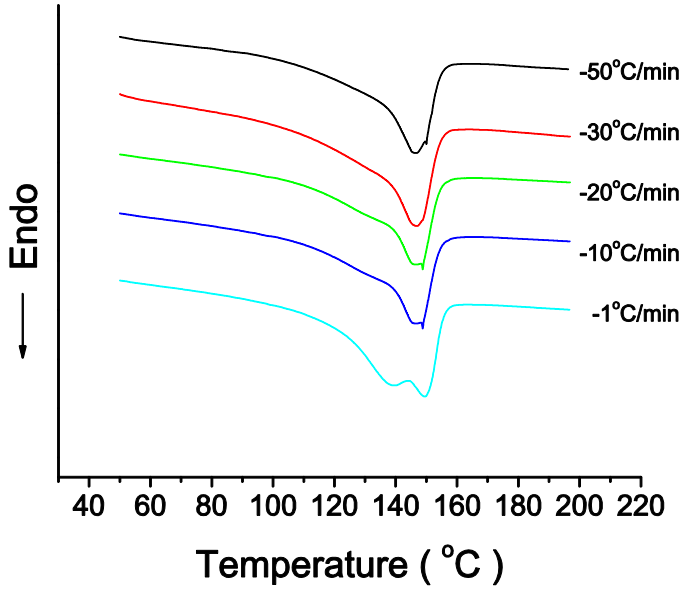

(a) WB260

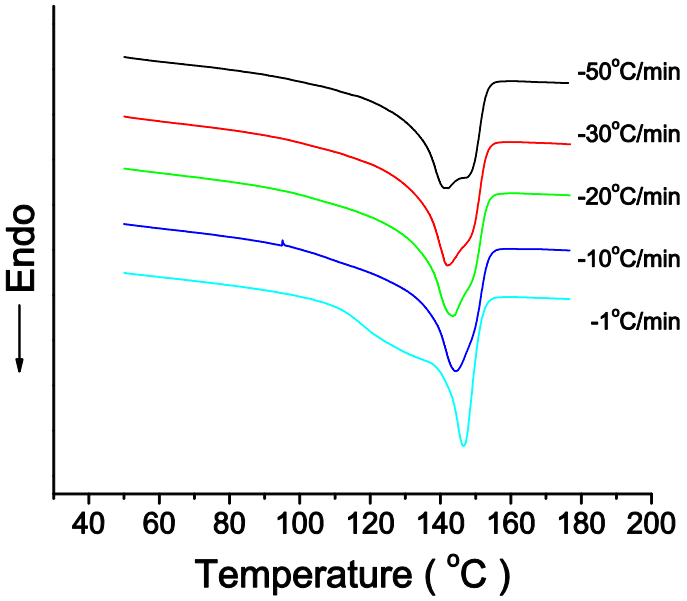

(b) J-A

Figure 6.6. DSC thermograms of 2nd heating scan of pure copolymers that were cooled down at different cooling rates; (a) WB260 and (b) J-A.

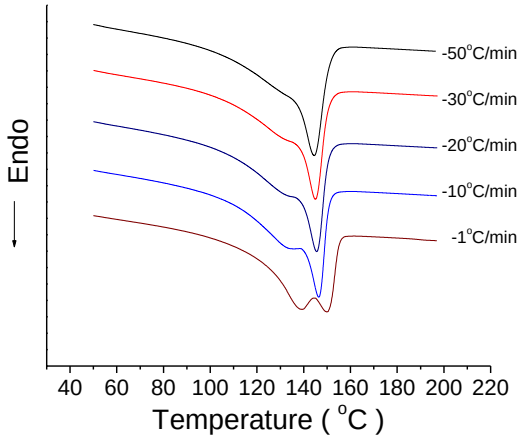

(a) 0.1 phr

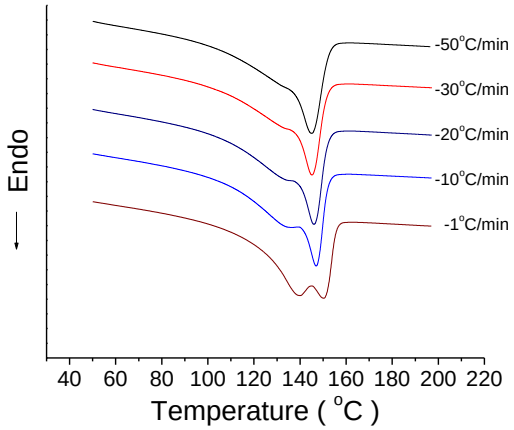

(b) 0.3 phr

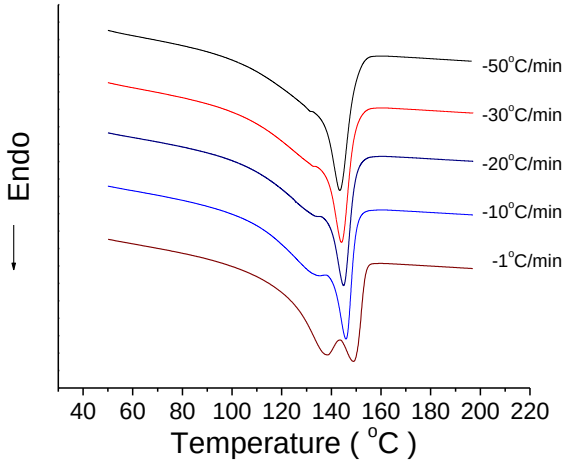

(c) 0.5 phr

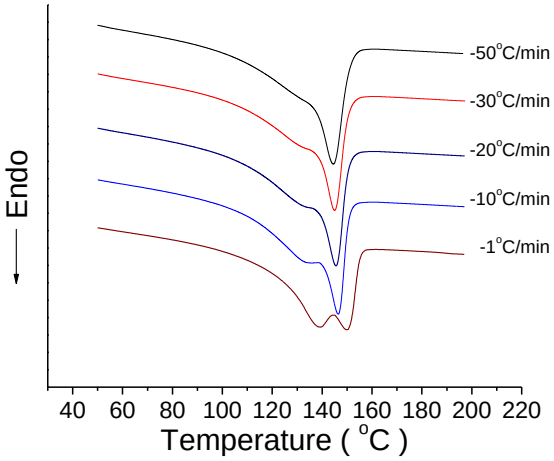

(d) 1.0 phr

Figure 6.7. DSC thermograms of 2nd heating scan of WB260 with various T-5 contents; a) 0.1 phr, b) 0.3 phr, c) 0.5 phr and d) 1.0 phr after crystallization at different cooling rates.

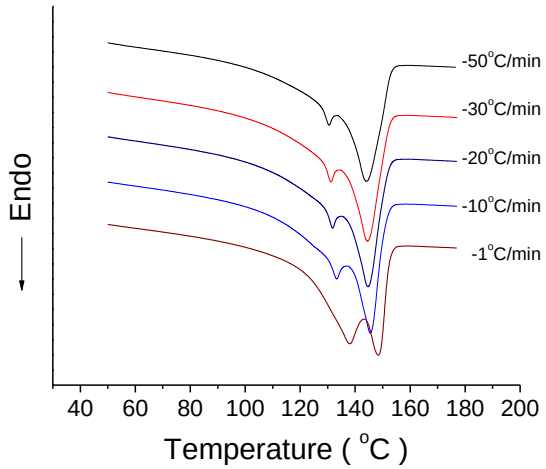

(a) 0.1 phr

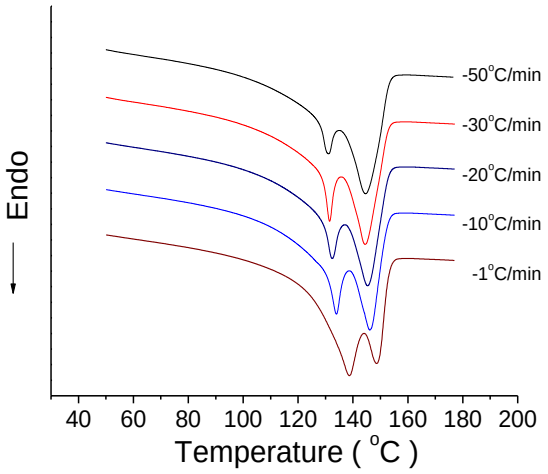

(b) 0.3 phr

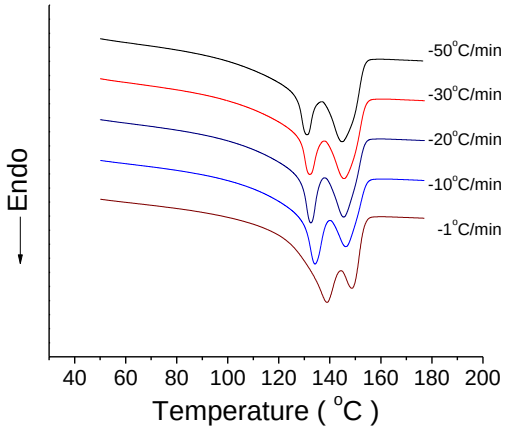

(c) 0.5 phr

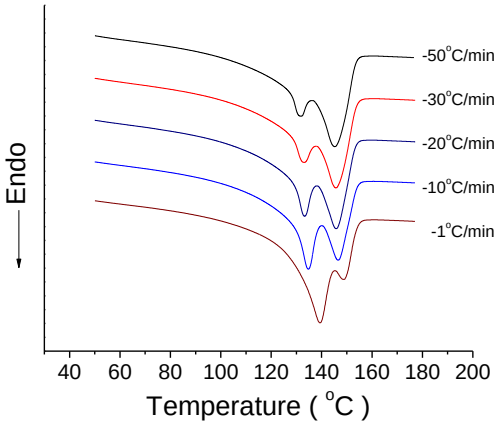

(d) 1.0 phr

Figure 6.8. DSC thermograms of 2nd heating scan of J-A with various T-5 contents; a) 0.1 phr, b) 0.3 phr, c) 0.5 phr and d) 1.0 phr after crystallization at different cooling rates.

Chapter 7

Extrusion Foaming of Propylene-Ethylene Copolymers for EPP Application

7.1. Introduction

Expanded polypropylene (EPP) bead foam is widely used in various industry areas; automotive parts, high-end packaging, and toys. EPP bead foam can provide highly resilient property as well as diversified geometry with very low density. Conventional manufacturing process of EPP bead is a batch foaming process in which solid polypropylene (PP) pellets should be impregnated with a physical blowing agent for about 1 hour. The low productivity from the batch process is one of the reasons why EPP beads are very expensive in industry. Therefore continuous extrusion foaming is believed a viable alternative process for manufacturing EPP beads. On the other hand, PP copolymer is more appropriate than homo PP for EPP application in that homo PP generally shows inferior impact property at low temperature [1-4]. Specifically, PP copolymers can be divided into random copolymer and block copolymer. It is known that a propylene-ethylene copolymer has random configuration of two monomers in the main backbone of polymer chains, because the polymerization reaction gets started with two mixed monomers from the beginning. Whereas a propylene-

ethylene block copolymer is polymerized through stepwise process in which homo PP polymerized in the first stage is blended with the two monomers for the second stage to polymerize ethylene-propylene rubber (EPR) in the matrix of homo PP [5-13].

However few researches on foaming behavior of the two copolymers have been reported. When it comes to foaming of homo PP, it is known that PP has weak melt strength and narrow processing window compared to other commodity polymers. When the melt strength of a polymer is weak, the cell walls separating the bubbles may not have enough strength to bear the extensional force and may rupture easily during foaming. When cell coalescence takes place, not only are the cell density and cell size uniformity deteriorated, but also the volume expansion ratio is greatly sacrificed due to the accelerated gas loss through ruptured cell walls. As a result, homo PP foams usually have high open-cell content and thus are unsatisfactory for many applications [14-21].

In this study, research focus was about the feasibility of two propylene-ethylene copolymers, a random copolymer (RC-PP) and a block copolymer (BC-PP), for continuous manufacturing process of EPP beads by carrying out extrusion foaming using n-butane as a blowing agent. Talc was used as a nucleating agent to enhance the cell population density based on heterogeneous bubble nucleation.

7.2. Experimental

7.2.1. Material and Compounding

As base materials in this study, RC-PP (R200P) and BC-PP (BA212E) were supplied by Hyosung Corp. and Borealis Gmbh respectively. The two resins have the same melt flow index of 0.3 g/10min (ASTM D1238, 230℃/2.16 kg).

As a nucleating agent for the extrusion foaming, talc (Cimpact CB7, Luzenac) was utilized. The talc was compounded along with the two copolymers using an intermeshing co-

rotating twin-screw extruder (W&P ZSK-30, 40:1 L/D, 30mm Ø). The screw rotating speed was 250 rpm and the extrusion temperature was 180℃. The blowing agent used in this study was n-butane (BOC Canada, 99%).

7.2.2. Surface Etching Experiment

As to the two copolymers, solvent etching experiment was executed using n-pentane. The first step is to make cross-sections of two pure resins by breaking the compression-molded samples after dipping in liquid nitrogen. Subsequently the two fractured samples were soaked in the liquid n-pentane for 3 days in an ambient condition. Subsequently the specimens were rinsed and dried. SEM analysis was conducted to observe the change of fracture surface of the two polymers.

7.2.3. Thermal Analysis

The thermal property of the two copolymers was investigated using a differential scanning calorimetry (DSC). Calorimeter model DSC 2910 from TA Instruments was utilized. Samples for the DSC experiments were taken from the initially received pellets with a sample size of 10.0 mg. The samples were heated from room temperature up to 200℃ and then maintain for 10 minutes to eliminate the thermal history. Subsequently the samples were cooled down at a ramp rate of 10℃/min under a nitrogen purge and then second heating and second cooling were performed at a ramp of 10℃/min and -50℃/min respectively. During the second heating and cooling processes in the DSC analysis, the melting and crystallization thermograms of the two copolymers were recorded.

7.2.4. Extensional Viscosity Measurement

Given that the rheological property is critical in polymer foaming, measurements of uniaxial extensional viscosity of two copolymers, RC-PP and BC-PP, were performed using an Extensional Viscosity Fixture (EVF, TA Instrument Inc.) attached to the ARES rheometer (Figure 7.1). The design of this device has been introduced by other researchers [22-23]. Rectangular samples of 18 mm x 10 mm x 0.8 mm in dimensions were prepared with a compression molding machine. Values of uniaxial extensional viscosity were obtained varying the temperature at three different extensional rates of 0.5, 1.0, and $3.0s^{-1}$. Since the melting temperatures of two copolymers are about 20℃ apart, RC-PP was measured at 155℃ and 165℃, whereas BC-PP was tested at 175℃ and 185℃.

7.2.5. Experimental Set-up and Procedure

Figure 7.2 shows a schematic of a single-screw foam-extrusion system used in this study. This machine consists of a 5 hp extruder drive with a speed-control gearbox, a ¾" single screw extruder (Brabender 05-25-000, Germany), a mixing screw of 30:1 L/D ratio (Brabender 05-00-144), two positive displacement equipments (ISCO syringe pump 260D), a gear pump (Zenith, PEP-II 1.2 cc/rev) for controlling the melt flow rate, a heat exchanger containing homogenizing static mixers (Labcore, model H-04669-12) for homogenizing the melt temperature, a gas injection port for injecting the blowing agent, six band heaters, four pressure transducers (Dynisco PT462B-10M-6/18) for detecting the pressure at several locations, and six temperature controllers and six thermocouples for controlling the temperatures of the extrusion barrel, the mixer, the heat exchanger, the gear pump and the die. Both the shaping and foaming were done in the filamentary die. The die diameter was 1.5 mm and the channel length was 6.0 mm. The designated amount of n-butane (i.e., 5 and 10 wt%) was then injected into the extrusion barrel using a syringe pump while the PP

copolymer resin was being fed into the hopper of single-screw extruder. The mixing screw and the static mixer generated a shear field to completely dissolve the blowing agent in the polymer melt. The single-phase polymer/gas solution went through the gear pump and was fed into the heat exchanger where it was cooled to the desired temperature. The cooled polymer/gas solution entered the die and experienced a rapid pressure drop. This rapid pressure drop caused a sudden decrease in the solubility of n-butane in the polymer, and hence a large number of bubbles were nucleated almost instantaneously in the polymer matrix and a cellular foam structure was created.

7.2.6. Foam Characterization

As for foam characterization, the collected foam samples were randomly chosen, and examined for acquiring the microstructure using a SEM (JEOL, JSM-6060). The foam samples were dipped in liquid nitrogen and then fractured to expose the cellular structure. The fractured surface was then coated with gold and the microstructure of the cross-section was obtained through the SEM. The volume expansion ratio of each sample was calculated as the ratio of the density of the original sample (ρ_0) to the measured density of the foam sample (ρ_f). The cell population density (N_f), the number of cells per cubic centimeter, was estimated by the Equation (7.1), where the area of the micrograph was A cm^2, the number of cells, n, and the magnification factor M.

$$N_f = \left(\frac{nM^2}{A} \right)^{3/2} \times \frac{\rho_0}{\rho_f} \tag{7.1}$$

The open-cell content of the foam samples was quantified using a gas pycnometer (Quantachrome Co.). The open-cell content is a porosity determined by calculating the ratio of gas-accessible cellular volume to the remaining volume occupied by closed cells and cell walls. In order to obtain the open-cell content (*OC*), the geometric volume (V_{geo}) and the

displacement volume (i.e., solid volume) (V_{dis}) of a foam sample should be determined. The geometric volume (V_{geo}) is determined by the measurement of the sample weight using a balance and a foam density based on the water displacement method described in ASTM D792-00. The displacement volume (V_{dis}) can be obtained using a gas pycnometer in accordance with ASTM D6226-98. The gas pycnometer consists of two chambers, with known volumes, connected by a valve. One of the chambers, the calibrated sample chamber, can be accessed for the insertion of the test sample and is connected to a high-purity gas source. The pressure in the sample chamber is increased to a predetermined pressure (P_1). The valve between the two chambers is then opened and the accordingly reduced pressure (P_2) is recorded. The ratio of the pressure change, P_1/P_2, is directly related to the volume of the sample chamber displaced by the specimen (i.e., due to the volume of closed cells and cell walls). This displacement volume (V_{dis}) can be calculated as follows:

$$V_{dis} = V_{chamber} - \frac{V_{\exp}}{\frac{P_1}{P_2} - 1} \tag{7.2}$$

where $V_{chamber}$ is the volume of the sample chamber and V_{exp} is the volume of non-accessible chamber. As described in ASTM D6226-98, the open-cell content can be calculated as shown in Equation (7.3).

$$OC = \frac{V_{geo} - V_{dis}}{V_{geo}} \times 100 \tag{7.3}$$

From the open-cell content, the ultimate closed-cell content (CC) can be acquired using Equation (7.4).

$$CC = 100 - OC \tag{7.4}$$

7.3. Results and Discussion

7.3.1. Surface Etching

Figure 7.3 shows two distinctive cross-sections of two copolymers following the etching experiment with n-pentane. RC-PP (R200P) does not exhibit any voids on the surface, which indicates that RC-PP is a homogeneous-phase polymer. On the other hand, the etched of BC-PP (BA212E) shows a number of tiny voids on the surface whose diameters are less than 1 mm. It is believed that n-pentane extracted the ethylene-propylene rubber phase embedded in the matrix of homo polypropylene to make lots of fine voids. Taking the stepwise polymerization process of BC-PP into account, the surface etching experiment indicates that BC-PP has heterogeneous phase rather than homogeneous phase.

7.3.2. Melting and Crystallization Temperature

In Figure 7.4, the melting and crystallization temperatures of RC-PP and BC-PP are shown in the DSC thermograms. RC-PP exhibited the melting peak at ~143 ^{o}C, and that of BC-PP was detected at ~164 ^{o}C. From the cooling curves on the DSC thermograms, the crystallization peak temperatures were 89°C and 118 ^{o}C for RC-PP and BC-PP respectively.

7.3.3. Extensional Viscosity

Measurements of the uniaxial extensional viscosities were made using the Extensional Viscosity Fixture attached to the ARES rheometer. Considering the fact that the two copolymers have different melting temperatures by about 20°C, RC-PP was characterized at 155°C and 165°C, whereas BC-PP was tested at 175°C and 185°C. Values of the uniaxial extensional viscosities are presented in Figure 7.5. The RC-PP does not exhibit strain hardening regardless of temperature and the strain rate. BC-PP also shows no significant

strain hardening behavior in most conditions. However only high strain rate, 3 s^{-1}, induces strain hardening at 175 ^{o}C, which will be beneficial to achieve higher closed-cell content. This strain hardening only at high strain rate is attributed to shorter relaxation time of polymer chains during the extension. It is known that cell growth normally leads to high strain rate in the melt [24].

7.3.4. Cell Nucleation Behavior

As exhibited in Figure 7.6 (a) and (b), BC-PP shows much higher cell population density than RC-PP when no nucleating agent is introduced. It seems that the ethylene-propylene rubber phase dispersed in BC-PP plays a role of a cell-nucleating agent. In contrast, RC-PP is believed to undergo homogeneous cell nucleation without talc, which is why the cell population density is lower than BC-PP. Figure 7.7 shows the effect of die temperature, talc content, and n-butane content on cell population density. In case of RC-PP, the cell density proportionally increased with increasing talc content for 5% n-butane. For 10% n-butane, even small amount of added talc (i.e., 0.5 phr) dramatically enhanced the cell population density by more than one order of magnitude. As to BC-PP, 10^5 cells/cm^3 was achieved without talc probably due to heterogeneous nucleation effect of the dispersed phase. Therefore the effect of talc on cell population density was relatively less significant in BC-PP than RC-PP. It turned out that the effect of die temperature on cell nucleation was not prominent in most experimental conditions.

7.3.5. Volume Expansion Behavior

Figure 7.8 exhibits that the maximum volume expansion ratio of BC-PP foam is greater than that of RC-PP foam at both the blowing agent contents. It is well known that volume expansion ratio is a sensitive function of melt temperature [25]. For 10% n-butane, the

optimum temperatures for high expansion ratio were 130℃ and 140℃ respectively. As the talc content increases, the expansion ratio was reduced in most conditions. It is inferred that gas loss through cell-to-cell gas diffusion may become more significant as cell population density increases in the foam.

7.3.6. Closed-Cell Content

In Figure 7.9, the closed-cell contents of foamed samples were plotted for different compositions and die temperature. In the case of 5 wt% n-butane, no significant trend was observed. However, the closed-cell content was dramatically decreased with the increasing die temperature for 10 wt% n-butane. It is believed that strong plasticization effect of large amount of the blowing agent could substantially reduce melt strength of polymers. Therefore cell opening could be dominant especially at high temperature. The maximum closed-cell content of BC-PP was 92%, whereas that of RC-PP was 80%.

7.4. Summary

In this chapter, the random and block propylene-ethylene copolymer foams were manufactured through extrusion foaming process. From the experimental results, the effect of die temperature, n-butane and talc content on foaming behaviors were investigated. The surface etching experiment showed that RC-PP and BC-PP could be homogeneous and heterogeneous phase resin respectively, which could account for why two copolymers exhibited different cell nucleation behaviors. It was observed that cell population density proportionally increased with talc content for RC-PP, whereas the effect of talc was not prominent for BC-PP. Regarding the volume expansion ratio, it turned out that BC-PP was more favorable than RC-PP. When it comes to the closed-cell content, 92% could be

achieved from BC-PP foam. It means that BC-PP is more appropriate than RC-PP for EPP bead foam application where closed-cell structure is strongly preferred.

7.5. References

[1] L. J. Gibson and M.F. Ashby, *Cellular Solids: Structure and Properties*, Cambridge University Press, New York (1997)

[2] S. C. Tjong, and S. A. Xu, *Polym. Int.*, 44: 95 (1997)

[3] J. Ito, K. Mitani and Y. Mizutani, *J. Appl. Polym. Sci.*, 46:1221 (1992)

[4] T. Yamaguchi, M. Yamaguchi, and K. Senda, *U.S. Patent* 6,355,696 (2002)

[5] E. P. Moore, *Polypropylene handbook*, Hanser, 149–164, New York (1996)

[6] Union Carbide Corporytion Technical manual, vol IV. Product technology. Union Carbide Corporation, Danbury (1986)

[7] T. Nomura, T. Nishio, H. Sato, and H. Sano, *Kobunshi Ronbunshu*, 50, 27 (1993)

[8] T. Nomura, T. Nishio, S. Moriya, and M. Hashimoto, *Kobunshi Ronbunshu*, 51:569 (1994)

[9] L. Dorazio, C. Mancarella, E. Martuscelli, and G. Sticotti, *Polymer*, 34:3671 (1993)

[10] K. Nitta, T. Kawada, M. Yamahiro, H. Mori, and M. Terano, *Polymer*, 41:6765 (2000)

[11] J. Ito, K. Mitani, and Y. Mizutani, *J. Appl. Polym. Sci.*, 46:1235 (1992)

[12] D. J. Walsh, and J. S. Higgins, *Macconachie A, Polymer blends and mixtures*, Imperial College, London, 219 (1985)

[13] I. Fumio, *Practical polymer alloy design. Industrial Investigation*, Tokyo, 119–135 (1998)

[14] D. Klempner, and K. C. Frisch, *Handbook of Polymeric Foams and Foam Technology*, NY, 266 (1991)

[15] C. B. Park, V. Padareva, P. C. Lee, and H. E. Naguib, *Journal of Polymer Engineering*, 39, 3, 239-260 (2004)

[16] C. R. Thomas, *The Formation of Cellular Plastics. Br. Plast.* 38, 552 (1965)

[17] B. I. Chaudhary, and R. P. Barry, *Foams*, 99, 19 (1999)

[18] K. Kaji, M. Hatada, I. Yoshizawa, and C. Kohara, *J. Appl. Polym. Sci*., 37, 2153 (1989)

[19] M. L. Kozma, J. D. Bambara, and R. F. Hurley, *U.S. Patent* 5,859,076 (1999)

[20] B. I. Chaudhary, and B. A. Malone, *U.S. Patent* 5,962,545 (1999)

[21] S. Abe, *U.S. Patent* 6,414,047 B1 (2002)

[22] M. Sentmanat, B. N. Wang, and G. H. Mckinley, *J. Rheol.* 49, 585-606 (2005)

[23] J. Meissner, and J. Hostettler, *Rheol. Acta* 33, 1-21 (1994)

[24] Q. Guo, J. Wang, C. B. Park, and M. Oshima, *Ind. & Eng. Chem. Res.* 45, 6153-6161 (2006)

[25] H. E. Naguib, C. B. Park, U. Panzer, and N. Reichelt, *Polym. Eng. & Sci.*, 42, 1481-1492 (2002)

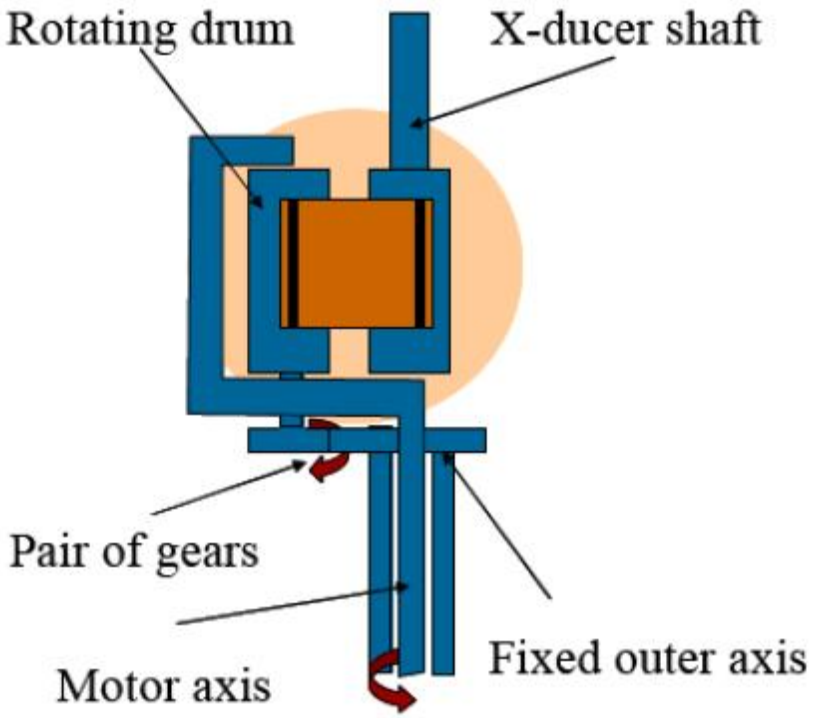

Figure 7.1. Schematic of the ARES-EVF (Extensional Viscosity Fixture).

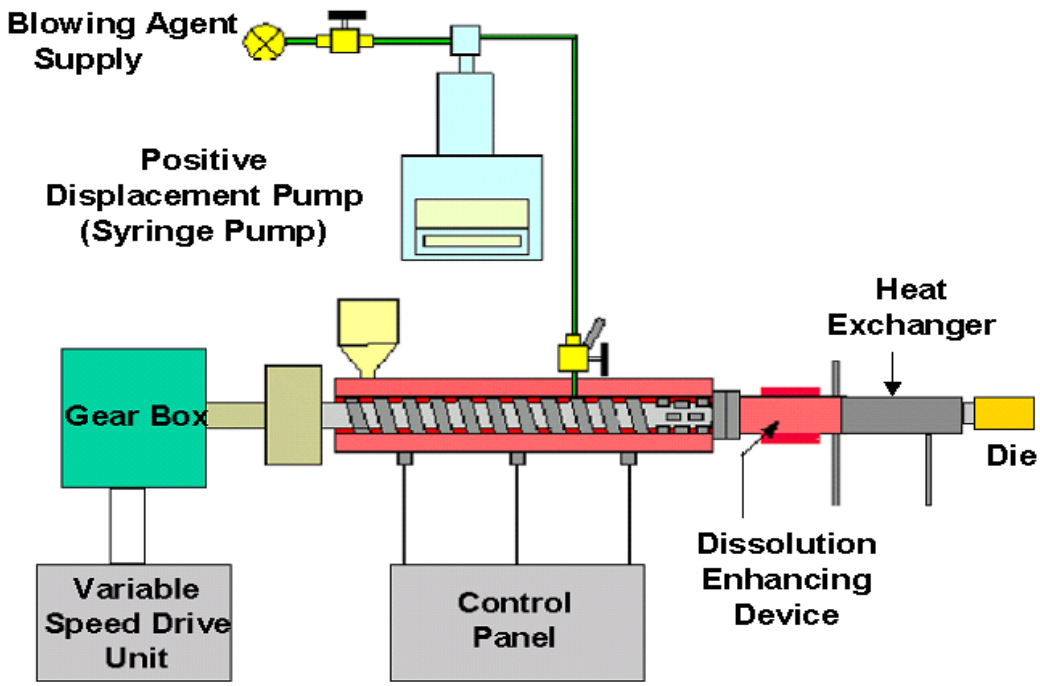

Figure 7.2. Experimental set-up of a single extrusion system for foaming with a filamentary die.

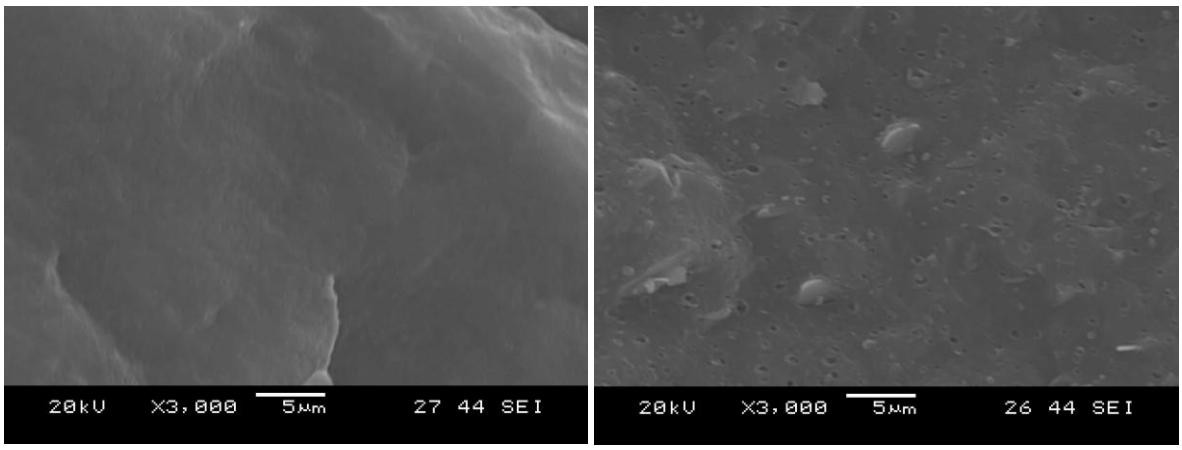

(a) (b)

Figure 7.3. SEM micrographs of the etched surfaces of neat copolymers; (a) RC-PP (R200P) and (b) BC-PP (BA212E).

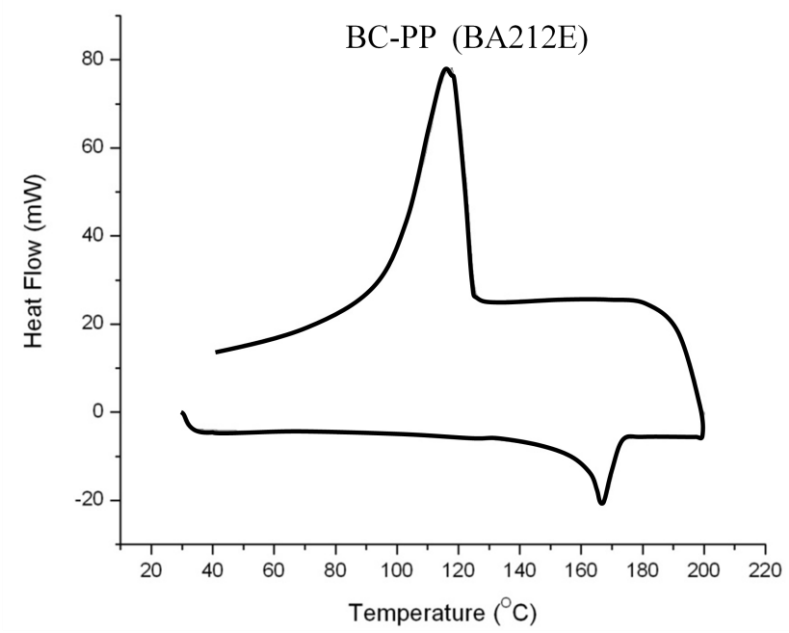

(a) BA212E

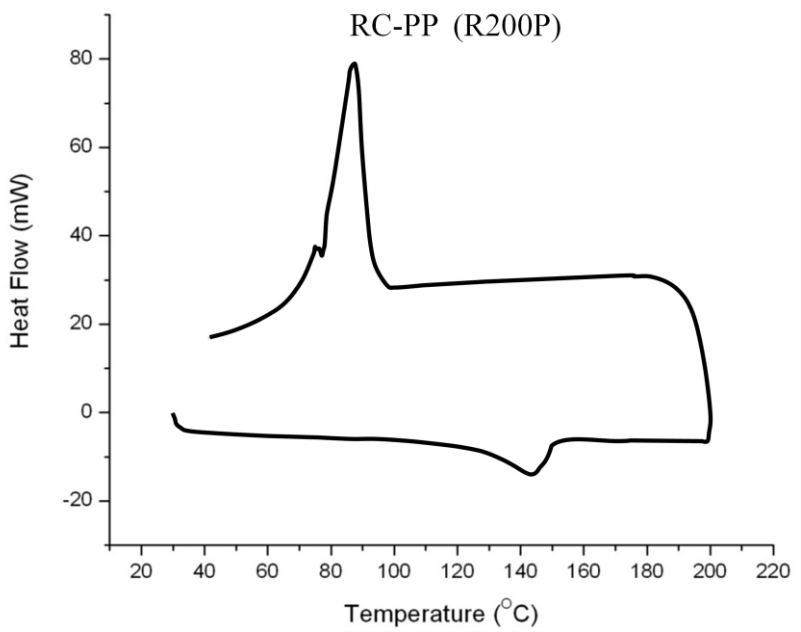

(b) R200P

Figure 7.4. DSC thermograms of BC-PP (BA212E) and RC-PP (R200P) at the ramp of 10℃/min (heating) and -50℃/min (cooling).

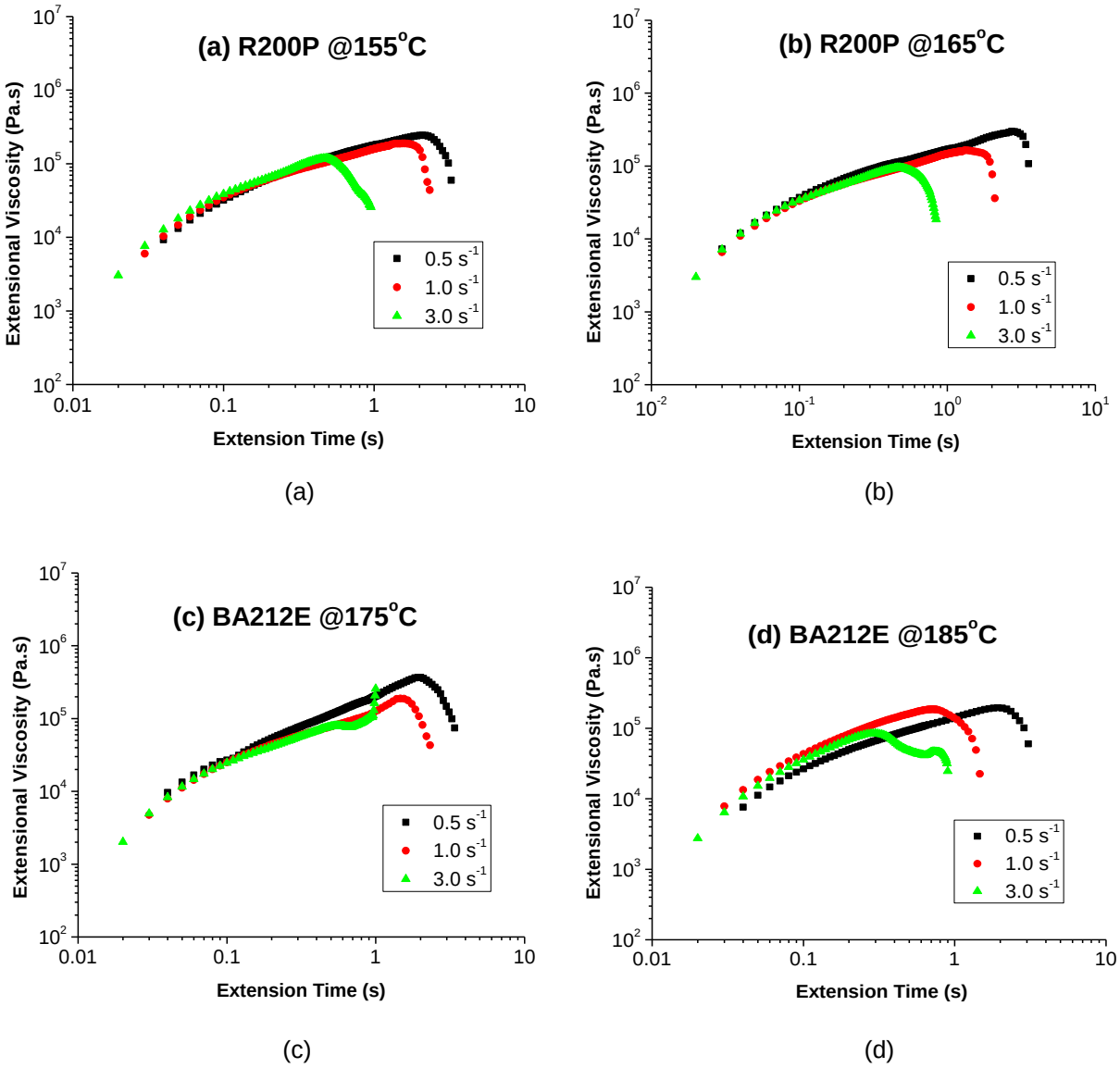

Figure 7.5. Extensional viscosity of neat copolymers at different temperatures and strain rates; (a) R200P at 155℃, (b) R200P at 165℃, (c) BA212E at 175℃, and (d) BA212E at 185℃.

140 °C 130 °C 120 °C

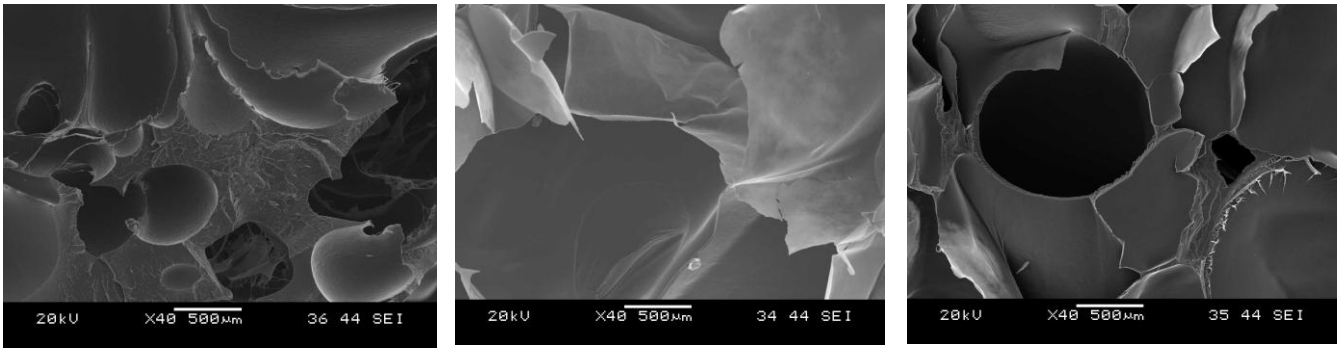

(a)

150 °C 140 °C 130 °C

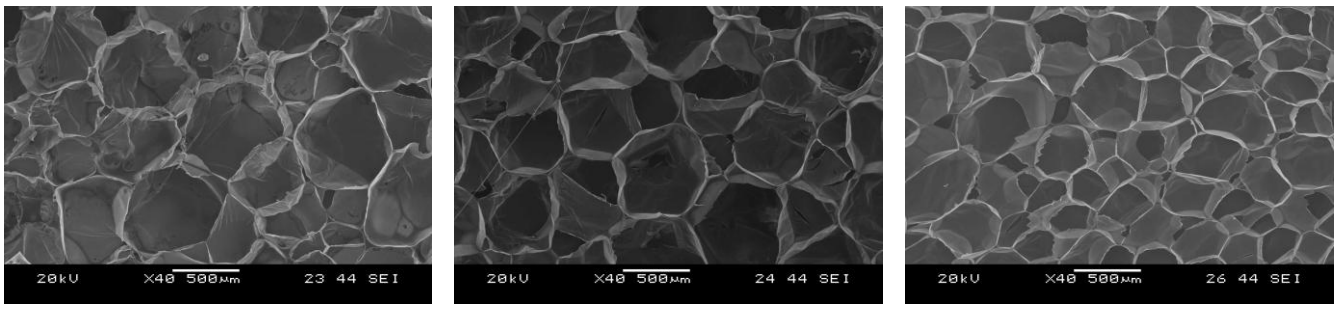

(b)

Figure 7.6. SEM micrographs of cross-sections of foamed samples at different die temperature without talc; (a) R200P with 10% n-butane and (b) BA212E with 10% n-butane.

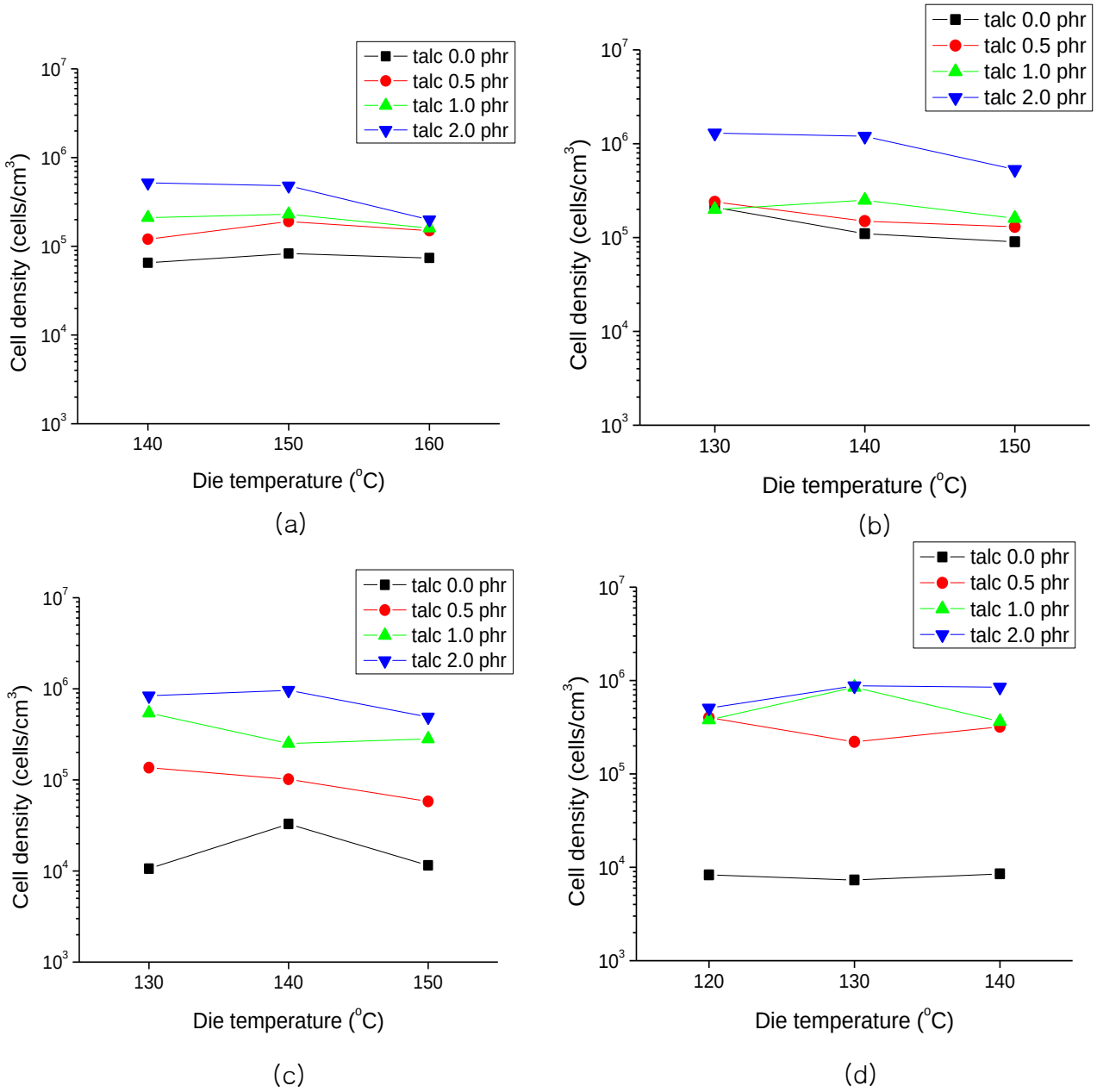

Figure 7.7. Cell population density of expanded foams at different die temperature; (a) BA212E with 5 % n-butane, (b) BA212E with 10 % n-butane, (c) R200P with 5 % n-butane and (d) R200P with 10 % n-butane.

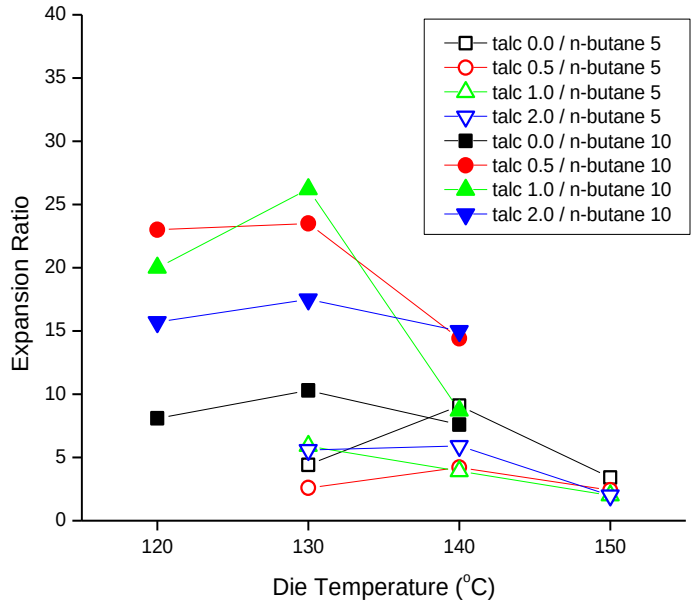

(a)

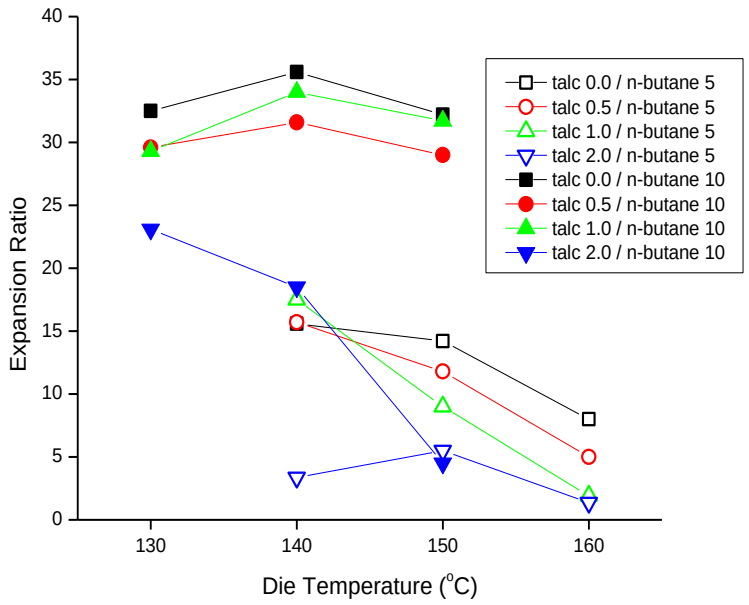

(b)

Figure 7.8. Volume expansion ratio of foamed R200P(a) and BA212E(b) at various compositions and die temperature.

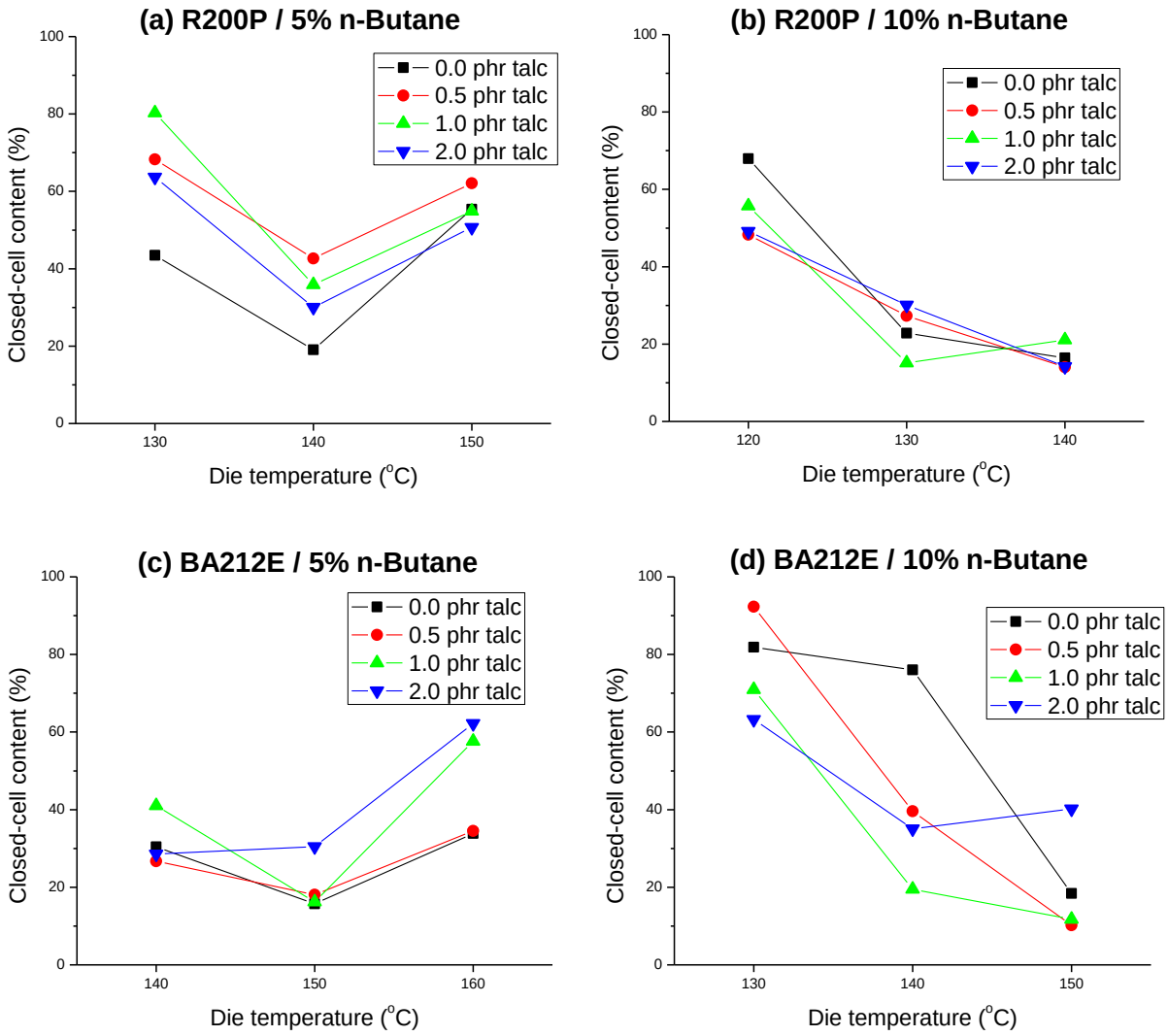

Figure 7.9. Closed-cell content of expanded foams at different conditions; (a) R200P with 5% n-butane, (b) R200P with 10% n-butane, (c) BA212E with 5% n-butane, and (d) BA212E with 10% n-butane.

Chapter 8

Study on Steam Chest Molding Process for EPP Bead Foams

8.1. Introduction

In the steam chest molding process for manufacturing expanded polypropylene (EPP) beads foams, high temperature steam can work as an effective heating medium that can heat up beads and lead to sintering among beads in a 3-dimensional mold cavity [1-3]. In addition to that, the steam diffuses into the beads and then expands the softened cellular structure thanks to pressure difference just like a blowing agent when the pressurized steam is removed in the mold cavity. However some of steam may remain as condensed water in the cells of EPP beads after the steam chest molding is over. Therefore the condensed water can make negative effects on the final foam products. In particular some dimensional defects can take place. The most typical issue is shrinkage of bead foam products. On this account, annealing at relatively high temperature after steam chest molding is needed especially for highly expanded beads. Based on a few previous researches, Nakai et al developed a numerical model on steam chest molding by investigating the fundamental aspects of evaporation, condensation of steam and heat conduction [4-8].

Figure 8.1 illustrates the principles of the steam chest molding process. The free volume between the beads should be removed in order to achieve superior mechanical properties of the final bead foam. In this sense, the ventilation of mold cavity is expected to be helpful to get rid of the free volume as well as the entrapped water in the free volume [9].

This study deals with the basic principles and procedure of steam chest molding process for EPP beads. Even though steam chest molding is an integral process for EPP technology, no research has been carried out on the processing condition. Specifically the optimum annealing time for steam-molded foam was investigated. Furthermore mechanical property of EPP bead foam was correlated with steam pressures. Finally the effect of steam pressure on dimensional stability was experimented by conducting steam chest molding of EPP beads.

8.2. Experimental

8.2.1. Material

For the steam chest molding, 3 kinds of EPP beads were supplied by JSP. Table 8.1 shows the detailed specification of EPP beads used in this study. These beads have 3 different expansion ratios: 15 fold, 30 fold, and 45 fold.

8.2.2. Experimental Set-up

A lab-scale of steam chest molding machine ((DPM-0404VS, DABO PRECISION, Korea) was installed by connecting the pipes of high-pressure steam, cooling water, and compressed-air. The dimension of the mold cavity was 30 cm × 30 cm × 10 cm. Figure 2.13 in Chapter 2 shows the actual steam chest molding machine used in the experiments.

8.2.3. Experimental Procedure

As illustrated in Figure 8.2, the basic process of steam chest molding comprises; 1) bead filling in the mold cavity, 2) 1st steam injection from fixed mold, 3) 2nd steam injection from moving mold, 4) 3rd steam injection from both molds, 5) water cooling, 6) mold-opening and ejection. However there is a depressurization step right before water cooling for further expansion of beads caused by pressure difference. Moreover, vacuum is applied after water cooling in order to remove remaining water in the bead foam. Steam chest molding was performed using 3 kinds of EPP beads with different expansion ratio. Subsequently the dimensional stability was studied for three EPP bead foams. After the steam molding, the weight change of the molded foams with time was monitored at different annealing temperatures. Scanning electron microscopy (SEM) analysis was carried out to observe the internal cell structure as well as the interface between beads in steam-molded foams. For the purpose of seeing the effect of steam pressure on the mechanical property, tensile test was conducted in accordance with ASTM D638-03. As a method to compare the dimensional stability, the warpage length for bead foams was defined and measured in this research.

8.3. Results and Discussion

8.3.1. Relationship between Annealing and Shrinkage

After the steam chest molding with 3 kinds of EPP beads was conducted, it turned out that the ×30 foam as well as the ×45 foam significantly shrank in two hours at ambient condition. Nevertheless the ×15 foam did not bring about any shrinkage unlike the highly expanded foams. Figure 8.3 (a) shows the severely shrunk foam sample on the left hand side. However the shrinkage of steam-molded foam did not appear when the foam was annealed at 80°C for 3 hours as shown on right hand side of Figure 8.3 (a). With regard to the ×30 foam

and the ×45 foam, it was obvious that annealing of steam-molded foams significantly suppressed the shrinkage that could be a critical defect of the final bead foam. More interestingly, the shrunk bead foam recovered the original shape and dimension after it was annealed at 80°C for 5 hours as demonstrated in Figure 8.3 (b). It is believed that the recovery is attributed not only to elastic recovery of cell wall but also to cell expansion by evaporation pressure of the condensed water in the cells. However a great deal of tiny wrinkles on the surface of seam-molded foam was not eliminated even after 24 hour annealing as revealed in Figure 8.3 (b).

To account for the reason of this phenomenon, SEM analysis of EPP beads seen in the Figure 6.2 in the Chapter 6 shows that cell wall thickness of the ×15 bead was about 15 μm, which is much thicker than the ×30 bead (~4 μm thick) and the ×45 bead (~2 μm thick) even though the cell sizes are similar. It means that when the molded-foam cools down, the remnant steam in the cell condensates and gives rise to vacuum state. It is believed that cell walls of the ×30 and ×45 beads were not thick enough to endure the vacuum in the cell. On the other hand, the ×15 bead could maintain its original dimension because of the even thicker cell wall. In this sense, the effect of cell wall thickness on shrinkage can be understood. It is likely that annealing had an effect of not only preventing vacuum state but also enhancing diffusion rates of steam and air. Therefore the remaining steam could diffuse out through the cell wall as time goes on. Besides, air could diffuse into the cells thanks to high diffusivity elevated by annealing until the equilibrium was reached. It is believed that this is how annealing can protect steam-molded foam whose cell wall is very thin from the dimensional deformation. Figure 8.4 supports this explanation by revealing the morphology of cell walls. The shrunk molded foam without annealing had highly rugged cell wall, whereas annealed foam showed by far even cell walls.

8.3.2. Weight Change of Steam-molded Foam during Annealing

As mentioned earlier, condensed water can be trapped in the cells after the steam chest molding. Therefore the remnant water was expected to gasify and maintain cell structure during the annealing. Finally most of water can diffuse out of the molded foam and overall weight of the molded foam can decrease accordingly. With a view to monitoring the weight change of steam-molded foam, annealing experiment was conducted at 4 different temperatures. Figure 8.5 exhibits that the weight of molded foam decreased as time goes on. In particular when annealed at 70°C and 95°C the weight quickly diminished and finally reached the plateau within 2 hours. However the weight of molded foam gradually decreased with time for annealing at 25°C and 50°C. Basically higher ambient temperature can dramatically improve diffusivity of steam by softening the cell wall of EPP bead. At relatively lower temperature, it is most likely that the gradual weight loss is attributed to lower diffusion rate of steam through the more rigid cell wall. According to these experimental results, It is believed that higher temperature is more favorable for annealing in order to shorten the process time of annealing stage.

8.3.3. Effect of Steam Pressure on Tensile Strength

In a bid to investigate the effect of steam pressure on the mechanical property of final bead foams, steam injection pressure was varied as tabulated in Table 8.2. Following the steam molding with ×45 EPP beads, the steam-molded foams were annealed at 80°C for 3 hours. Subsequently tensile test was executed using the specimens of the molded bead foams. Figure 8.6 shows that the pressure condition of #3 provided the highest tensile strength. SEM pictures in the Figure 8.7 back up the tensile test results in that #3 pressure condition showed most severely ripped EPP beads on the fracture surface of tensile test specimen. It seems that

each bead could expand enough to provide stronger adhesion strength between beads at the #3 condition, compared to other steam pressure conditions.

8.3.3. Effect of Steam Pressure on Dimensional Stability

Annealing after steam molding could prevent shrinkage of the molded bead foams. Nevertheless slight warpage took place depending on steam pressure conditions. For the purpose of quantifying the dimensional stability of the molded foams, warpage length was defined as shown in Figure 8.8 (a) in this study. Figure 8.8 (b) shows the results of warpage length measurement of bead foams that were steam-molded at different pressure conditions of #1~#5 in Table 8.2.

It is interesting that the least warpage length was also acquired from #3 steam pressure condition just like the tensile test result. It is believed that dimensional stability is directly related to the extent of bead adhesion depending on steam pressure.

8.4. Summary

Taking it into account that mechanical property as well as dimensional stability is very important in the application of EPP bead foam, research efforts have been made not just to understand the principles of steam chest molding of EPP beads but also to find the optimum processing condition in this study. Since steam pressure is a critical parameter in steam chest molding, the steam pressure was varied and resulting bead foams were tested schematically.

It was discovered that annealing at higher temperature (up to 95°C) was more appropriate to reduce the processing time for annealing, considering the fact that annealing was required to avoid shrinkage especially for highly expanded EPP beads. In terms of tensile test, #3 steam pressure condition showed the highest tensile strength. In addition this result

coincided with that of dimensional stability test obtained by measuring warpage length of steam-molded bead foams. SEM experiment visually supported these test results by showing the fractured surface of EPP bead foams.

8.5. References

[1] N. J Mills and A. Gilchrist, *Cell. Polym*., 18(3), 157 (1999)

[2] K.W. Suh, *Handbook of Polymeric Foams and Foam Technology*, D. Klempner and C. Frisch, Eds., Hanser Publishers, Munich, 151 (1991)

[3] N. J. Mills, *Cell. Polym*., 16, 194 (1997)

[4] S. Nakai, K. Taki, I. Tsujimura, M. Ohshima, *Polym. Eng. Sci*., 48(1), 107-115 (2008)

[5] C. T. Yang and S. T. Lee, J. Cell. Plast., 39, 59 (2003)

[6] G. Frederick, G. A. Kaepp, C.M. Kudelko, P.J. Schuster, F. Domas, U.G. Haardt, and W. Lenz, *S.A.E. Trans*, 104(5), 394 (1995)

[7] A. Mahapatro, N. J. Mills, and G.L.A. Sims, *Cell. Polym*., 17, 252 (1998)

[8] I. Beverte, *Mech. Compos. Mater.,* 34, 115 (1998)

[9] C. T. Bellehumeur, J. Vlachopoulos, *SPE, ANTEC, Technical Papers*, 1, 1112 (1998)

Table 8.1. EPP beads with different expansion ratios

Grade	Expansion Ratio	Bulk Density (g/L)
ARPRO 5446	x 15	60.9
ARPRO 5425	x 30	31.3
ARPRO 5415	x 45	20.9

Table 8.2. Steam chest molding conditions

No.	Steam Pressure (bar)		
	1st Injection (fixed mold)	2nd Injection (moving mold)	3rd Injection (fixed/moving)
#1	1.6	2.8	1.8 / 3.0
#2	1.8	3.0	2.0 / 3.2
#3	2.2	3.6	2.4 / 3.8
#4	2.6	3.4	2.8 / 3.5
#5	2.8	3.4	3.0 / 3.5

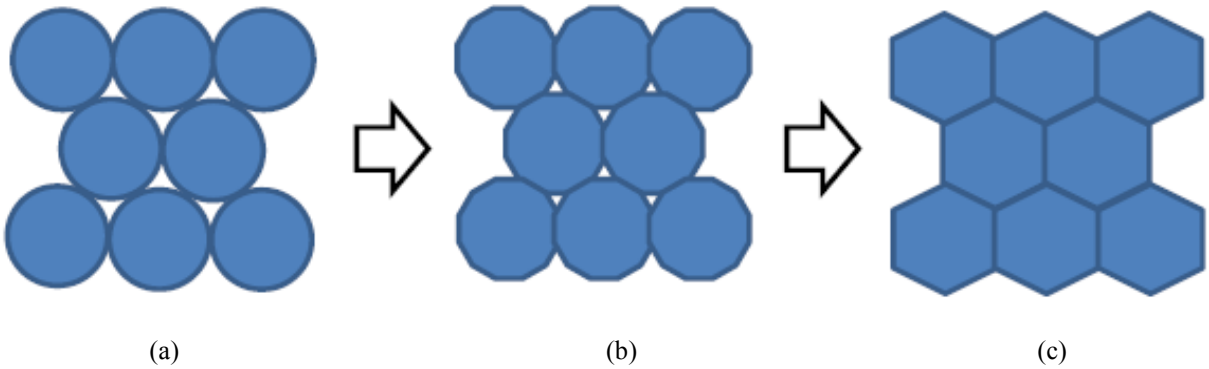

Figure 8.1. Model of bead sintering; (a) Initial packing, (b) Intermediate stage and (c) ideally sintered bead foam.

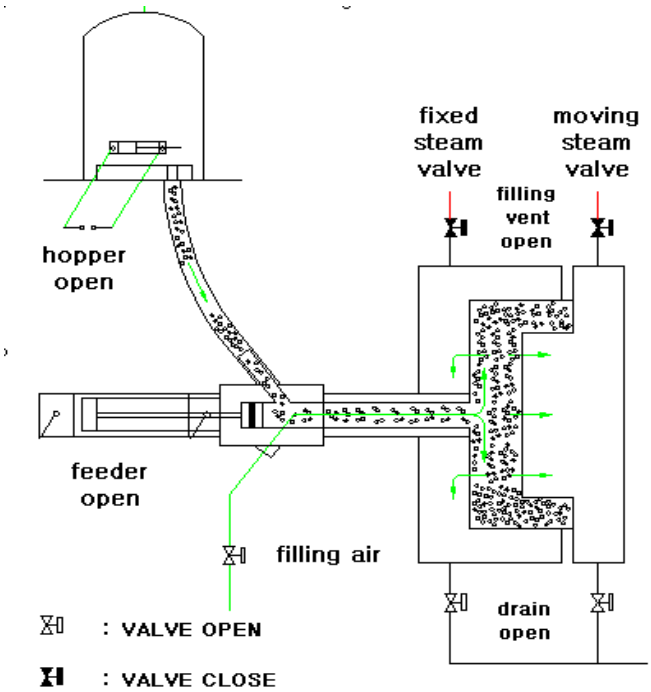

(a) Bead filling process

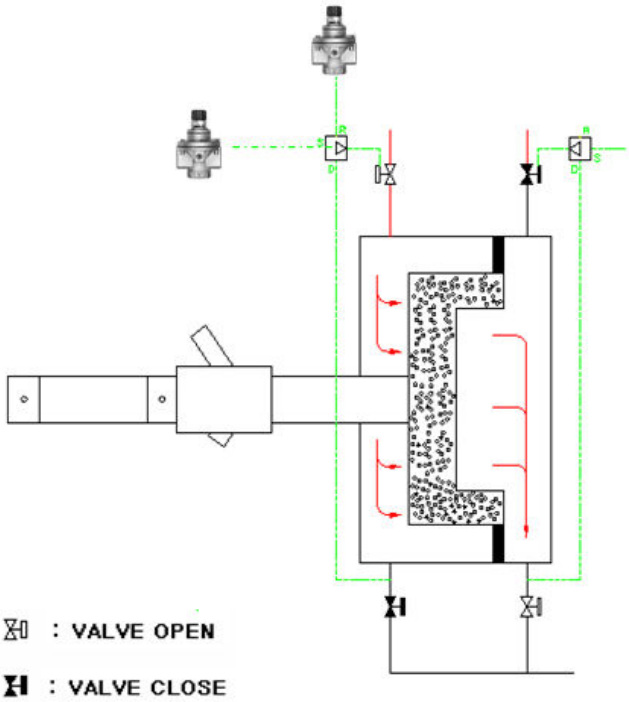

(b) 1st steam injection from fixed mold

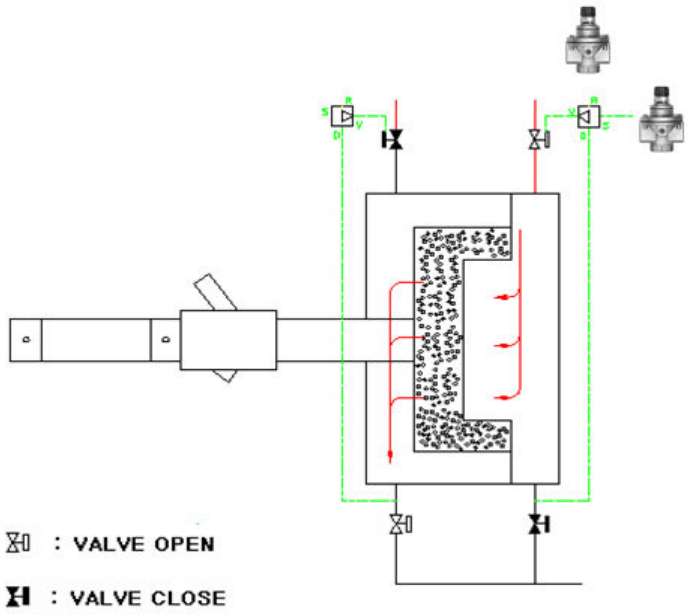

(c) 2nd steam injection from moving mold

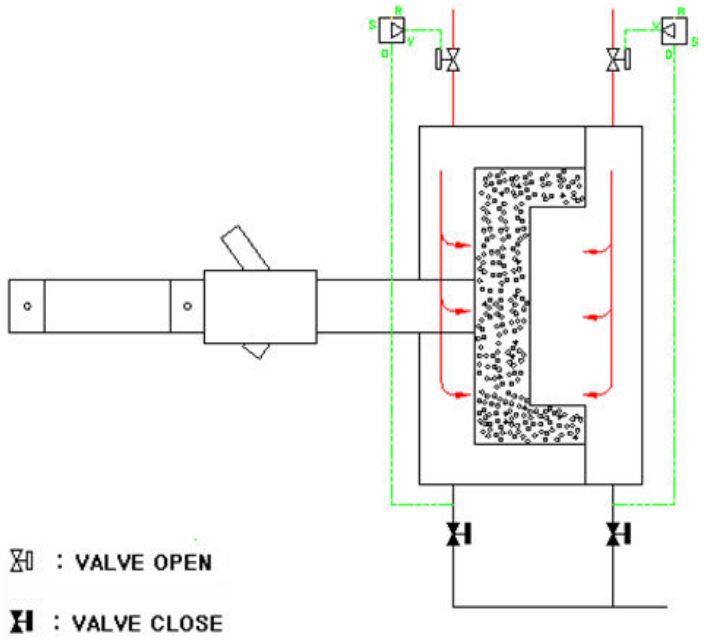

(d) 3rd steam injection from both molds.

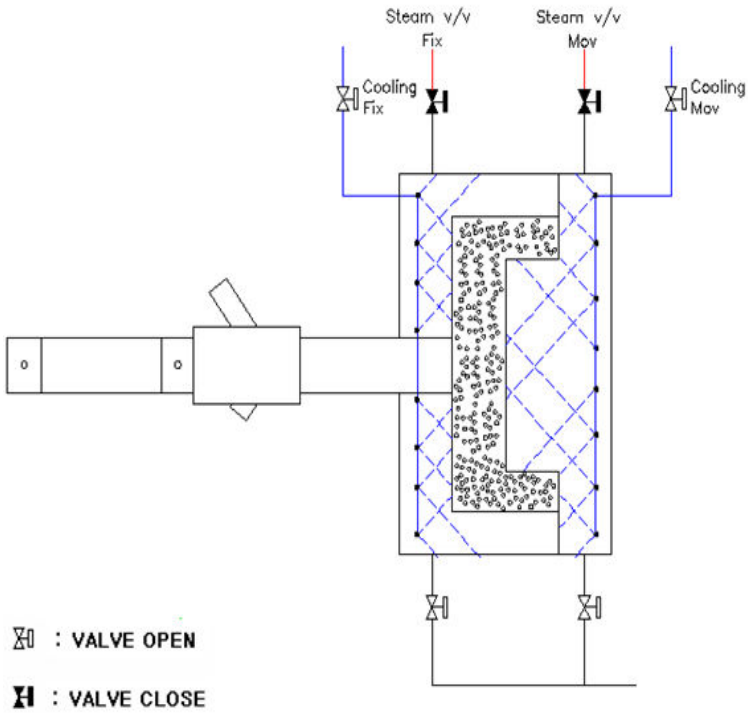

(e) Water cooling process

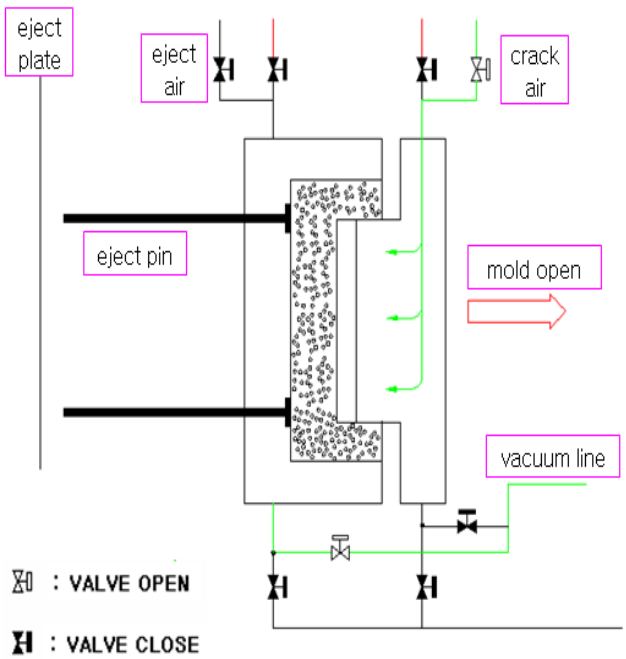

(f) Mold opening and release

Figure 8.2. Process of steam chest molding.

(a)

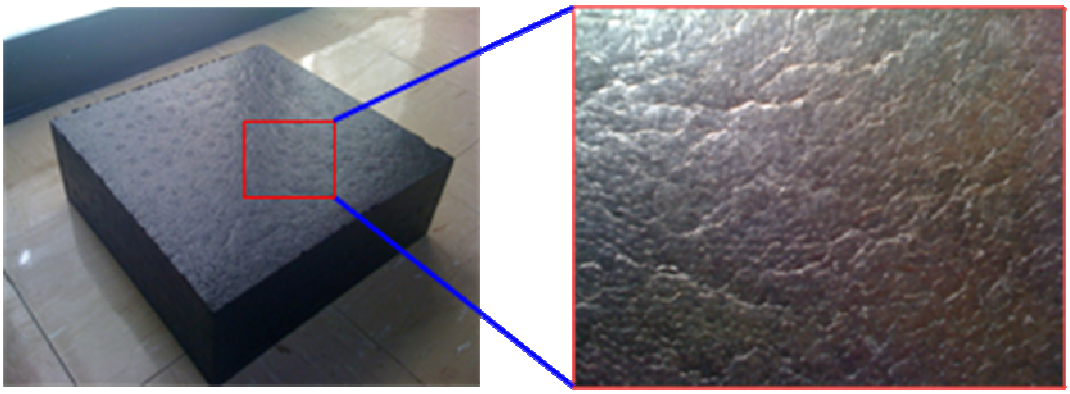

(b)

Figure 8.3. Shrinkage of EPP foam (× 45) and recovery through oven annealing;

(a) foam with shrinkage without annealing (left hand side) and normal foam after annealing (right hand side); (b) recovered foam by annealing after shrinkage.

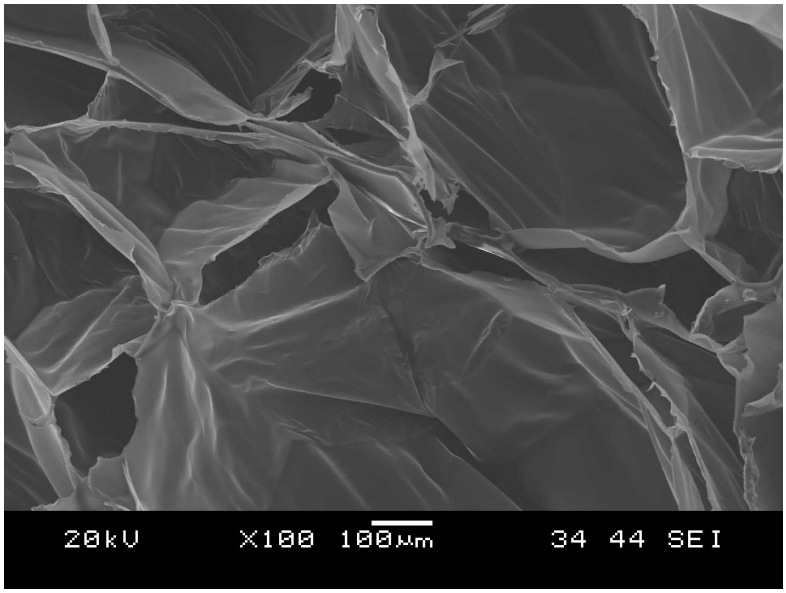

(a)

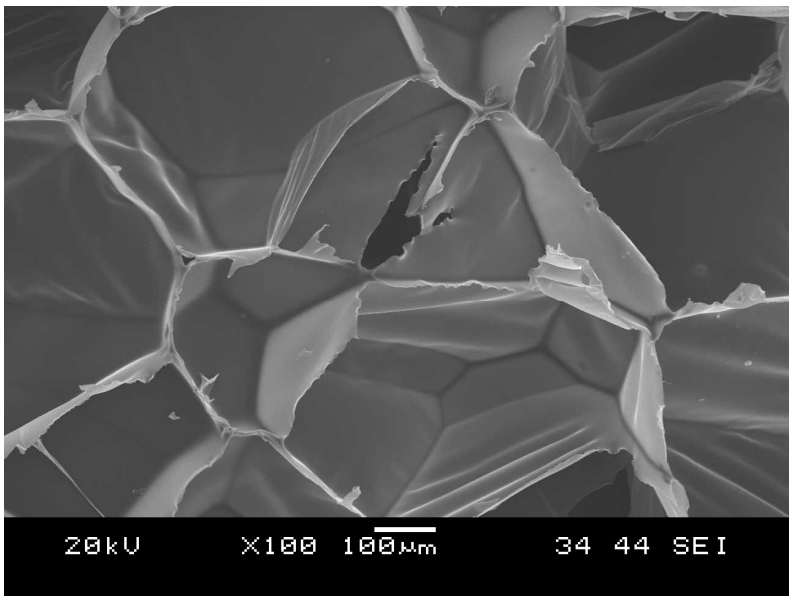

(b)

Figure 8.4. SEM photographs of cross-sections of EPP foams; (a) shrunk foam without annealing, (b) normal foam with annealing after steam chest molding.

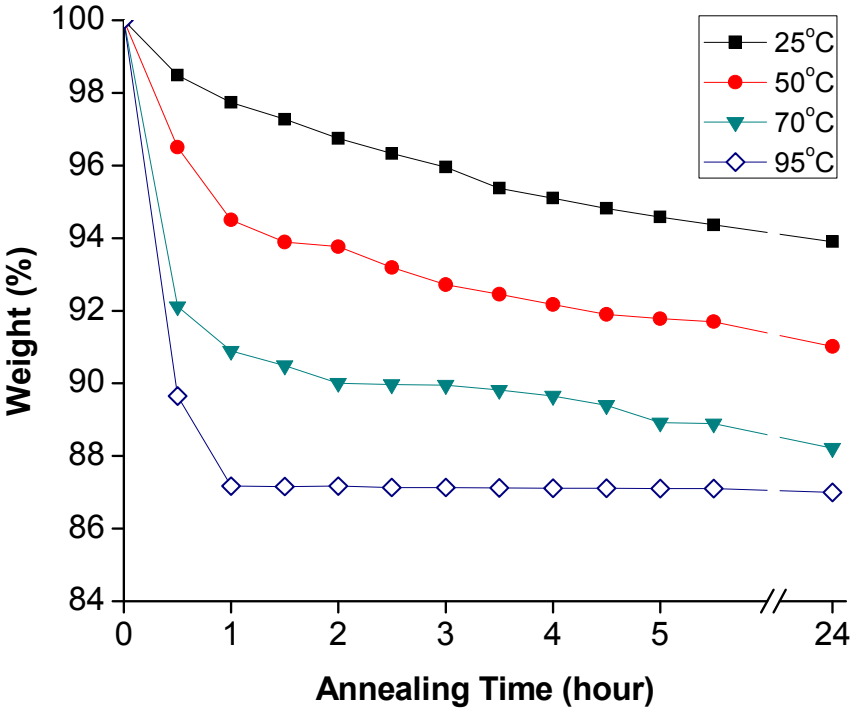

Figure 8.5. Weight loss of EPP foams (x 45) after steam chest molding depending on annealing time and temperature.

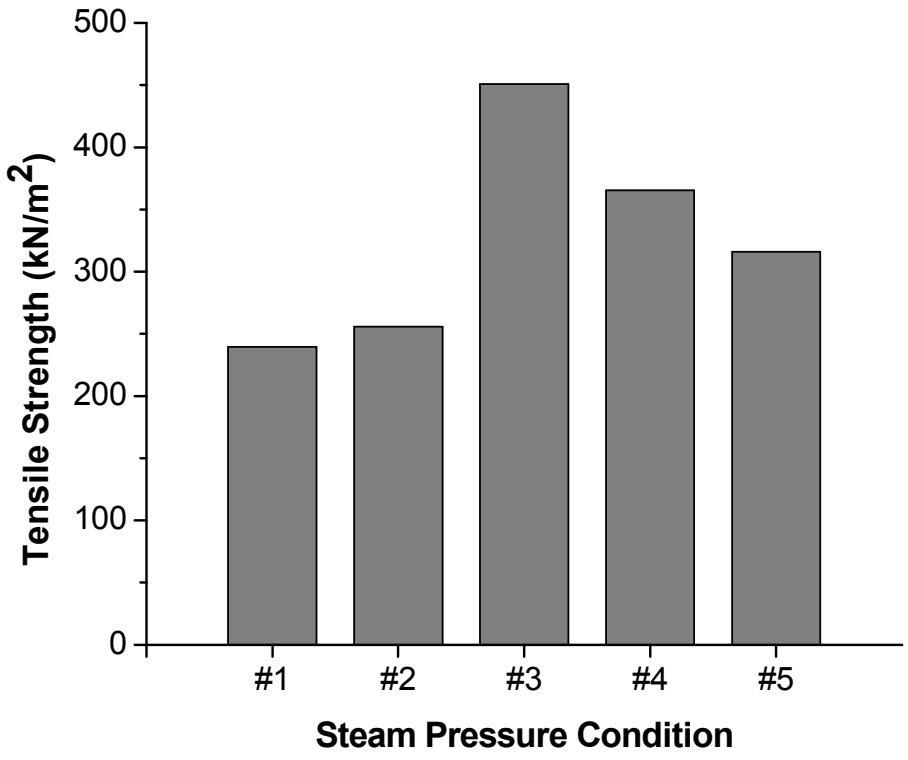

Figure 8.6. Tensile strength of EPP foams (× 45) that were steam-molded at different steam pressure conditions.

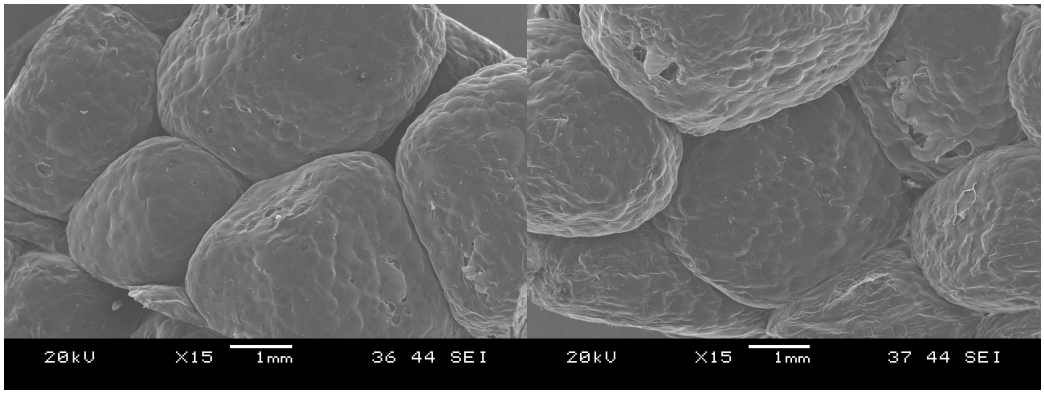

(a) (b)

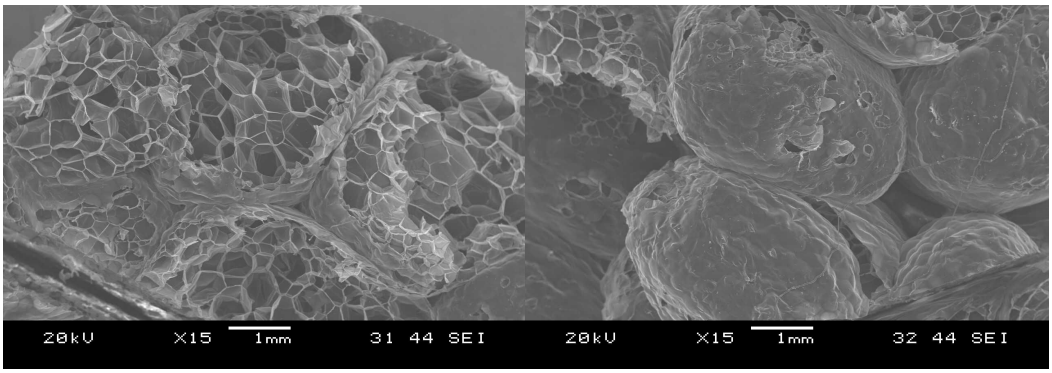

(c) (d)

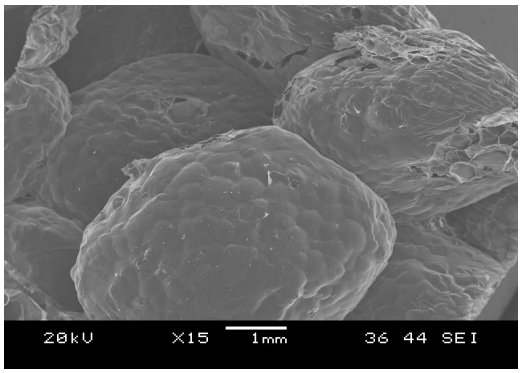

(e)

Figure 8.7. SEM photographs of fracture surface of EPP foam (x 45) during tensile test; Steam molding conditions of (a) ~ (e) were described in Table 8.2.

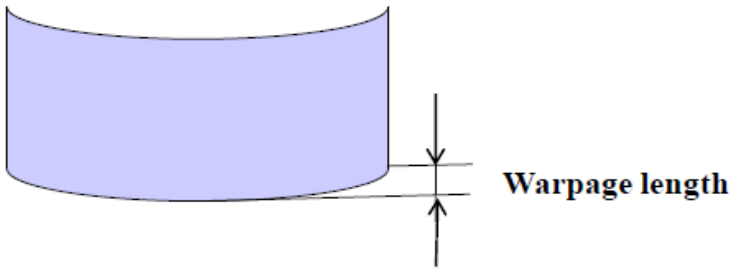

(a)

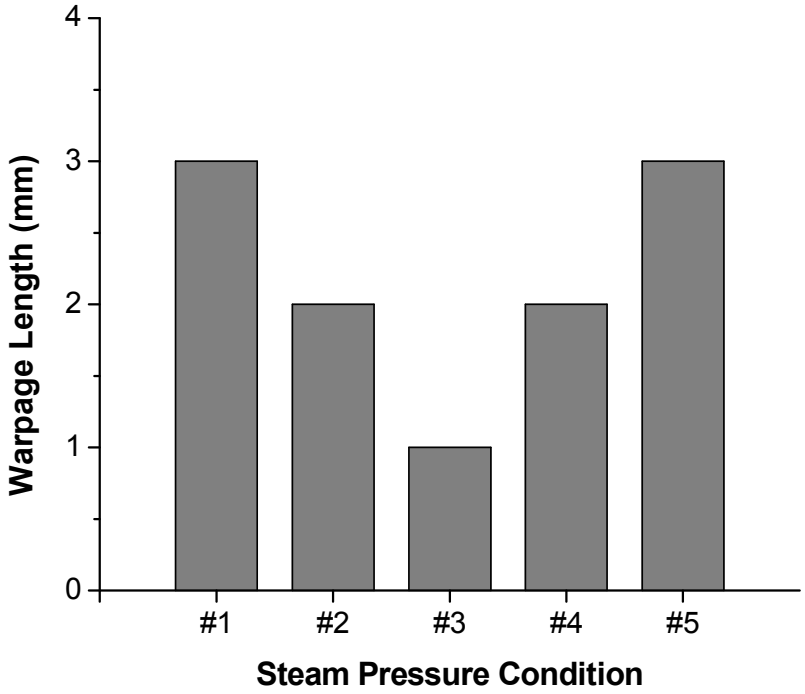

(b)

Figure 8.8. Warpage measurement of EPP foam (x45); (a) definition of warpage length, (b) warpage length depending on steam pressure.

Chapter 9

Summary and Recommendations

9.1. Summary of Major Contributions

In this thesis, the new foaming processes and the principles for manufacturing PS and PP bead foams have been systematically studied. Although EPS and EPP bead foams are very similar in the aspect of final foam products, the basic manufacturing processes are quite different due to the unique characteristics of two commodity polymers. In addition, it was found that the two bead foam technologies had some drawbacks that can limit the range and the extent of applications in industry. In brief, EPS bead foam process still has a few issues related to the volatile organic compound, n-pentane. Besides more advanced physical properties of EPS foams are still demanded by some application areas despite the fact that EPS has been widely being used for a long time. Especially the excellent thermal insulation property has been aimed at by many researchers and engineers. In the case of EPP bead foams, the low productivity and high transportation cost are still restricting the dramatic expansion of market volume and application

areas in spite of many advantages of EPP bead foams such as outstanding resilient property, environmentally benign raw material, recyclability, etc. From this point of view, this thesis study was undertaken not only to scientifically comprehend the basic principles of material characteristics and foaming processes of the two most popular bead foam technologies, EPS and EPP bead foams, but also to develop advanced viable bead foam processes. Based on the results of the thesis study, the major contributions could be summarized as follows.

9.1.1. Technical Achievements

- **Development of the viable foaming processes for VOC-free EPS bead foam technology.**

Research efforts have been made to manufacture the cell-nucleated PS beads that have desirable cellular characteristics required for VOC-free EPS bead foam process. Batch foaming and extrusion foaming were executed changing both compositions and processing parameters in order to find the most suitable process for producing the nucleated PS beads. The targeted cell structure was successfully obtained from batch foaming experiment thanks to plasticization effect of carbon dioxide as well as the solubility-enhancing effect of PDMS. Furthermore, the optimum process conditions were determined about the pre-expansion of the nucleated beads as well as about re-pressurization of the pre-expanded beads just prior to the steam chest molding.

- **Bi-cellular PS foam was successfully fabricated through extrusion foaming process.**

In an attempt to fabricate the bi-cellular PS foam, extrusion foaming was conducted using co-blowing agents of water and n-butane along with precipitated silica. The bi-cellular foam

structure in PS could be effectively generated by changing the ratio of n-butane/water/silica content as well as die temperature in the extrusion foaming process. Presumably water trapped in the pore of silica contributed to the formation of the smaller cells, whereas both the excessive water that was not absorbed by silica particles and n-butane primarily resulted in the larger cell surrounded by the smaller cells. The precipitated silica particles were believed to function as a water carrier in the PS melt due to their strong hydrophilic characteristic, which was conducive to the dispersion of water despite its low solubility.

- **The continuous extrusion foaming process was demonstrated to produce expanded PP beads.**

The conventional EPP beads are highly expensive, not only because the transportation cost is high, but also because the production process is an inefficient batch foaming process which needs tremendous investment for the production facilities. Therefore extrusion foaming which is a continuous foaming process was performed in order to see the feasibility of replacing the traditional batch foaming process. The random and block propylene-ethylene copolymers were extrusion-foamed by varing the die temperature, n-butane content and talc content. Higher volume expansion ratio was achieved from the block propylene-ethylene copolymer. In addition, when it comes to the closed-cell content, the maximum value was 92%, which was obtained from the block propylene-ethylene copolymer foam.

- **Optimum processing conditions of steam chest molding were determined.**

Based on understanding of the principles of steam chest molding, it was possible to identify the optimum processing condition for EPP beads. Now that steam pressure plays an important role in sintering beads in the steam chest molding process, the steam pressure was

varied and resulting bead foams were tested schematically. Regarding annealing process required for avoiding shrinkage, it turned out that annealing at higher temperature (up to 95°C) was very effective to reduce the processing time. Tensile test and dimensional stability test showed the most desirable results at the same steam pressure condition. SEM analysis visually backed up these experimental results by showing the morphology of fractured surface of EPP bead foams.

9.1.2. Scientific Accomplishments

- **Quantitative measurement of solubility and diffusivity of n-pentane in PS and PP at ambient condition.**

With a view to observing the transportation behaviors of n-pentane in PS and PP, the solubility and diffusivity of n-pentane in PS and PP at room temperature and atmospheric pressure were quantitatively measured and compared. A series of sorption and desorption experiments were schematically carried out. It was discovered that sorption and desorption of n-pentane in PP were much faster than in PS although n-pentane had high solubility in both PS and PP. The molecular chains of PS should be in a glassy or frozen state because the glass transition temperature is about 107°C, whereas PP is in a rubbery state. On this account, the mobility of n-pentane is believed to be restricted in PS. Moreover the concentration-dependent diffusivities of n-pentane in PS and PP were numerically calculated.

- **The scientific principles and fundamental mechanisms in the conventional EPP process were identified**

It was identified that gas impregnation at an elevated temperature led to the formation of higher melting crystals aside from the innate alpha crystal of PP. The newly created crystals can

contribute to the significant improvement of melt strength of PP due to the cross-linking effect. In other words, the substantially enhanced extensional viscosity can prevent cell openings during the stage of cell growth. Accordingly very high closed-cell content can be achieved in the conventional EPP process. Besides, it was understood that the high temperature crystals play a crucial role in maintaining overall cellular structure at the stage of steam chest molding of EPP beads. In addition, beta crystallization behaviors of PP were investigated by changing the cooling rates as well as by introducing a functional additive that was believed to promote the epitaxial beta crystallization in PP.

9.2. Recommendations

The following suggestions can be made for the direction of future research on bead foam technology:

1. As to the production of nucleated PS beads, more experimental efforts on extrusion foaming will be valuable by using various blowing agents and nucleating agents in the aspect of reducing cost through a continuous process. Moreover, the mechanical equipments such as a pre-expander, stepwise pressurizing chamber directly connected to a steam chest molding machine should be designed and manufactured in order to develop commercially viable VOC-free EPS technology.

2. Thermal insulation property of bi-cellular PS foam should be measured depending on material compositions and foam-processing parameters. Furthermore, instead of water, ethanol should be tested as a blowing agent, because ethanol has higher solubility than water although it has a hydrophilic feature.

3. Following the extrusion foaming of ethylene-propylene copolymers, an underwater pelletizer can produce expanded spherical beads by cutting the foamed strands. Therefore steam chest molding experiment will be conducted using bulk amount of expanded PP beads in order to investigate the final mechanical properties as well as dimensional stabilities of PP bead foams. Moreover, extensive experiments on extrusion foaming should be needed since higher closed-cell content is required for excellent sintering of PP beads.

4. It may be possible to apply the VOC-free EPS process to EPP technology. It will be highly valuable to develop VOC-free expandable PP beads foam process by manufacturing the nucleated PP beads using batch foaming or extrusion foaming process. If this study would succeed, the impact of the expandable PP beads technology on bead foam industry should be tremendous.

5. Based on the deep understanding about PS and PP bead foams, it will be possible to develop expandable (or expanded) poly lactic acid (PLA) beads foam which is a popular biodegradable polymer. Aside from PLA bead foams, bead foams of high-temperature durable polymers will also be worth trying to invent, because bead foams using steam chest molding is the only process that can embody low density foam products with complicated 3-dimensional geometry.